

STRUCTURAL STUDIES OF PMM/PGM
FROM *PSEUDOMONAS AERUGINOSA*

A Dissertation
presented to
the Faculty of the Graduate School
University of Missouri-Columbia

In Partial Fulfillment
Of the Requirements for the Degree
Doctor of Philosophy

by

CATHERINE A. REGNI

Dr. Lesa J. Beamer, Dissertation Supervisor

DECEMBER 2005

The undersigned, appointed by the Dean of the Graduate School,
have examined the dissertation entitled.

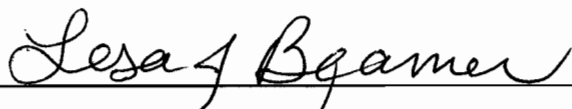
STRUCTURAL STUDIES OF PMM/PGM

FROM *PSEUDOMONAS AERUGINOSA*

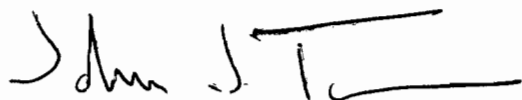
Presented by Catherine A. Regni

A candidate for the degree of Doctor of Philosophy of Biochemistry

And hereby certify that in their opinion it is worthy of acceptance.









ACKNOWLEDGMENTS

I would like to thank all of my committee members and members of the Biochemistry Department for invaluable advice and support. I would like to extend special thanks to Peter Tipton, for helping me to appreciate enzymes, and Jack Tanner, for sharing his knowledge about X-ray crystallography, and helping with data collection. And special thanks also to my adviser, Lesa, for several things, including but not limited to, unwavering patience, support, and many stimulating discussions about protein structure.

I would like to thank my family for encouragement, especially Agoston, for his endless support, and Margit, for inspiration.

This work was supported by NIH grant GM59653 and NIH training grant GM08396-13.

TABLE OF CONTENTS

	<u>Page</u>
ACKNOWLEDGMENTS	ii
LIST OF TABLES.....	iv
LIST OF FIGURES	v
ABSTRACT.....	vi
CHAPTER	
1. Introduction.....	1
2. Crystallization and initial crystallographic analysis of PMM/PGM from <i>Pseudomonas aeruginosa</i>	8
3. Crystal structure of PMM/PGM: An enzyme in the biosynthetic pathway of <i>P.</i> <i>aeruginosa</i> virulence factors.....	18
4. Structural basis of diverse substrate recognition by the enzyme PMM/PGM from <i>P. aeruginosa</i>	58
5. Roles of active site residues in <i>Pseudomonas aeruginosa</i> Phosphomannomutase/Phosphoglucomutase.....	92
6. Structural analysis of intermediate complexes in PMM/PGM.....	113
7. Conclusion.....	140
VITA.....	142

LIST OF TABLES

Table	Page
3-1. Data collection statistics.....	49
3-2. Refinement summary.....	49
3-3. Geometry of metal binding loop.....	50
4-1. Data collection and refinement statistics.....	81
4-2. Enzyme-ligand hydrogen bond contacts in PMM/PGM complexes.....	82
5-1. Kinetic parameters for PMM/PGM site directed mutants.....	106
5-2. Kinetic parameters for PMM/PGM S108 mutants.....	107
6-1. Data collection and refinement statistics for intermediate complexes.....	129
6-2. Pairwise superposition data.....	130
6-3. Comparison of all PMM/PGM structures.....	131
6-4. Hydrogen bond contacts in intermediate structures.....	132

LIST OF FIGURES

Figure	Page
2-1. Biosynthetic pathway of alginate.....	15
2-2. Diffraction pattern of native PMM/PGM crystal.....	16
3-1. Biosynthetic pathways of alginate and LPS.....	42
3-2. Structure, topology, and electrostatic surface of PMM/PGM.....	43
3-3. Superposition of PMM/PGM and PGM from rabbit muscle.....	45
3-4. Details of PMM/PGM active site.....	46
3-5. Schematic of proposed reaction mechanism for PMM/PGM.....	48
4-1. Mechanism and overall structure of PMM/PGM.....	85
4-2. Interactions between PMM/PGM and its phosphosugar substrates.....	86
5-1. Active site of PMM/PGM with glucose 1-phosphate bound.....	109
5-2. Electrostatic potential of PMM/PGM active site.....	110
5-3. Scheme 1.....	111
6-1. Superposition of PMM/PGM structures.....	133
6-2. Active site of PMM/PGM.....	134
6-3. Difference map of dephospho-PMM/PGM complex.....	135
6-4. Difference map of phospho-PMM/PGM complex.....	136

**STRUCTURAL STUDIES OF PMM/PGM FROM *PSEUDOMONAS
AERUGINOSA***

Catherine A. Regni

Dr. Lesa J. Beamer, Dissertation Supervisor

ABSTRACT

The human pathogen *Pseudomonas aeruginosa* expresses a variety of cell surface polysaccharides, including alginate, lipopolysaccharide (LPS), and rhamnolipid. *P. aeruginosa* is the primary cause of chronic lung infections in cystic fibrosis (CF) patients, and these molecules contribute to its virulence. This dual-specificity enzyme phosphomannomutase/phosphoglucomutase (PMM/PGM) is required for the production of these molecules. The structure of PMM/PGM was previously solved in our laboratory, showing that the protein has four domains organized in a “heart shape,” with the active site in a deep cleft formed by residues from each domain. Recently, we have determined the structures of PMM/PGM bound to its two substrates, two products, and an intermediate at 2.0 Å resolution or higher. These structures reveal the structural basis for diverse substrate recognition by the enzyme and pinpoint residues important for accomplishing the dynamic reorientation step of the reaction.

CHAPTER 1 INTRODUCTION

Pseudomonas aeruginosa expresses a variety of cell surface polysaccharides. These molecules include the mucoid substance alginate, lipopolysaccharide (LPS) and rhamnolipid. Alginate is composed of random polymers of D-mannuronic and L-guluronic acid, while LPS is a complex glycolipid composed of a hydrophobic lipid-containing region, central core polysaccharides, and repeating O-antigen polysaccharides. Rhamnolipid is a glycolipid with a detergent-like structure, containing one or two rhamnose units. The biosynthetic pathways of alginate, LPS and rhamnolipid share common steps. Alginate and LPS A-band polysaccharide production begin with fructose 6-phosphate, which is eventually converted to GDP-mannose. Glucose is converted to dTDP-L-rhamnose, which is the precursor for rhamnolipid and LPS core sugars. These reactions occur in the cytosol.

P. aeruginosa is the primary cause of chronic lung infections in cystic fibrosis (CF) patients, and alginate, LPS and rhamnolipid contribute to its virulence [1], [2]. During chronic infection, the bacterium converts to the mucoid phenotype, meaning it produces alginate. This molecule forms a viscous coating around the bacterium, which helps protect it from the host immune response. The alginate coating is also believed to diminish the effectiveness of many antibiotics against *P. aeruginosa*. At later stages of infection, *P. aeruginosa* abandon their planktonic lifestyle and form surface-attached communities called biofilms. These communities have defined structure interspersed with fluid-filled channels, and protect the bacteria from environmental insults (dehydration, etc). Rhamnolipid, a surfactant, maintains these channels allowing nutrients to flow through the biofilm [2].

Because of their role in *P. aeruginosa* pathogenesis, enzymes responsible for the biosynthesis of alginate, LPS and rhamnolipid are attractive candidates for inhibitor design. In collaboration with Peter Tipton's laboratory we have focused on the enzymes of alginate biosynthesis. His group has conducted the mechanistic characterization of key enzymes in the alginate biosynthetic pathway, while the Beamer group has performed structural studies by X-ray crystallography. To date, the crystal structures of the enzymes encoded by the *algC* and *algD* genes have been determined [3], [4]. The corresponding protein products are the dual-specificity phosphomannomutase/phosphoglucomutase (PMM/PGM), and GDP-mannose dehydrogenase (GMD), respectively. GMD catalyzes the committed step of alginate biosynthesis. In contrast, PMM/PGM participates in the alginate, LPS and rhamnolipid pathways. The enzymes of alginate biosynthesis are present at low levels within the bacterium, even when large amounts of alginate are produced [5]. Therefore, the genes encoding these enzymes were identified by their ability to complement non-alginate producing strains of *P. aeruginosa* and confer the alginate producing phenotype. The additional roles of PMM/PGM were discovered more recently. By complementation, PMM/PGM was found to be required for rhamnolipid and LPS core sugar biosynthesis [6, {Coyne, 1994 #51}].

PMM/PGM is a member of the α -D-phosphohexomutase enzyme superfamily. Members of this superfamily play varied roles in carbohydrate metabolism and other biosynthetic pathways. As the name suggests, the PMM/PGM enzymes can utilize mannose- and glucose-based phosphosugars. These enzymes are found primarily in bacteria. In contrast, the PGM members are highly specific for glucose. PGM is best known for its role in providing substrates that enter the glycolytic pathway. Other members include phosphoglucosamine mutase (PNGM) and phosphoacetylglucosamine mutase (PAGM), although these proteins have been less extensively characterized. PNGM and PAGM are involved in the biosynthesis of UDP-N-acetylglucosamine, which is an essential common precursor for bacterial cell wall components

and is also required for the posttranslational N-acetylglucosamine modification of eukaryotic proteins [7].

PMM/PGM is a monomeric enzyme with 463 amino acid residues. It requires divalent magnesium for maximum activity and glucose 1,6-bisphosphate (G16P) as an activator. PMM/PGM catalyzes the transfer of a phosphoryl group between the C(6) and C(1) positions of α -glucose- and α -mannose-based substrates with equal efficiency, and the reaction is readily reversible. The eukaryotic analog PGM, from rabbit muscle, has been studied extensively and shows a 6000-fold preference for glucose-based substrates [8]. Both enzymes are phosphorylated at a serine residue (108 in PMM/PGM and 116 in PGM), and this phosphoryl group is transferred to the substrate. The substrate then reorients to return a phosphoryl group to the serine residue, so that the catalytic cycle can begin again.

Enzyme-catalyzed reactions involving the transfer of a phosphoryl group are central to metabolism, and the chemistry of this group transfer is well characterized. The reaction catalyzed by PMM/PGM has been proposed to proceed via general acid/base catalysis, based on mechanistic and structural studies with PGM [9]. However, it has also been proposed that the mechanism utilizes an ensemble of amino acids, based on studies of several site-directed mutants [10]. Since the PMM/PGM active site contains several positively charged residues, electrostatics may facilitate ionization of the substrate [10]. Studies on PGM also suggested that the phosphorylated serine residue was essential for catalysis, so a site-directed mutant of PMM/PGM, S108A, was made to test the assertion. Surprisingly, the mutant retained 5% of the activity of the wild-type enzyme, significant for a supposedly “essential” residue [10]. It has been proposed that another active site residue can be phosphorylated as an alternative, but to date this residue has not been identified [10].

The reaction catalyzed by PMM/PGM poses interesting challenges to the enzyme, which are explored in the work herein. The research presented ranges from the initial purification and

crystallization of PMM/PGM to detailed structural investigations probing each step of the reaction. The contents of each chapter are outlined below.

Chapter 2 – “Crystallization and initial crystallographic analysis of phosphomannomutase/phosphoglucomutase from *Pseudomonas aeruginosa*.”

This chapter describes the overexpression construct, purification of the enzyme, crystallization of the native enzyme and selenomethionine derivative, and X-ray data collection.

Chapter 3 – “Crystal structure of PMM/PGM: An enzyme in the biosynthetic pathway of *P. aeruginosa* virulence factors.”

This chapter describes determination of the three-dimensional structures of wild-type PMM/PGM and a site-directed mutant, S108A. The architecture of the protein and fold of its four domains are presented in detail. The active site is identified in a cleft of the protein and residues important to catalysis, such as phosphoserine 108 and the metal binding loop, are located. The flexibility of domain 4 is postulated.

Chapter 4 – “Structural basis of diverse substrate recognition by the enzyme PMM/PGM from *P. aeruginosa*.”

Chapter four focuses on structures of PMM/PGM with each of its four substrates, revealing how the enzyme exploits the phosphate group, the conserved structural feature, to utilize these otherwise structurally diverse ligands. Here, the flexibility of domain 4 is demonstrated by closure of the active site cleft around the substrates. In addition, two distinct binding orientations are observed for 1- and 6-phosphosugars.

Chapter 5 – “Roles of active site residues in *Pseudomonas aeruginosa* Phosphomannomutase/Phosphoglucomutase.”

The structures presented in Chapter 4 are used to design site-directed mutants in the active site of PMM/PGM to probe the catalytic reaction. It is postulated that the positive electrostatic environment created by an ensemble of residues in the active site facilitates the catalytic reaction.

The data show that no single residue is absolutely essential for catalysis, including phosphoserine 108.

Chapter 6 – “Structural analysis of intermediate complexes in PMM/PGM.”

Chapter six probes the remaining uncharacterized step of the PMM/PGM reaction: the interaction with its bisphosphorylated intermediate. In the normal course of the reaction, this intermediate binds to the dephosphorylated state of the enzyme. Our structural analysis shows that the PMM/PGM complex with G16P is highly similar to the enzyme substrate complexes. Furthermore, as part of this study, we isolated a second complex with G16P, bound the phospho-enzyme. Although a “non-productive” complex, this structure has provided unexpected insights into the most interesting feature of the PMM/PGM reaction: the reorientation of the intermediate that occurs between phosphoryl transfers.

Chapter 7 – “Conclusion: Overall significance and future directions”

This chapter explores the implications of the work presented and proposes experimental avenues for the future.

References

1. Rocchetta, H.L., L.L. Burrows, and J.S. Lam, *Genetics of O-antigen biosynthesis in Pseudomonas aeruginosa*. Microbiol. Mol. Biol. R., 1999. **63**(3): p. 523-553.
2. Govan, J.R.W. and V. Deretic, *Microbial pathogenesis in cystic fibrosis - Mucoicid Pseudomonas aeruginosa and Burkholderia cepacia*. Microbiol. Rev., 1996. **60**(3): p. 539-574.
3. Regni, C., P.A. Tipton, and L.J. Beamer, *Crystal structure of PMM/PGM: an enzyme in the biosynthetic pathway of P. aeruginosa virulence factors*. Structure, 2002. **10**(2): p. 269-79.
4. Snook, C.F., P.A. Tipton, and L.J. Beamer, *Crystal Structure of GDP-Mannose Dehydrogenase: A Key Enzyme of Alginate Biosynthesis in P. aeruginosa*. Biochemistry, 2003. **42**(16): p. 4658-68.
5. Schlichtman, D., A. Kavanaugh-Black, S. Shankar, and A.M. Chakrabarty, *Energy metabolism and alginate biosynthesis in Pseudomonas aeruginosa: role of the tricarboxylic acid cycle*. J Bacteriol, 1994. **176**(19): p. 6023-9.
6. Olvera, C., J.B. Goldberg, R. Sanchez, and G. Soberon-Chavez, *The Pseudomonas aeruginosa algC gene product participates in rhamnolipid biosynthesis*. FEMS Microbiol Lett, 1999. **179**(1): p. 85-90.
7. Shackelford, G.S., C.A. Regni, and L.J. Beamer, *Evolutionary trace analysis of the alpha-D-phosphohexomutase superfamily*. Protein Sci, 2004. **13**(8): p. 2130-8.

8. Ray, W.J., Jr., J.W. Burgner, 2nd, and C.B. Post, *Characterization of vanadate-based transition-state-analogue complexes of phosphoglucomutase by spectral and NMR techniques*. *Biochemistry*, 1990. **29**(11): p. 2770-2778.
9. Ray, W.J., Jr., C.B. Post, and J.M. Puvathingal, *Comparison of rate constants for (PO₃⁻) transfer by the Mg(II), Cd(II), and Li(I) forms of phosphoglucomutase*. *Biochemistry*, 1989. **28**(2): p. 559-69.
10. Naught, L.E., C. Regni, L.J. Beamer, and P.A. Tipton, *Roles of active site residues in P. aeruginosa phosphomannomutase/phosphoglucomutase*. *Biochemistry*, 2003. **42**: p. 9946-9951.

CHAPTER 2

CRYSTALLIZATION AND INITIAL CRYSTALLOGRAPHIC ANALYSIS OF PHOSPHOMANNOMUTASE/PHOSPHOGLUCOMUTASE FROM *PSEUDOMONAS AERUGINOSA*

Reproduced with permission from Regni, C.A., P.A. Tipton, and L.J. Beamer,
*Crystallization and initial crystallographic analysis of
phosphomannomutase/phosphoglucomutase from Pseudomonas aeruginosa*. Acta
Crystallogr. D, 2000. **56**(Pt 6): p. 761-2. Copyright 2000 International Union of
Crystallography. (<http://journals.iucr.org/>).

Abstract

The enzyme phosphomannomutase/phosphoglucomutase (PMM/PGM) catalyzes the conversion of mannose 6-phosphate to mannose 1-phosphate in the second step of the alginate biosynthetic pathway of *P. aeruginosa*. PMM/PGM has been crystallized by hanging drop vapor diffusion in space group $P2_12_12_1$. Crystals diffract to 1.75 Å resolution on a synchrotron X-ray source under cryocooling conditions. PMM/PGM substituted with selenomethionine has been purified and crystallizes isomorphously with the native enzyme. Structure determination by MAD phasing is underway. Because of its role in alginate biosynthesis, PMM/PGM is a potential target for therapeutic inhibitors to combat *P. aeruginosa* infections.

1. Introduction

The infectious bacterium *Pseudomonas aeruginosa* secretes a protective exopolysaccharide called alginate that forms a viscous capsule around the organism. This alginate coating is believed to contribute the bacteria's widespread resistance to antibiotics and its ability to evade the host's immune response (Govan & Deretic, 1996). Chronic *P. aeruginosa* infections are the leading cause of morbidity and mortality in cystic fibrosis patients (Govan & Deretic, 1996), and are also common in cancer, burn, and immunocompromised patients. Because of alginate's role in the pathogenicity of *P. aeruginosa*, enzymes in the alginate biosynthetic pathway are attractive candidates for clinical inhibitors.

Pseudomonad alginate is a linear polymer of (1-4)-linked β -D-mannuronate and α -L-guluronate residues. Many of the mannuronate residues are O-acetylated at the 2- or 3-position, or both. The alginate biosynthetic pathway as it is currently understood is shown in Fig. 1. PMM/PGM is encoded by the *algC* gene, and catalyzes the conversion of mannose 6-phosphate to mannose 1-phosphate in the second step of the alginate biosynthetic pathway. It is also required for A band lipopolysaccharide biosynthesis where it utilizes glucose 6-phosphate as a substrate. These dual biosynthetic roles for PMM/PGM were confirmed by *algC* mutants that lacked the alginate phenotype and O-side chain and core lipopolysaccharides (Ye *et al.*, 1994). PMM/PGM has a molecular weight of 50,200 Da and is reported to be a monomer in solution (Ye, *et al.*, 1994). It

requires Mg^{2+} for maximal activity, and is activated by glucose-1,6-bisphosphate. The reaction is believed to proceed through a phosphoenzyme intermediate at serine 108 (Shankar *et al.*, 1995).

P. aeruginosa PMM/PGM shows only moderate sequence identity (30-50%) with other bacterial phosphomannomutases and phosphoglucomutases, and very little homology with the rabbit muscle PGM which has been structurally characterized by Ray and coworkers (Ray *et al.*, 1993). *P. aeruginosa* PMM/PGM differs from rabbit muscle PGM in a number of its functional characteristics as well, including its substrate specificity and metal ion preference (Ye, *et al.*, 1994).

2. Materials and Methods

The *algC* gene was amplified from *Pseudomonas aeruginosa* strain PAO1 by the polymerase chain reaction using primers based on the published sequence. The forward primer incorporated an *NdeI* site and the reverse primer incorporated a *BamHI* site, so the amplicon could be cloned directly into the pET3-a (Novagen) vector. The resulting construct was used to transform BL21(DE3) cells. Freshly transformed cells were grown to an optical density at 600 nm of ~0.6 and expression of the *algC* gene was induced by the addition of IPTG to a final concentration of 0.4 mM. Cells were harvested 4-5 hours after induction and stored at $-78^{\circ}C$ until use. PMM/PGM was purified to homogeneity following the published procedure (Ye, *et al.*, 1994). Approximately 200 mg of purified protein was obtained from 17 g of frozen cell paste. MALDI mass spectrometric analysis

(Mass Consortium, La Jolla, CA) of the purified PMM/PGM indicates two predominant species differing by approximately 77 daltons, consistent with isolation of both phospho- and dephospho-forms of the enzyme (a phosphate group is 79 daltons).

Initial crystallization screens employed conditions found in the Hampton Research Crystal Screen kits 1 and 2. The PMM/PGM solution was at 12-15 mg/ml in 10 mM MOPS buffer, pH 7.0. Crystals grow by hanging drop vapor diffusion from 1.4 M Na,K tartrate, and 100 mM Na HEPES pH 7.5 from drops containing 2 μ l of protein and 2 μ l of well buffer. Crystals grow from heavy precipitate in drops; *de novo* growth time varies widely, from two weeks to four months. Use of micro- and macro-seeding techniques has reliably produced crystals within several weeks. A solution of 40% glycerol and 1.4 M Na,K tartrate was used to cryoprotect the PMM/PGM crystals for low temperature data collection. Crystals were transferred gradually into solutions of increasing glycerol concentration, and were flash-frozen in the nitrogen stream for data collection.

To facilitate structure solution, a selenomethionine (SeMet) substituted PMM/PGM (eight methionine residues) was produced in *E. coli* by growing bacteria in minimal media and in the presence of SeMet and lysine, threonine, phenylalanine, leucine, isoleucine and valine to inhibit methionine biosynthesis (Van Duyne *et al.*, 1993). The SeMet-substituted enzyme was active, and was purified by the same protocol as the wild-type enzyme. Approximately 50 mg of purified protein was obtained from a 2 L culture broth. Incorporation of selenomethionine was verified by MALDI mass spectrometry (data not shown). The SeMet protein did not crystallize *de novo*, but native PMM/PGM

crystals were successfully used to seed into SeMet PMM/PGM drops containing the crystallization buffer described above plus 1.0 mM β -mercaptoethanol. SeMet protein concentration was 6 mg/ml for seeding. Small *de novo* SeMet crystals produced from seeding with native crystals were used as seeds to grow larger SeMet PMM/PGM crystals for data collection.

The SeMet PMM/PGM crystallizes isomorphously with the native enzyme. Although the SeMet PMM/PGM crystals were quite sensitive to radiation damage at room temperature (lifetime on rotating anode < 1 hour), the cryoprotectant used for the native crystals is also suitable for the SeMet crystals and extends crystal lifetime in the beam indefinitely. Presumably because of their smaller size, the SeMet PMM/PGM crystals diffract to a nominal resolution of 2.2 Å on a synchrotron X-ray source.

3. Results and Discussion

A native data set to 1.75 Å for PMM/PGM was collected from a single crystal on beamline X8C at Brookhaven National Laboratory (Table 1 and Fig. 2). Data were collected at approximately -170° C using the cryoprotectant described above. X-ray wavelength was 0.98 Å, oscillation angle was 0.75° , and crystal to detector distance 130 mm. Crystals belong to space group $P2_12_12_1$ and have unit cell parameters of $a=70.89$, $b=73.02$, $c=92.57$ Å, $\alpha=\beta=\gamma=90^{\circ}$. Data were processed using DENZO and Scalepack (Otwinowski & Minor, 1997). Packing density calculations for PMM/PGM indicate $V_m=2.43$ Å³ Da⁻¹ assuming one molecule of PMM/PGM per asymmetric unit. This

corresponds to a solvent fraction of about 49%, a typical value for protein crystals (Matthews, 1968).

The protein of known structure most closely related to PMM/PGM is PGM from rabbit. Several models derived from rabbit PGM structure were used for molecular replacement attempts. However, no solution was found, presumably due to the low sequence identity between the two proteins (~21%). Structure determination efforts will proceed via the SeMet PMM/PGM crystals that were recently used in MAD experiments at beamline X8C at Brookhaven National Laboratory. Refinement of PMM/PGM with 1.75 Å native data should provide an excellent starting point for studies of enzyme-inhibitor complexes.

This work was supported by a grant from the Children's Miracle Network of the University of Missouri Health Sciences Center. We acknowledge Cicely Miederhoff for assistance with crystallization trials. We thank Leon Flaks and the support staff of beamline X8C at the National Synchrotron Light Source of Brookhaven National Laboratory for providing synchrotron facilities.

FIGURES

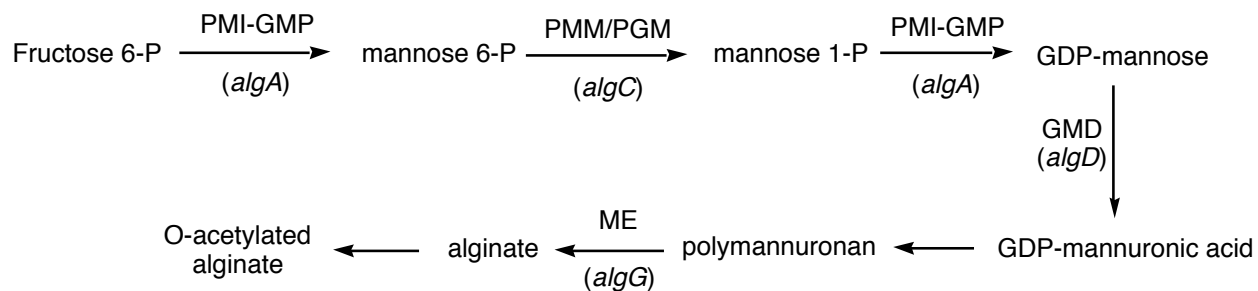


Figure 1. Biosynthetic pathway of alginate in *P. aeruginosa*. Several key enzymes are indicated: **PMI-GMP**, phosphomannose isomerase-GDP pyrophosphorylase; **PMM/PGM**, phosphomannomutase/phosphoglucomutase; **GMD**, GDP-mannose dehydrogenase; **ME**, mannuronan epimerase. Genes encoding each enzyme are indicated in italic.

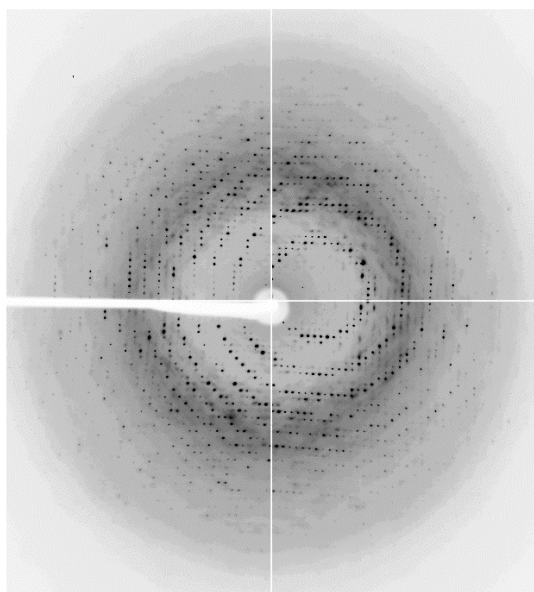


Figure 2

11

Figure 2. Diffraction pattern of native PMM/PGM crystals at beamline X8C at the National Synchrotron Light Source.

References

1. Govan, J. R. & Deretic, V., (1996). *Microbiol. Rev.* **60**: 539-74.
2. Matthews, B. W., (1968). *J. Mol. Biol.* **33**: 491-7.
3. Otwinowski, Z., and Minor, W., (1997). *Methods in Enzymol.* **276**: 307-326.
4. Ray, W. J., Jr., Post, C. B., Liu, Y. & Rhyu, G. I., (1993). *Biochemistry* **32**: 48-57.
5. Shankar, S., Ye, R. W., Schlichtman, D. & Chakrabarty, A. M., (1995). *Adv. Enzymol. Relat. Areas Mol. Biol.* **70**: 221-55.
6. Van Duyne, G. D., Standaert, R. F., Karplus, P. A., Schreiber, S. L. & Clardy, J., (1993). *J. Mol. Biol.* **229**: 105-24.
7. Ye, R. W., Zielinski, N. A. & Chakrabarty, A. M., (1994). *J. Bacteriol.* **176**: 4851-7.

CHAPTER 3

CRYSTAL STRUCTURE OF PMM/PGM: AN ENZYME IN THE BIOSYNTHETIC PATHWAY OF *P. AERUGINOSA* VIRULENCE FACTORS

Reproduced with permission from Regni, C., L.E. Naught, P.A. Tipton, and L.J. Beamer, *Crystal structure of PMM/PGM: An enzyme in the biosynthetic pathway of P. aeruginosa virulence factors*. Structure, 2002. **10**: p. 269-279. Copyright 2002 Elsevier Science Ltd.

Abstract

The enzyme phosphomannomutase/phosphoglucomutase (PMM/PGM) from *P. aeruginosa* is required for the biosynthesis of two bacterial exopolysaccharides: alginate and lipopolysaccharide (LPS). Both of these molecules play a role in the virulence of *P. aeruginosa*, an important human pathogen known for its ability to develop antibiotic resistance and cause chronic lung infections in cystic fibrosis patients. The crystal structure of PMM/PGM shows that the enzyme has four domains, three of which have a similar three-dimensional fold. Residues from all four domains of the protein contribute to the formation of a large active site cleft in the center of the molecule. Detailed information on the active site of PMM/PGM lays the foundation for structure-based inhibitor design. Inhibitors of sufficient potency and specificity should impair the biosynthesis of alginate and LPS, and may facilitate clearance of the bacteria by the host immune system and increase the efficacy of conventional antibiotic treatment against chronic *P. aeruginosa* infections.

Introduction

Pseudomonas aeruginosa is a widespread Gram-negative bacterium, commonly found in fresh water and soil. It is also a deadly opportunistic human pathogen that causes life-threatening infections in immuno-compromised hosts, including cystic fibrosis (CF), burn, and chemotherapy patients [1]. *P. aeruginosa* is a leading cause of hospital-acquired infections, and one of the top three pathogens responsible for sepsis by Gram-negative bacteria [2]. Chronic *P. aeruginosa* infections are notoriously difficult to treat due to the organism's ability to grow in a biofilm and become resistant to a wide variety of antibiotic agents.

CF patients are highly susceptible to lung infections by *P. aeruginosa*, presumably due to the unique environment of the CF lung. The CF genetic defect impairs the ability of patients to clear bacteria from their airways, and may also decrease the effectiveness of the immune response. Many CF patients have a history of colonization by *P. aeruginosa* that spans more than a decade, and the establishment of chronic lung infections by *P. aeruginosa* is correlated with a poor prognosis for these patients. Despite the development of new anti-infective agents and intensive drug therapy, these infections are still the most common cause of morbidity and mortality in CF patients [3].

Several factors affecting the virulence of *P. aeruginosa* infections have been identified, including exopolysaccharides such as alginate [3] and LPS [2]. One of the hallmarks of chronic *P. aeruginosa* infections in the CF lung is the conversion of the bacterium to a mucoidy (alginate-producing) phenotype [3]. Alginate is a repeating polymer of β -D-mannuronate and α -L-guluronate residues, and is secreted by the bacteria in response to environmental stress (dehydration, nitrogen starvation, etc.) and during the formation of bacterial biofilms [4]. The viscous alginate coating is believed to play a role in the organism's resistance to antibiotics and also to reduce the effectiveness of the host immune system. Alginate is present in sputum samples of CF patients and antibodies to alginate are present in all CF patients with chronic *P. aeruginosa* infections [3].

Changes in LPS phenotype are also associated with the development of chronic *P. aeruginosa* infections [2]. LPS is a complex glycolipid found in the outer membrane of gram-negative bacteria. It has a tripartite structure consisting of a hydrophobic lipid-containing region that is part of the bacterial membrane, central core polysaccharides, and repeating O-antigen polysaccharide chains that extend out from the surface of the cell. In chronic *P. aeruginosa* infections, the composition of the O-antigen polysaccharide changes

from a heteropolymeric (B-band) to a homopolymeric (A-band) form. Although not fully understood, the conversion to A-band phenotype appears to be beneficial to the bacterium by reducing its immunogenicity and sensitivity to certain antibiotics [2]. LPS is the major antigen component of immune complexes isolated from the sputum of CF patients with chronic *P. aeruginosa* [5]. In addition, because of its ability to over-stimulate the immune system, the presence of LPS in the lungs likely contributes to the cycle of infection/inflammation that eventually leads to irreversible lung damage in the CF patient.

In *P. aeruginosa*, the biosynthetic pathways of alginate and LPS share several common steps (Fig. 1). The *algC* gene is strategically placed in these pathways, leading to the production of the key intermediate GDP-mannose which is necessary for both alginate and LPS A-band polysaccharide biosynthesis. *AlgC* encodes the enzyme PMM/PGM which has both phosphomannomutase and phosphoglucomutase activities. It was originally identified by complementation as essential for alginate biosynthesis [6] where it catalyzes the conversion of mannose 6-phosphate to mannose 1-phosphate. More recently, it was found that PMM/PGM has an additional role in LPS biosynthesis, converting glucose 6-phosphate to glucose 1-phosphate in the production of sugar precursors destined for the core region of LPS [7, 8]. Homologs of several enzymes in the LPS and alginate biosynthetic pathways have been identified in *P. aeruginosa* [9], and therefore these steps may be difficult targets for inhibition. However, there is no known homolog of PMM/PGM. Thus this enzyme appears to play a key role in the production of both of these bacterial virulence factors in *P. aeruginosa*.

The relevance of PMM/PGM to the pathogenesis of *P. aeruginosa* infections has been shown using an *algC* knockout strain. Mouse models of infection show this strain is less virulent than the wild-type bacteria [10, 11]. In addition, *algC* is up-regulated as a response to bacterial attachment to a surface during biofilm formation [12]. Cells unable to

up-regulate *algC* are less able to remain attached to a glass surface in *in vitro* biofilm models. While not an essential enzyme for the bacteria, effective inhibition of PMM/PGM may be expected to interfere with alginate and LPS production, and impair biofilm maintenance, thereby making the bacteria more susceptible to the host immune response and traditional antibiotic therapy.

PMM/PGM is part of a family of phosphohexomutases that catalyze intramolecular phosphoryl transfer by way of a phosphorylated enzyme intermediate [4]. The protein has 463 residues and exists as a monomer in solution. The active form of the enzyme is phosphorylated at Ser108 and requires Mg^{2+} for full activity. The activator glucose 1,6-bisphosphate is required to maintain the enzyme in the phosphorylated state. The mechanism of PMM/PGM is believed to closely parallel that of a related protein: phosphoglucomutase (PGM) from rabbit muscle. PMM/PGM shows limited but significant sequence identity to rabbit PGM that has been extensively characterized by Ray and colleagues ([13] and references therein). After the initial transfer of the phosphoryl group from the enzyme, the reaction of both enzymes is believed to proceed via diffusional reorientation of the bis-phosphorylated intermediate in the active site, followed by a second phosphoryl transfer to regenerate the phosphorylated form of the enzyme.

The dual roles of PMM/PGM in alginate and LPS biosynthesis of *P. aeruginosa* make the enzyme an attractive target for inhibitor design. However, little is known about the details of the enzymatic mechanism or protein structure that will aid such design efforts. To this end, we have initiated detailed mechanistic and structural studies of the protein, and report here the determination of the three-dimensional structure of the wild-type protein and an active site mutant of the enzyme.

Results

Structure determination and description

The crystal structure of PMM/PGM from *P. aeruginosa* was determined by MAD phasing using crystals of the selenomethionine-substituted protein and has been refined to 2.2 Å. This model was used to solve the structure of an active site mutant (S108A) of the enzyme that has been refined to 1.75 Å resolution (see Experimental procedures and Tables 1 and 2). Comparison of the selenomethionine-substituted wild-type enzyme structure with that of the S108A mutant shows that there are no significant differences attributable to the substitution of selenomethionine for methionine, and that the structure of the S108A mutant is very similar to the wild-type protein with the exception of the mutated residue. In the following sections, we describe features of the wild-type protein, and indicate differences with the S108A mutant when relevant.

PMM/PGM contains four domains (Fig. 2a) of approximately equal size, arranged in an overall “heart” shape. Each domain contains both α -helices and β -sheet. Domains 1-3 share a common topological core: a mixed α/β structure consisting of a four-stranded β -sheet sandwiched between two α -helices (Fig. 2b, c). The strands in the β -sheet are in the order 2134, with strand 4 antiparallel to the rest. Although they are structurally similar, the amino acid relationship between the three domains is undetectable by standard sequence alignment methods: the amino acid identity between any two superimposed pairs is less than 20% (based on structural superposition with MAPS [14] using the C_{α} pairs automatically aligned by this program). Each domain has several insertions relative to the common core: domain 1 has two additional α -helices and three extra β -strands; domain 2 has one extra α -helix; and domain 3 has three additional α -helices and one extra β -strand. Despite the common topology and 3-dimensional fold of domains 1-3, the PMM/PGM

structure does not contain a pseudo 3-fold axis; however, an approximate 2-fold axis (176° rotation) is found between domains 1 and 3. While it appears the first three domains of the protein arose from an ancient gene duplication event, domain 4 is unrelated structurally to the others, and is a member of the TATA-box binding protein-like fold superfamily [15]. It consists of a 4-stranded antiparallel β -sheet flanked by two α -helices, and two short β -strands.

The four domains of PMM/PGM pack as a relatively compact structure. The polypeptide proceeds through each domain sequentially, with only one chain crossing between domains. Extensive contact surface areas of 993 and 1300 \AA^2 (15 and 21% respectively, of their total surface areas) are found between domain pairs 1-2 and 2-3. Domains 1 and 3 also have a significant interface area of 547 \AA^2 despite the intervening domain 2. Domain 4 has less extensive interactions with the rest of the molecule: 660 \AA^2 total shared surface area with domain 3, involving only 11% of its total surface area. The 3-4 domain interface also stands out for its high gap volume, a measure of the complementarity of the interacting surfaces [16]. Its gap volume index [gap volume (\AA^3)/interface accessible surface area (\AA^2)] is 2.39 \AA , more than twice that of the other two consecutive domain interfaces, and is similar to those typically found in dimeric protein interfaces [16]. The low surface complementarity of this interface, combined with its relatively small surface area, leads us to suggest conformational flexibility between domain 4 and the rest of the molecule. Flexibility between domain 4 and the rest of the protein has also been indicated for rabbit PGM [17].

The crystal structure shows that the active site of PMM/PGM is found in the center of the protein, in a deep cleft formed by atoms in 67 residues distributed across all four domains. The cleft has a solvent accessible surface area of approximately 1100 \AA^2 in the wild-type protein [18]. Topologically equivalent loops in domains 1-3 (between strands 3

and 4 of the conserved core) point toward the active site, clustering residues involved in enzyme activity/specificity (see following sections). Residues from domain 4 also contribute to the cleft, and are primarily located on strands 3 and 4 of the antiparallel β -sheet. Although the overall charge of the protein is negative (calculated pI = 5.24), the active site has a net positive charge as would be expected for binding of its anionic substrate and intermediate (Fig. 2d).

Structural relatives

The overall fold of PMM/PGM is found in one other protein of known structure that of PGM from rabbit muscle. This protein is involved in the synthesis and breakdown of glycogen, and is an essential enzyme in humans. Rabbit muscle PGM has been extensively characterized, both mechanistically and structurally [13, 17, 19, 20]. As its name implies, PGM is highly specific for glucose-based substrates, showing a 6000-fold preference for glucose over mannose in the biosynthetic direction of the reaction [21]. This contrasts with pseudomonad PMM/PGM that shows equal preference for glucose- and mannose-based substrates [22]. The two enzymes also have differing metal-binding specificity: both require Mg^{2+} for maximum activity, but rabbit PGM is also activated by Co^{2+} and Ni^{2+} .

The relationship of the two proteins was originally shown by amino acid sequence comparisons that clearly identify the conservation of important functional elements, despite a relatively low overall sequence identity (22%). A structural alignment of the two proteins (Fig. 3) shows that they share the same overall heart shape and four-domain architecture. Since PGM has a total of 561 residues, 98 more than PMM/PGM, it has several additional secondary structural elements; these tend to fall on the periphery of the molecule, distant from the active site. The two structures (3PMG and 1K35 PMM) can be aligned with a

root-mean-square (rms) deviation of 1.8 Å for 312 C_α residues [14]. This alignment shows that critical residues in the active site are in very similar positions, including the active site serine, metal-binding loop, and phosphate-binding site (see following section).

Multiple structures of PGM are available in the PDB, including four with various metal ions (3PMG, 1VKL, 1LXT, and 1JDY) and two in complex with an intermediate or inhibitor (1C4G, 1C47). With the exception of 3PMG that has been refined to 2.4 Å [17], the resolution of all of these structures is 2.7 Å. The two PGM complexes, although deposited, have not been described in a publication. One of these is a complex with the reaction intermediate glucose 1,6-bis-phosphate (G16P); the other is a covalent complex with the inhibitor glucose 1-phosphate, 6-vanadate (G1P6V). Although the overall sequence homology of PMM/PGM with rabbit PGM is relatively low, many residues involved in the active site are highly conserved, and these complexes can provide approximate models for binding of substrate to PMM/PGM. References to these PGM structures are included in the following sections when relevant.

Details of active site

Sequence comparisons and biochemical and mutational analyses have indicated residues important for the activity and specificity of PMM/PGM [4]. These can be grouped into four distinct regions of the protein: 1) the active site serine (residue 108) involved in phosphoryl group transfer; 2) a metal-binding loop (residues 242-246) that chelates a Mg²⁺ ion required for activity; 3) a sugar-binding loop (residues 324-328) predicted to contain residues that distinguish between related sugar substrates; and 4) the distal phosphate-binding site (containing Arg421) believed to interact with the bis-phosphorylated reaction intermediate. Since the reaction intermediate contains two phosphate groups (and therefore the enzyme has two phosphate-binding sites), we will hereafter refer to them as either

proximal (near Ser108) or distal (opposite end of active site near Arg421). In the following section, we describe the structural elements of each of these regions in detail, and conclude with a description of the binding of a tartrate molecule in the active site of the S108A mutant structure.

Active site serine

PMM/PGM catalyzes reversible intramolecular phosphoryl transfer from the 1 to the 6 position of its sugar substrates by way of a phosphoenzyme intermediate. Sequence comparisons with rabbit PGM suggested Ser108 as the site of phosphorylation and mutagenesis experiments have confirmed its important role in enzyme activity [22]. In the crystal structure of the wild-type PMM/PGM, Ser108 appears to be fully phosphorylated as judged by electron density maps (Fig. 4a); the phosphorylation state of the enzyme is supported by mass spectrometry (data not shown). Two oxygens of the phosphate group interact with other residues in the active site: one serves as a ligand to the bound metal ion (see next section), and another forms a hydrogen bond with the side chain of the neighboring residue, His109. The loop containing Ser108 is quite well defined in electron density maps. However, the backbone dihedral angles of this residue fall in the disallowed region of a Ramachandran plot ($\Phi = 50^\circ$, $\Psi = -115^\circ$) defining a rare type II' β -turn. Presumably this unusual conformation reflects a functional requirement for maintaining this residue in a specific orientation for enzyme activity. This conformation is retained in the S108A mutant structure where the backbone angles of Ala108 are $\Phi = 60^\circ$ and $\Psi = -115^\circ$, despite the fact that it no longer acts as a ligand for the metal.

Metal-binding loop

In PMM/PGM, a bound Mg^{2+} ion is required for full activity and presumably serves to activate the phosphate group of Ser108 for transfer by stabilizing negative charge on the phosphoryl group or leaving group during catalysis. The role of the metal ion in activation

has been extensively characterized for rabbit PGM [23]. In the crystal structure of wild-type PMM/PGM, phosphoserine 108 and the metal-binding loop are in close proximity to each other, with a terminal oxygen atom from the phosphorylated serine providing one ligand for the bound metal ion (Fig. 4b). Three other metal ligands come from the carboxylate side chains of aspartates 242, 244, and 246. The metal ion in the crystal structure is believed to be Zn^{+2} , rather than Mg^{+2} that is required for enzymatic activity (see Experimental Procedures). In the S108A mutant of PMM/PGM, the phosphoserine residue is absent, and a new ligand replaces it in the crystal structure: an oxygen atom from the carboxylate group of a tartrate molecule, presumably arising from the precipitant used for crystallization: 1.4 M Na, K tartrate. Ligand bond distances for the wild-type and mutant structures are given in Table 3 and are consistent with those seen in other Zn^{2+} binding sites [24, 25]. In both structures, the metal-ligand geometry is approximately tetrahedral.

Sugar-binding loop

PMM/PGM belongs to a sub-class of phosphohexomutases that are primarily found in bacteria and often function in the synthesis of exopolysaccharides. This sub-class demonstrates dual substrate specificity for glucose and mannose, which are epimers at the C2 position of the sugar ring. They have a conserved sequence motif in domain 3, 324-GEMS(G/A)-328, which has been postulated to act as a sugar-binding loop and determine the specificity (or lack thereof) for glucose versus mannose [4]. In the PMM/PGM structure, the loop containing these residues is solvent accessible and forms part of the active site cleft (Fig. 4b). The side chains of Glu325, Ser327, and His329, another highly conserved residue, point toward Ser108 and the metal-binding loop, and should be available to interact with bound substrates.

The sugar-binding loop in domain 3 has also been called the “specificity loop” [17] and was proposed to determine the relative binding affinity of glucose versus mannose

for members of the phosphohexomutase family. Enzymes with a strong preference for glucose, like rabbit PGM, have a different sequence signature, 374-GEESFG-379, on the equivalent loop in domain 3 [4]. However, comparison of the PMM/PGM structure with that of PGM and analysis of the residues in PGM complexes that interact with bound sugars, suggest that this loop alone is probably insufficient for determining the sugar binding affinities. In the rabbit PGM complexes, residues from the sugar-binding loop do indeed contact the bound sugars: the side chains of Glu375 and Ser377 (analogous to Glu325 and Ser327 in PMM/PGM) are within hydrogen bonding distance of O3 on the glucose ring. However, no contacts are apparent between residues on the sugar-binding loop and O2, the site at which mannose and glucose are epimers. In the PGM complex with G16P, a residue (Thr356) from a different loop in domain 3 does form a hydrogen bond with O2 of the bound sugar. However, since PMM/PGM has an identical residue at the equivalent position (Thr306), the structural determinants for the high specificity of PGM for glucose-based substrates remain unclear.

Distal phosphate-binding site

After phosphoryl transfer from Ser108, the active site of PMM/PGM must temporarily accommodate an intermediate with two phosphate groups at positions 1 and 6 of the sugar. A cluster of positively charged, conserved residues is found at the end of the active site distal to Ser108. These include Arg421 and Arg432 from domain 4, and also Lys285 from domain 3. Mutagenesis data for one of these residues, Arg421, reveals a crucial role in enzyme activity. The mutant strain 8858 of *P. aeruginosa* was isolated as deficient in alginate production [6]. This strain shows a single mutation in the *algC* gene, changing residue 421 of PMM/PGM from an arginine to a cysteine. Kinetic data (P. Tipton, unpublished data) shows that the R421C mutant of PMM/PGM has a K_m for glucose 1-phosphate of 20 μM , several-fold higher than the K_m of the wild-type enzyme. However, the kinetic parameters V/K and V_{max} are dramatically reduced, suggesting that the

primary effect of the mutation is not on substrate binding.

In the crystal structure of PMM/PGM, Arg421 is approximately 14 Å away from Ser108 and the metal-binding loop. The two phosphate groups on G16P are separated by approximately 10 Å. Thus, a small conformational change, such as a rotation of domain 4, could position this residue for binding of the intermediate. The important role of Arg421 is supported by its high sequence conservation with other phosphohexomutases and also by structural data on rabbit PGM. In the PGM complex with G16P, the analogous residue (Arg502) is 3.4 Å from the 1-phosphate group of the sugar. However, in the PGM complex with inhibitor G1V6P, Arg514 (analogous to Arg432 in PMM/PGM) appears to make the best interaction with this phosphate group (2.4 Å) with a second contact mediated by Thr18 from domain 1. Therefore, it seems likely that other residues in PMM/PGM, like Arg432 and possibly residues in other domains, may also be important in forming the distal phosphate-binding site.

Binding of tartrate to S108A mutant

Attempts to observe a PMM/PGM complex with substrate or intermediates by X-ray crystallography have not yet been successful, possibly due to the high concentration (>1 M) of Na, K-tartrate necessary for crystallization. However, in the S108A mutant structure, a tartrate molecule binds in the active site, providing the fourth ligand for the bound metal ion in lieu of phosphoserine 108. Tartrate is a four-carbon carbohydrate, with carboxylate groups at C1 and C4, and hydroxyl groups at C2 and C3. While its presence in our structure was fortuitous (due to its role as precipitant in crystallization), tartrate may serve as a useful scaffold for future efforts at inhibitor design.

Multiple interactions are found between the S108A mutant enzyme and the bound tartrate (Fig. 4c). In the absence of phosphoserine 108, an oxygen from a carboxylate

group of tartrate provides the fourth ligand for the bound metal ion, completing its tetrahedral coordination sphere. In total, five of the six tartrate oxygens appear to interact with the protein. Direct hydrogen bonds to tartrate are mediated by the side chains of four residues: Lys118, Arg247, His 308, and His 329. An additional residue, Asp18, is involved in a water-mediated contact. Although PMM/PGM was crystallized in a mixture of (+/-) tartrate, only the (+) stereoisomer, in the energetically favorable trans conformation, is found in the active site, indicating some specificity of binding. Modeling of the (-) stereoisomer indicates that while it could still coordinate the metal ion and avoid steric conflicts with protein residues, it would be unable to make the additional contacts with Lys118 and His329, although it could potentially pick up a new contact with the side chain of His109.

Although tartrate is smaller than the 6-carbon substrates of the enzyme, and linear rather than cyclic, it may make some interactions analogous to those with its glucose or mannose-based substrates. In the PGM complexes, the residues analogous to Lys118 and Arg247 (Lys129 and Arg292) both contact the proximal phosphate/vanadate group of the bound intermediate/inhibitor. An additional residue in PGM, Lys388, is in a spatially similar position to His329 in PMM/PGM, and also contacts the proximal phosphate/vanadate group. His308 of PMM/PGM, however, is most closely aligned with a partially buried tryptophan in rabbit PGM that makes no contacts with bound sugars. Therefore, with the exception of His308, residues of PMM/PGM involved in binding tartrate seem to be equivalent to a subset of those used by PGM to bind its physiologically-relevant ligands.

Implications for enzyme mechanism

In alginate and LPS biosynthesis, PMM/PGM catalyzes the transfer of a phosphoryl group from the 6- to the 1-position of mannose or glucose-based substrates

(Fig. 5). Based on the well-studied mechanism of rabbit PGM, the reaction of PMM/PGM has been proposed to proceed through the following steps: 1) binding of mannose or glucose 6-phosphate to the active (phosphorylated) state of the enzyme; 2) transfer of the enzyme phosphoryl group from Ser108 to the 1-position of the sugar substrate, creating a bis-phosphorylated intermediate; 3) diffusional reorientation of the intermediate in the active site placing the phosphoryl group at position 6 near the active site serine; and 4) regeneration of the phospho-enzyme by transfer of the phosphoryl group at position 6 of the sugar back to Ser108. Salient features inherent to this mechanism include a key role for Ser108 in phosphoryl transfer, and as-yet-unidentified residues to assist in general acid/base catalysis. In addition, the mechanism implies significant reorientation of the intermediate in the active site without allowing its release into solution, as well as specific binding of the same substrate in two distinct orientations. Finally, the enzyme must be able to accommodate both glucose and mannose-based substrates. The implications of the crystal structure for these issues are discussed below.

The proposed mechanism for PMM/PGM predicts a critical role for Ser108 in phosphoryl transfer during catalysis. Indeed, the presence of an active site serine is strongly conserved in members of the phosphohexomutase family, including rabbit PGM, and the crystal structure of the wild-type protein confirms that this residue is in fact phosphorylated. Therefore, it was surprising to find that site-directed mutants of this residue (S108A and S108V) retain significant catalytic activity (V_{\max} and V/K approximately 5% of wild-type) [22]. Although diminished, this activity is substantially more than that expected after removal of a catalytically “required” residue. Furthermore, like the wild-type enzyme, the S108A mutant shows substrate inhibition and requires G16P as an activator, implying that a phosphorylated residue on the enzyme is still involved in activity. The crystal structure suggests that the residue adjacent to Ser108, His 109, may be a candidate for an alternative phosphorylation site. In the wild-type structure, the δN of

His109 is 3.0 Å from the O1P of phosphoserine 108. Manual rotation of this side chain can bring the εN of His109 to within 1.2 Å of the O1P atom of phosphoserine and to within 3.0 Å of the bound Zn⁺² ion. Thus it seems fairly small structural changes, like side chain rotation or a minor shift of the protein backbone, could position His109 for a role in catalysis. BLAST [26] searches of Genbank reveal that a related PMM/PGM from *Xylella fastidiosa* (44% identical to the *P. aeruginosa* enzyme) completely lacks the conserved active site serine; it is replaced by a glycine. However, this protein retains a histidine at the position equivalent to 109, and also has additional histidines at positions 110 and 112 (residue numbers refer to the *P. aeruginosa* enzyme).

The structure of PMM/PGM provides clues about other residues important for activity. The proposed mechanism for the enzyme specifies a role for a general base in initiating transfer of the phosphoryl group from Ser108 to the substrate, through abstraction of a proton from the 6-hydroxyl group of the sugar. Since no direct structural information for a substrate or inhibitor is yet available, we have identified possible candidates based on their location in the active site and proximity to the bound intermediate/inhibitor in superimposed PGM complexes. Two residues in PMM/PGM stand out as possible candidates for this role: His308 and His329. As noted previously, both of these residues are in the active site cleft and interact with the bound tartrate molecule in the S108A mutant structure. In the PGM complexes, the ζN of Lys388 (analogous to His329) is 3.2 Å from O6. Without a bound substrate or intermediate in the active site, it is impossible to precisely define the position of O6, and other residues in its likely vicinity include Arg20 and Arg247. They may also be candidates for the general base.

Following abstraction of its proton, the O6 of mannose/glucose performs a nucleophilic attack on phosphoserine 108, catalyzing transfer of the phosphoryl group to the sugar. This process is aided by a general acid on the protein that donates a proton to the

side chain oxygen of Ser108. We have identified two residues that are strong candidates for the general acid: His109 and Lys118. In the structure of native PMM/PGM, both of these residues appear to be well positioned to act as proton donors. Although His109 is immediately adjacent to Ser108, the geometry of the unusual type II' turn in this loop allows its δN to be positioned 3.0 Å from O1P of the phosphate group of Ser108. A second possibility for the general acid is Lys118, also a highly conserved residue. In the wild-type structure of PMM/PGM, the ζN of Lys118 is 2.9 Å from O3P of the phosphoserine, and 3.1 Å from O2P. In both the wild-type and mutant PMM/PGM structures, the Lys118 side chain appears to be firmly anchored in the active site, making potential additional contacts with non-liganding side chain oxygens of Asp244 and Asp246 in the metal-binding loop. Site-directed mutagenesis supports involvement of residue 109 in catalysis: an H109Q mutant shows diminished activity; characterization of a Lys118 mutant is underway (P. Tipton, unpublished data).

During catalysis, the phosphoryl group on Ser108 is transferred to the substrate, and a second phosphoryl group, approximately 10 Å away, is transferred back to the same serine residue. This implies significant movement on the part of either the enzyme or the intermediate. Nuclear magnetic resonance studies of rabbit PGM [27] support the latter possibility: reorientation of the bis-phosphorylated reaction intermediate in the active site. In order to exchange the positions of the 1- and 6-phosphate groups, a 180° rotation about an axis defined by O3 and C5 of the intermediate is required. In the PGM complexes, it is not possible to perform this rotation without causing significant steric clashes in the active site. Therefore, it appears likely that the intermediate must first dissociate from its high-affinity binding site deep in the active site, diffuse into the larger active site cleft, rotate 180°, and then re-bind in the opposite orientation. This presents an unusual challenge for the enzyme, which must release and re-bind its intermediate without losing it to the bulk solution, and may explain the presence of such a large active site cleft in the enzyme, despite

the small size of its substrates. It also seems likely that conformational flexibility between domain 4 and the rest of the protein may facilitate this process, with domain 4 potentially moving to aid reorientation or prevent dissociation of the intermediate during catalysis. Changes in the volume and surface area of the active site cleft are evident when comparing PGM structures, some of which arise from a rotation of domain 4 relative to the rest of the protein ([17] and L. Beamer, unpublished data).

It has been proposed [20] that electrostatic interactions between the positively charged active site and the anionic substrate/intermediates of PGM may provide sufficient non-directional binding energy to allow the dramatic reorientation of the intermediate without dissociation from the active site. It seems reasonable that the bis-phosphorylated intermediate, which is tetra-anionic, should be more tightly associated with the positively charged active site, than the di-anionic substrates. However, in the proposed mechanism for PGM and PMM/PGM, it is this highly charged intermediate, rather than the substrate, that must dissociate and reorient in the active site, which is seemingly in conflict with its higher binding affinity. Therefore, the relative roles of electrostatic attraction versus other factors, like potential conformational changes in the enzyme, during catalysis remain to be elucidated.

Implications for inhibitor design

The key role of PMM/PGM in the biosynthesis of virulence factors from *P. aeruginosa* makes it an attractive target for inhibitor design. The underlying function of both alginate and LPS is to form a protective barrier around the bacterium. Disruption of this barrier, or perhaps even small changes in its permeability or stability, may increase the effectiveness of the host immune response and conventional antibiotic therapy. This would be of great benefit to CF patients and others who are colonized by antibiotic resistant strains

of *P. aeruginosa*. In addition, since phosphohexomutases with dual substrate specificity are found primarily in bacteria, inhibitors developed for PMM/PGM in *P. aeruginosa* may serve as models for fighting infections by other organisms such as *Vibrio cholerae*, *Klebsiella pneumoniae*, and *Mycobacterium tuberculosis*.

Several features of PMM/PGM should facilitate design of inhibitors. First, the enzyme's natural substrates are small molecules with well-studied chemistry that should lend themselves to the design and synthesis of related molecules that can function as inhibitors or inactivators. The structure of the S108A PMM/PGM mutant reveals that even simpler carbohydrates like tartrate can effectively utilize residues in the active site for binding, and might serve as a scaffold for design of more potent inhibitors. Second, detailed mechanistic studies of the enzyme mechanism are underway [22] and several molecules with inhibitory activity (e.g., xylose 1-phosphate, 1-deoxyglucose 6-phosphate) have already been characterized ([22] and P. Tipton, unpublished data). Finally, a high-resolution view of the active site is now available, providing detailed three-dimensional information on residues that might be utilized for inhibitor binding.

The potential clinical utility of PMM/PGM inhibitors is complicated by the presence of the essential eukaryotic PGM homolog that is found in many tissues and organs. In particular, the similarity of the active sites of these two proteins provides a challenging, but hopefully not insurmountable, hurdle for inhibitor design. Several important differences between the two enzymes might be exploited to overcome this challenge. PMM/PGM owes its dual substrate activity for glucose and mannose to a lack of specificity for epimers at the C2 position of the sugar. PGM, on the other hand, is highly specific for binding of glucose. Therefore, inhibitors based on mannose stereochemistry should be effectively excluded from binding to PGM. In addition, although the enzymes are clearly related, their overall sequence identity is rather low, so there are many differences in residues in non-conserved

areas of the active site. Some of these have been noted in the discussion (e.g., His308 versus Trp358). It should be possible to design inhibitors that interact with or are excluded by residues that differ between the two proteins. Such a strategy has been successful with more closely related proteins, including the isoforms of human cyclooxygenase [28]. As in that case, since the structures of both enzymes are now known, these and other specific design questions can be addressed in a structural context at atomic detail.

Future studies that will facilitate inhibitor design include continued characterization of enzyme mechanism and additional site directed mutagenesis to confirm our proposed role for many residues in activity. A direct comparison of high-resolution structures of PMM/PGM and PGM in complex with bound substrates/inhibitors should be extremely useful, especially in addressing questions about enzyme specificity and potential conformational changes in the protein during catalysis. Characterization of PMM/PGM complexes has been recalcitrant to date, but alternative approaches to stable complex formation, including the formation of covalent adducts, are under investigation. Eventually, this work should provide a better understanding of the enzyme's ability to efficiently catalyze a reaction with two different substrates, accommodate a dramatic rotation of the reaction intermediate in the active site, and bind the intermediate with high affinity in two different orientations.

Experimental procedures

Crystallization and data collection

Purification and crystallization of native and SeMet PMM/PGM were carried out as previously described [29]. A four wavelength MAD data set and 1.75 Å native data set were collected at -180° C at beam line X8C at the National Synchrotron Light Source of

Brookhaven National Laboratory. Statistics for the X-ray diffraction data are presented in Table 1. A mutant of PMM/PGM (S108A) was crystallized in conditions similar to the wild-type protein [29] and in the same space group ($P2_12_12_1$), but with slightly different cell constants ($a = 71.1$, $b = 71.3$, $c = 94.4$ Å). Macroseeding was used to produce large single crystals for data collection. The S108A crystals diffracted to high resolution and a complete data set was collected using a Rigaku rotating anode generator and R-AXIS IV area detector (Table 1).

Structure solution and refinement

The eight SeMet sites in the PMM/PGM monomer were located and refined using the program SOLVE [30]. Final Z-score and figure of merit were 56.0 and 0.53, respectively. Density modification of phases from SOLVE was performed with DM [31] yielding good quality electron density maps ($fom = 0.79$). Improved maps were obtained from the program SHARP [32] by refining the SeMet sites obtained from SOLVE followed by density modification with SOLOMON [33] using 46% solvent content. These maps revealed the location of several surface exposed loops that were absent in the SOLVE/DM maps. The model was built interactively using O [34] in combination with iterative cycles of simulated annealing and positional refinement, initially with CNS [35], and in the final stages with REFMAC 5.0 [36] with individual, restrained B-factors. Progress was monitored by use of R_{free} and 5% of the data were set aside for cross-validation before refinement. Water molecules were placed automatically by WATPEAK [37] in peaks greater than 3.0σ in $F_o - F_c$ maps and within hydrogen bonding distance to nitrogen or oxygen atoms of the protein. The final model of the wild-type protein contains 455 of the 463 residues, 167 water molecules, one metal ion modeled as Zn^{2+} , and a phosphorylated serine residue (Ser108). No restraints on the metal-ligand geometry were used at any point in refinement. The first seven residues at the NH_2 -terminus could not be unambiguously placed in electron density and were omitted from the model; density for the side chains of

the following residues was also not well-defined and they have been truncated to alanine: L9, P10, R20, V23, T31, R55, K66, E98, E129, E136, I138, K140, N141, S145, V147, R164, E205, K219, E221, K224, K229, K316, Q357, Q397, E400, N402, K415, E439, and K445. Two stretches of more than 10 residues in domain 1, 9-35 and 131-146, have relatively high average B-factors ($>60 \text{ \AA}^2$) and the electron density maps in those regions are not as clear as for the rest of the molecule. Density for the protein backbone is continuous except for small breaks near residues 34 and 215. Refinement of a 1.75 \AA data set of native PMM/PGM (without SeMet) collected at beamline X8C did not proceed well, as judged by the inability to reduce R_{free} below 31%. When the S108A mutant protein became available, it was found to crystallize more reproducibly than the wild-type and to produce crystals with high quality diffraction (better than 1.5 \AA a synchrotron source). Since the S108A data set presented here is of equal resolution and refinement proceeded smoothly (see below), we opted not to further pursue refinement of the native data set. Refinement statistics are shown in Table 2

Rigid-body refinement starting with the 2.2 \AA model of the wild-type SeMet protein was used to refine the structure of the S108A mutant. The model was further refined with CNS [35] and REFMAC [36] to 1.75 \AA using individual, restrained B-factors. Water molecules were selected as above. The final model of the S108A mutant contains 459 protein residues, 435 water molecules, one Zn^{2+} ion, and one tartrate molecule ($\text{C}_4\text{H}_2\text{O}_6$)²⁻ (Table 2). The first four residues at the NH_2 -terminus could not be unambiguously placed in electron density and were omitted from the model; density for the side chains of the following residues was also not well defined and they have been truncated to alanine: K5, Q78, E124, E129, E136, E139, S145, L156, E205, K219, E221, K224, Q357, and E438. Refinement statistics are shown in Table 2.

The metal ion in both PMM/PGM structures has been modeled as Zn^{2+} ion. Initial attempts to use Mg^{2+} in the wild-type model resulted in a 10σ positive density peak at the position of the metal in F_o-F_c maps. Subsequent metal analysis by inductively-coupled argon plasma emission spectroscopy (Chemical Analysis Laboratory, University of Georgia) of both the protein sample and of the tartrate solution used for crystallization revealed numerous contaminating ions, including Ca^{2+} , Zn^{2+} and others at lower levels (data not shown). Based on the known high affinity binding of Zn^{2+} to rabbit PGM [38], and evaluation of the unrestrained metal-ligand bond lengths and geometry, Zn^{2+} was selected for the identity of the ion; this choice eliminated the positive density peak in F_o-F_c maps on the site of the ion, and refined to a reasonable B-factor with full occupancy in both structures.

Both the wild-type and S108A enzyme structures have good geometry, with 89% and 92.3%, respectively, of their residues lying in the most favored regions of the Ramachandran plot [39]. The models were also evaluated by ERRAT [40], 3D-1D profiles [41], SFCHECK [42], and WHAT_CHECK [43]. Figures were prepared with Molscript [44], MOLMOL [45], Bobscript [46], and Raster3D [47].

Biological implications

Enzymes with dual specificity for mannose and glucose-based substrates form a subset of the phosphohexomutase family. PMM/PGM enzymes are found in many different bacteria, and often play a role in the synthesis of bacterial exoproducts. PMM/PGM from *P. aeruginosa* is the first representative of this enzyme sub-family to be structurally characterized, and as such it provides a high quality model for other mutases with dual sugar specificity.

In the case of *P. aeruginosa*, an opportunistic human pathogen, PMM/PGM is an important enzyme in the biosynthesis of both alginate and LPS, two molecules that affect the pathogenicity of the organism. Inhibition of its biosynthetic roles may help make the bacteria more susceptible to the host immune system and conventional antibiotic treatment, providing a new approach to treating CF and other patients with chronic *P. aeruginosa* infections.

The high-resolution structure of PMM/PGM from *P. aeruginosa* provides a detailed view of the enzyme's active site and suggests residues involved in catalysis. The structure of an active site mutant of PMM/PGM reveals multiple interactions with a bound tartrate molecule that may serve as a useful scaffold for future efforts at inhibitor design. Together with the mechanistic and mutagenesis studies already underway, these structures provide new insights into the details of the enzymatic reaction and set the stage for structure-based inhibitor design.

Acknowledgments

We acknowledge Leon Flaks and the staff of beam line X8C of the National Synchrotron Light Source of Brookhaven National Laboratory for synchrotron time and technical expertise. This work was supported by NIH grant GM59653 and by a University of Missouri Research Board grant. We thank Melissa Myers for assistance with protein purification. We are grateful to John Burgner for alerting us to the high affinity binding of rabbit PGM to Zn^{2+} .

Accession numbers

The structures of wild-type PMM/PGM and the S108A mutant have been deposited with the Protein Data Bank and assigned the codes 1K35 and 1K2Y, respectively.

Figures

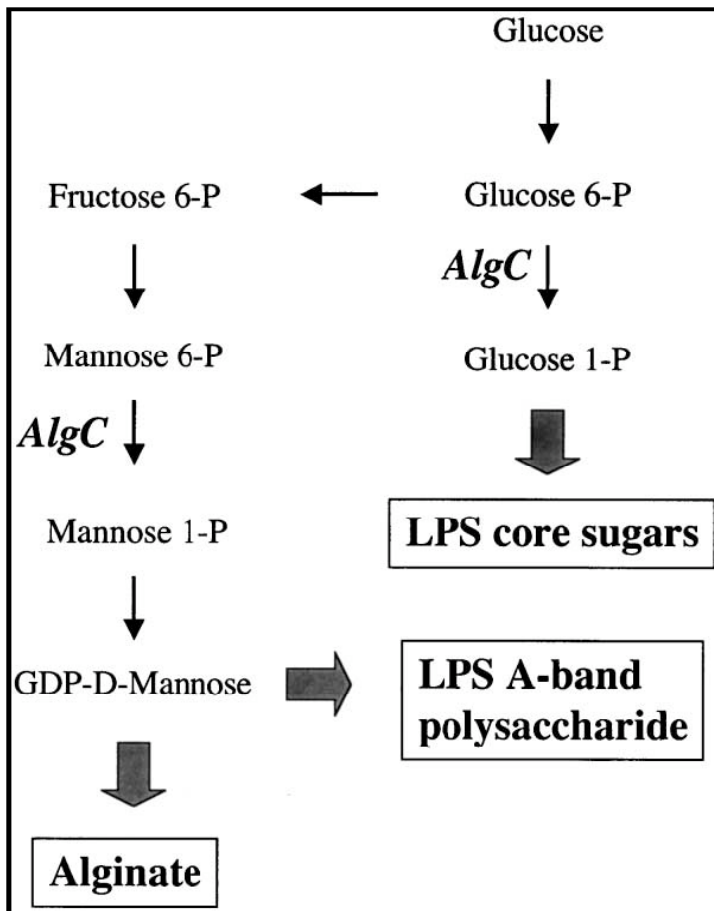


Fig. 1. A schematic illustrating the role of PMM/PGM from *P. aeruginosa* in the overlapping biosynthetic pathways of alginate and LPS. The enzyme catalyzes the conversion of mannose 6-phosphate to mannose 1-phosphate in the second step in the biosynthesis of alginate, and also in the production of A-band polysaccharide of LPS. A similar conversion of glucose 6-phosphate to glucose 1-phosphate is also catalyzed by PMM/PGM and produces sugars for the core region of LPS.

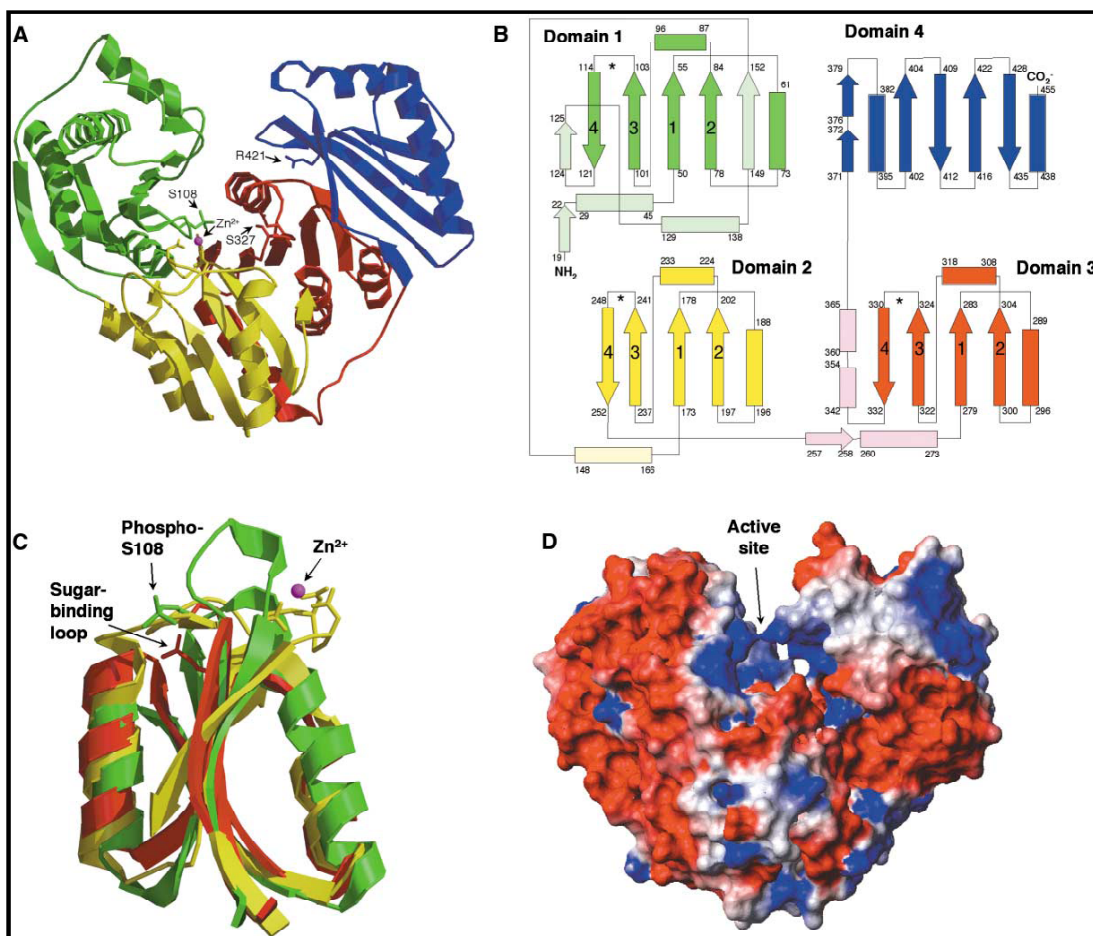


Fig. 2. **a)** Ribbon diagram of PMM/PGM colored by domain. Domain 1 (residues 1-153) is shown in green, domain 2 (residues 154-256) in yellow, domain 3 (residues 257-368) in red, and domain 4 (residues 369-463) in blue. Residues involved in enzyme activity/specificity are shown as sticks and highlighted with numbered arrows: 1) active-site phosphoserine (Ser108), 2) metal-binding loop (Zn^{2+} shown as magenta sphere), 3) Ser327 in the sugar-binding loop; 4) residue Arg421 in the distal phosphate-binding site.

b) Topology diagram of PMM/PGM, showing each domain in the same colors used in a). Helices are indicated by rectangles, and β -strands by arrows; strands that form a β -sheet are shown adjacent to one another. In domains 1-3, the four β -strands in the common topological core are numbered, and the loop between strands 3 and 4 is marked with an asterisk. Helices and strands that are not part of the common core are shown in lighter

colors. The α -helix preceding strand 1 of the common core is divergent in its three-dimensional orientation was therefore not included as part of the motif.

c) Superposition of C_α atoms in the common core regions of domains 1-3 using the same colors as in a). The 4-stranded β -sheet is in the center sandwiched between two conserved α -helices. The side chains of residues on the loop between strand 3 and 4 are shown as a stick models; residues outside of the core regions have been omitted for clarity. The rms deviation between core pairs is 1.39, 1.57, and 1.47 \AA^2 for domains 1-2, 1-3, and 2-3 (for 46, 29, and 42 C_α pairs, respectively) [14].

d) Electrostatic surface potential calculated by MOLMOL [45] of PMM/PGM showing the cluster of basic charge in the active site cleft. Red indicates negative charge; blue indicates positive. Protein is shown in the same orientation as **a**).

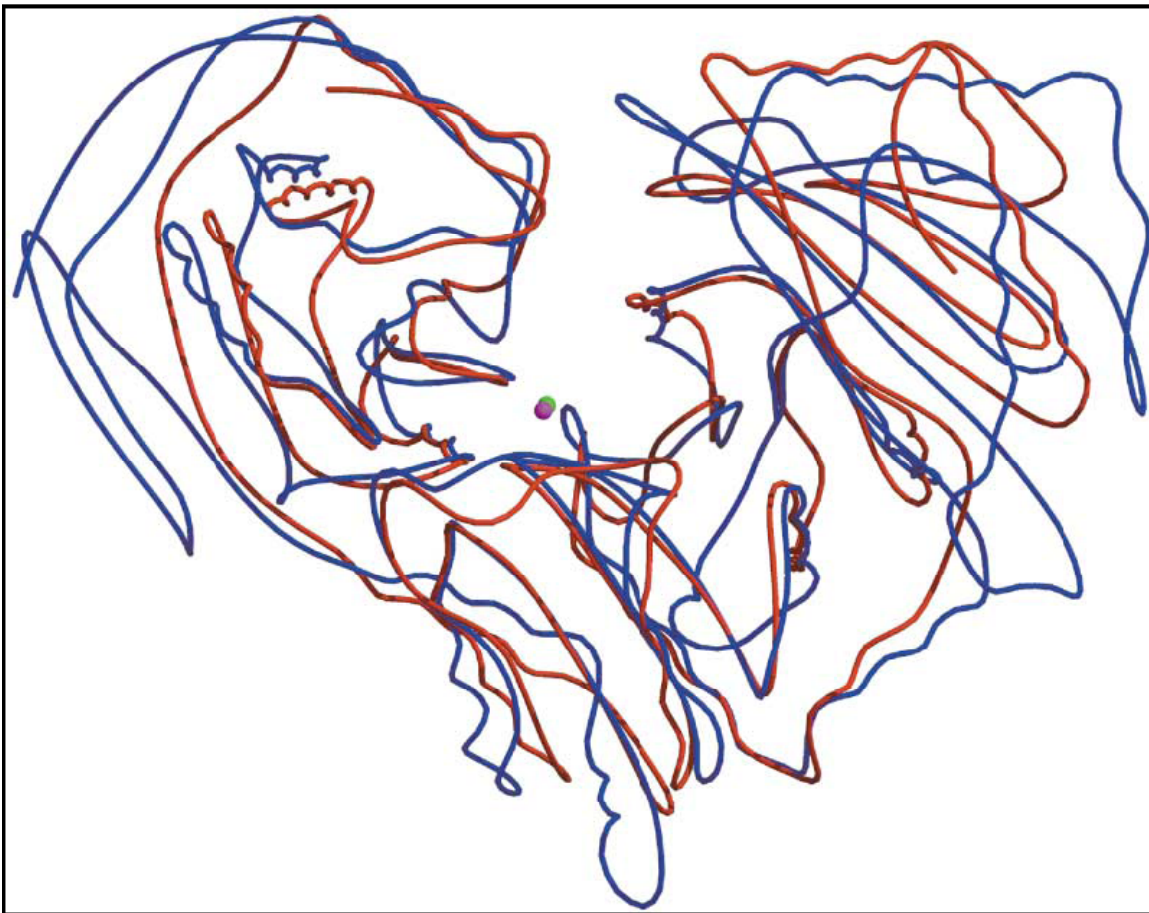


Fig. 3. Superposition of PMM/PGM from *P. aeruginosa* with PGM from rabbit muscle. PMM/PGM is shown in the same orientation as in Fig. 2a. A trace of the C_α atoms of each protein is shown with PMM/PGM in red, and PGM in blue. The Zn²⁺ ion from PMM/PGM is shown as a magenta sphere, and the Mg²⁺ ion from PGM is shown as a green sphere.

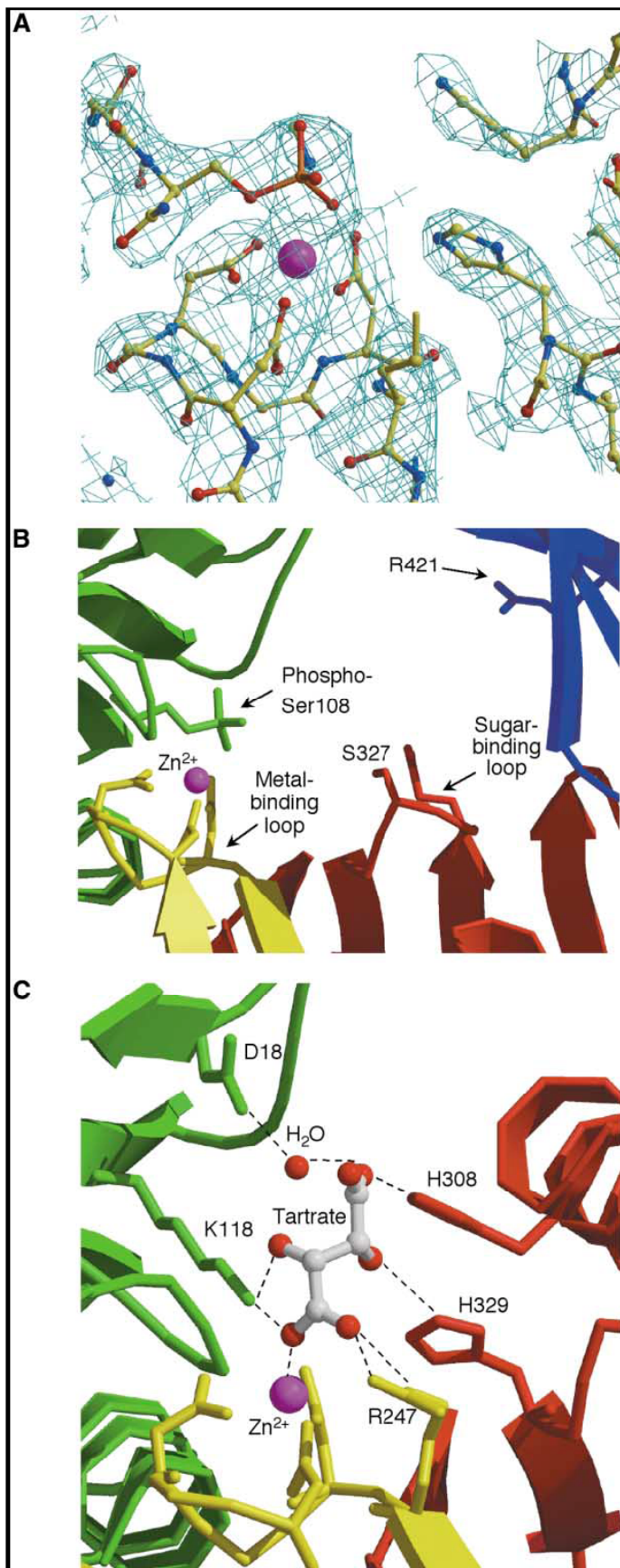


Fig. 4. a) Electron density map from the MAD data set using phases calculated by SHARP showing the active site of PMM/PGM in the vicinity of phosphoserine 108, and the metal-binding loop (residues 242-246) with bound Zn^{2+} ion (magenta sphere). Protein residues are shown as ball-and-stick model with yellow for carbon, red for oxygen, blue for nitrogen, and orange for phosphorus atoms. The electron density is contoured at 1.0σ and is shown in cyan.

b) Close-up view of residues in the active site of PMM/PGM, illustrating the four regions involved in enzyme activity/specificity. Residues in domains 1-4 are colored as in Fig. 2a.

c) Schematic illustrating binding of (+) tartrate in the active site of the S108A PMM/PGM mutant structure. Domains are colored as in Fig. 2a. Dashed lines indicate potential hydrogen bonds or salt bridges between the tartrate and protein residues. Except for the tartrate-Zn interaction (see Table 3), contact distances range from 2.8 to 3.1 Å and are between hydrogen-bonding partners.

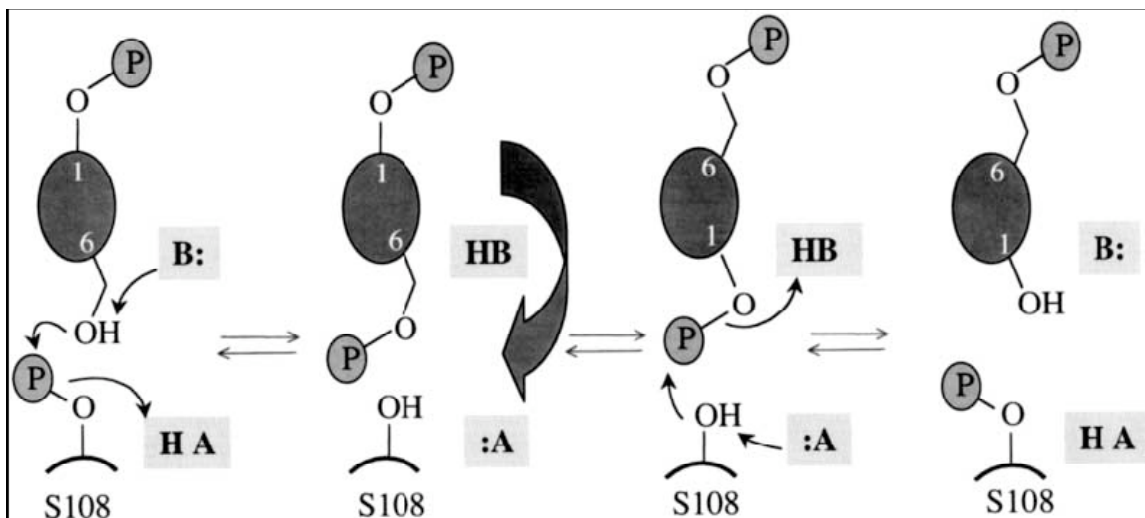


Fig. 5. Schematic of the proposed mechanism for the conversion of mannose 1-phosphate to mannose 6-phosphate by PMM/PGM. Phosphate groups are indicated by “P”, general base by “B:”, and general acid by “HA”. The reaction begins with binding of mannose 1-phosphate to the phosphorylated enzyme. A general base initiates transfer of the phosphoryl group from Ser108 to the substrate, through abstraction of a proton from the 6-hydroxyl group of the sugar. A general acid facilitates phosphoryl transfer to the sugar by protonating the hydroxyl oxygen of Ser108. The bis-phosphorylated intermediate is believed to reorient (indicated by large arrow) in the active site allowing transfer of the phosphoryl group from position 1 of the sugar back to Ser108. Candidate residues for the role of general acid and base are discussed in the text.

Tables

Table 1. Data collection statistics

Crystal	MAD				S108A
	$\lambda 1$	$\lambda 2$	$\lambda 3$	$\lambda 4$	
Wavelength (Å)	0.979151	0.979432	0.971480	0.986945	1.54
Resolution (Å)	2.2	2.2	2.2	2.2	1.75
R_{sym} (%)	7.1 (33.3)	6.4 (28.8)	7.1 (33.2)	6.4 (32.7)	5.3 (36.3)
R_{anom} (%)	5.4	4.4	5.7	4.3	-
Unique reflections	24,319	24,290	24,090	23,990	49,105
Observed reflections	185,144	192,257	95,570	89,620	240,203
Completeness (%)	96.5 (98.7)	96.7 (98.6)	96.3 (98.0)	95.0 (97.1)	97.4 (98.8)
$I/\sigma(I)$	27.8 (5.8)	30.0 (7.2)	19.7 (3.9)	20.1 (4.0)	28.5 (2.3)

Numbers in parentheses refer to statistics for the highest resolution shell

Table 2. Refinement summary

	Wild type	S108A mutant
Resolution (Å)	2.2	1.75
R_{cryst}	23.4	16.9
R_{free}	27.6	19.6
Rmsd bond distance (Å)	0.015	0.017
Rmsd bond angle (deg)	1.6	1.6
Total no. non-H atoms	3,565	3,893
Number of solvent molecules	166	435
Avg. protein B-value (Å ²)	46.4	32.2
Avg. solvent B-value (Å ²)	45.2	46.6
Heteroatoms	P-Ser, Zn ²⁺	Tartrate, Zn ²⁺

$R_{\text{cryst}} = \sum |F_o - F_c| / \sum |F_c|$ where F_o and F_c are observed and calculated structure factors, respectively. R_{free} is the R factor calculated from 5% of the reflections not included in refinement. P-Ser is a phosphorylated serine residue.

Table 3. Geometry of metal-binding loop

Bond lengths to Zn²⁺ in Å:

<u>Residue type & No.</u>	<u>Atom type</u>	<u>Wild type</u>	<u>S108A mutant</u>
D242	O	1.79	1.89
D246	O	2.22	2.03
D248	O	2.02	1.89
Phosphoserine 108	O	2.06	-
Tartrate	O	-	1.84

References

1. Lyczak, J.B., Cannon, C.L., and Pier, G.B. (2000). Establishment of *Pseudomonas aeruginosa* infection: lessons from a versatile opportunist. *Microbes Infect.* 2: 1051-1060.
2. Rocchetta, H.L., Burrows, L.L., and Lam, J.S. (1999). Genetics of O-antigen biosynthesis in *Pseudomonas aeruginosa*. *Microbiol. Mol. Biol. R.* 63: 523-553.
3. Govan, J.R.W., and Deretic, V. (1996). Microbial pathogenesis in cystic fibrosis - Mucoid *Pseudomonas aeruginosa* and *Burkholderia cepacia*. *Microbiol. Rev.* 60: 539-574.
4. Shankar, S., Ye, R.W., Schlichtman, D., and Chakrabarty, A.M. (1995). Exopolysaccharide alginate synthesis in *Pseudomonas aeruginosa*: enzymology and regulation of gene expression. *Adv. Enzymol. RAMB.* 70: 221-255.
5. Hoiby, N., Krogh Johansen, H., Moser, C., Song, Z., Ciofu, O., and Kharazmi, A. (2001). *Pseudomonas aeruginosa* and the in vitro and in vivo biofilm mode of growth. *Microbes Infect.* 3: 23-35.
6. Zielinski, N.A., Chakrabarty, A.M., and Berry, A. (1991). Characterization and regulation of the *Pseudomonas aeruginosa* algC gene encoding phosphomannomutase. *J. Biol. Chem.* 266: 9754-9763.
7. Coyne, M.J., Jr., Russell, K.S., Coyle, C.L., and Goldberg, J.B. (1994). The *Pseudomonas aeruginosa* algC gene encodes phosphoglucomutase, required for the synthesis of a complete lipopolysaccharide core. *J. Bacteriol.* 176: 3500-3507.

8. Ye, R.W., Zielinski, N.A., and Chakrabarty, A.M. (1994). Purification and characterization of phosphomannomutase/phosphoglucomutase from *Pseudomonas aeruginosa* involved in biosynthesis of both alginate and lipopolysaccharide. *J. Bacteriol.* *176*: 4851-4857.
9. Rocchetta, H.L., Pacan, J.C., and Lam, J.S. (1998). Synthesis of the A-band polysaccharide sugar D-rhamnose requires Rmd and Wbpw: Identification of multiple AlgA homologues, Wbpw and Orf488, in *Pseudomonas Aeruginosa*. *Mol. Microbiol.* *29*: 1419-1434.
10. Tang, H.B., DiMango, E., Bryan, R., Gambello, M., Iglewski, B.H., Goldberg, J.B., et al. (1996). Contribution of specific *Pseudomonas aeruginosa* virulence factors to pathogenesis of pneumonia in a neonatal mouse model of infection. *Infect. Immun.* *64*: 37-43.
11. Goldberg, J.B., Coyne, M.J., Jr., Neely, A.N., and Holder, I.A. (1995). Avirulence of a *Pseudomonas aeruginosa* algC mutant in a burned-mouse model of infection. *Infect. Immun.* *63*: 4166-4169.
12. Davies, D.G., and Geesey, G.G. (1995). Regulation of the alginate biosynthesis gene algC in *Pseudomonas aeruginosa* during biofilm development in continuous culture. *Appl. Environ. Microbiol.* *61*: 860-867.
13. Ray, W.J., Jr., Burgner, J.W., 2nd, and Post, C.B. (1990). Characterization of vanadate-based transition-state-analogue complexes of phosphoglucomutase by spectral and NMR techniques. *Biochemistry* *29*: 2770-2778.

14. Lu, G. (2000). TOP: A new method for protein structure comparison and similarity searches. *J. Appl. Crystallogr.* 33: 176-183.
15. Murzin, A.G., Brenner, S.E., Hubbard, T., and Chothia, C. (1995). SCOP: a structural classification of proteins database for the investigation of sequences and structures. *J. Mol. Biol.* 247: 536-540.
16. Jones, S., and Thornton, J.M. (1996). Principles of protein-protein interactions. *Proc. Natl. Acad. Sci. USA* 93: 13-20.
17. Liu, Y., Ray, W., and Baranidharan, S. (1997). Structure of rabbit muscle phosphoglucomutase refined at 2.4 Å resolution. *Acta Crystallogr. D* 53: 392-405.
18. Liang, J., Edelsbrunner, H., and Woodward, C. (1998). Anatomy of protein pockets and cavities: measurement of binding site geometry and implications for ligand design. *Protein Sci.* 7: 1884-1897.
19. Dai, J.B., Liu, Y., Ray, W.J., Jr., and Konno, M. (1992). The crystal structure of muscle phosphoglucomutase refined at 2.7- angstrom resolution. *J. Biol. Chem.* 267: 6322-6337.
20. Lin, Z., Konno, M., Abad-Zapatero, C., Wierenga, R., Murthy, M.R., Ray, W.J., Jr., et al. (1986). The structure of rabbit muscle phosphoglucomutase at intermediate resolution. *J. Biol. Chem.* 261: 264-274.

21. Lowry, O.H., and Passonneau, J.V. (1969). Phosphoglucomutase kinetics with the phosphates of fructose, glucose, mannose, ribose, and galactose. *J. Biol. Chem.* *244*: 910-916.
22. Naught, L.E., and Tipton, P.A. (in press). Kinetic mechanism and pH dependence of the kinetic parameters of *Pseudomonas aeruginosa* phosphomannomutase/phosphoglucosmutase. *Arch. Biochem. Biophys.*
23. Ray, W.J., Jr., Post, C.B., and Puvathingal, J.M. (1989). Comparison of rate constants for (PO₃⁻) transfer by the Mg(II), Cd(II), and Li(I) forms of phosphoglucomutase. *Biochemistry* *28*: 559-69.
24. Glusker, J.P. (1991). Structural aspects of metal liganding to functional groups in proteins. *Adv. Protein Chem.* *42*: 1-76.
25. Harding, M.M. (2001). Geometry of metal-ligand interactions in proteins. *Acta Crystallogr. D* *57*: 401-411.
26. Altschul, S.F., Gish, W., Miller, W., Myers, E.W., and Lipman, D.J. (1990). Basic local alignment search tool. *J. Mol. Biol.* *215*: 403-10.
27. Percival, M.D., and Withers, S.G. (1992). ¹⁹F NMR investigations of the catalytic mechanism of phosphoglucomutase using fluorinated substrates and inhibitors. *Biochemistry* *31*: 505-512.

28. Kalgutkar, A.S., Crews, B.C., Rowlinson, S.W., Garner, C., Seibert, K., and Marnett, L.J. (1998). Aspirin-like molecules that covalently inactivate cyclooxygenase-2. *Science* 280: 1268-1270.
29. Regni, C.A., Tipton, P.A., and Beamer, L.J. (2000). Crystallization and initial crystallographic analysis of phosphomannomutase/phosphoglucomutase from *Pseudomonas aeruginosa*. *Acta Crystallogr. D* 56: 761-2.
30. Terwilliger, T.C., and Berendzen, J. (1999). Automated MAD and MIR structure solution. *Acta Crystallogr. D* 55: 849-861.
31. Cowtan, K. (1994). Joint CCP4 and ESF-EACBM Newsletter on Protein Crystallography 31: 34-38.
32. LaFortelle, E.D., and Bricogne, G. (1997). Maximum-likelihood heavy-atom parameter refinement in the MIR and MAD methods. *Method Enzymol.* 276: 472-492.
33. Abrahams, J., and Leslie, A. (1996). Methods used in the structure determination of bovine mitochondrial F1 ATPase. *Acta Crystallogr. D* 52: 30-42.
34. Jones, T.A., Zou, J.Y., Cowan, S.W., and Kjeldgaard, M. (1991). Improved methods for building protein models in electron density maps and the location of errors in these models. *Acta Crystallogr. A* 47: 110-119.
35. Brünger, A.T., Adams, P.D., Clore, G.M., DeLano, W.L., Gros, P., Grosse-Kunstleve, R.W., et al. (1998). Crystallography & NMR system: A new software suite for macromolecular structure determination. *Acta Crystallogr. D* 54: 905-21.

36. Murshudov, G.N., Vagin, A.A., Lebedev, A., Wilson, K.S., and Dodson, E.J. (1999). Efficient anisotropic refinement of macromolecular structures using FFT. *Acta Crystallogr. D* 55: 247-255.
37. No. 4, C.C.P. (1994). The CCP4 suite: Programs for Protein Crystallography. *Acta Crystallogr. D* 50: 760.
38. Magneson, G.R., Puvathingal, J.M., and Ray, W.J., Jr. (1987). The concentrations of free Mg^{2+} and free Zn^{2+} in equine blood plasma. *J. Biol. Chem.* 262: 11140-11148.
39. Laskowski, R.A., McArthur, M.W., Moss, D.S., and Thornton, J.M. (1993). PROCHECK: A program to check the stereochemical quality of protein structures. *J. Appl. Crystallogr.* 26: 283-291.
40. Colovos, C., and Yeates, T.O. (1993). Verification of protein structures: patterns of nonbonded atomic interactions. *Protein Sci.* 2: 1511-9.
41. Bowie, J.U., Luthy, R., and Eisenberg, D. (1991). A method to identify protein sequences that fold into a known three- dimensional structure. *Science* 253: 164-70.
42. Vaguine, A.A., Richelle, J., and Wodak, S.J. (1999). SFCHECK: a unified set of procedures for evaluating the quality of macromolecular structure-factor data and their agreement with the atomic model. *Acta Crystallogr. D* 55: 191-205.
43. Hooft, R.W., Vriend, G., Sander, C., and Abola, E.E. (1996). Errors in protein structures. *Nature* 381: 272.

44. Kraulis, P. (1991). MOLSCRIPT: a program to produce both detailed and schematic plots of protein structures. *J. Appl. Crystallogr.* *24*: 946-950.
45. Koradi, R., Billeter, M., and Wuthrich, K. (1996). MOLMOL: a program for display and analysis of macromolecular structures. *J. Mol. Graphics* *14*: 51-5, 29-32.
46. Esnouf, R.M. (1997). An extensively modified version of MolScript that includes greatly enhanced coloring capabilities. *J. Mol. Graph. Model.* *15*: 132-4, 112-3.
47. Merritt, E.A., and Bacon, D.J. (1997). Raster3D: Photorealistic molecular graphics. *Method Enzymol.* *277*: 505-524.

CHAPTER 4

STRUCTURAL BASIS OF DIVERSE SUBSTRATE RECOGNITION BY THE ENZYME PMM/PGM FROM *P. AERUGINOSA*

Reproduced with permission from Regni, C., L.E. Naught, P.A. Tipton, and L.J. Beamer, *Structural basis of diverse substrate recognition by the enzyme PMM/PGM from P. aeruginosa*. Structure, 2004. **12**: p. 55-63. Copyright 2004 Elsevier Science Ltd.

ABSTRACT

Enzyme-substrate complexes of phosphomannomutase/phosphoglucomutase (PMM/PGM) reveal the structural basis of the enzyme's ability to use four different substrates in catalysis. High-resolution structures with glucose 1-phosphate, glucose 6-phosphate, mannose 1-phosphate, and mannose 6-phosphate show that the position of the phosphate group of each substrate is held constant by a conserved network of hydrogen bonds. This produces two distinct, and mutually exclusive, binding orientations for the sugar rings of the 1-phospho and 6-phospho sugars. Specific binding of both orientations is accomplished by key contacts with the O3 and O4 hydroxyls of the sugar, which must occupy equatorial positions. Dual recognition of glucose and mannose phosphosugars uses a combination of specific protein contacts and non-specific solvent contacts. The ability of PMM/PGM to accommodate these four diverse substrates in a single active site is consistent with its highly reversible phosphoryl transfer reaction and allows it to function in multiple biosynthetic pathways in *P. aeruginosa*.

Introduction

P. aeruginosa is an opportunistic human pathogen that produces life-threatening infections in cystic fibrosis patients, burn victims, and immuno-compromised hosts (Lyczak et al., 2000). *P. aeruginosa* is known to form antibiotic-resistant biofilms, and its infections are further complicated by the production of multiple bacterial exoproducts that contribute to virulence. Three of these virulence factors are alginate, lipopolysaccharide, and rhamnolipid. Alginate is an exopolysaccharide that forms a viscous protective coating around the bacteria in response to certain environmental factors and also during chronic cystic fibrosis lung infections (Govan and Deretic, 1996). Lipopolysaccharide is a complex glycolipid found in the outer membrane of Gram-negative bacteria, and is a potent inflammatory stimulant (Rocchetta et al., 1999). Rhamnolipid is a surfactant produced by *P. aeruginosa* that plays a critical role in biofilm maintenance (Olvera et al., 1999).

In *P. aeruginosa*, the enzyme PMM/PGM participates in the biosynthesis of all three of these virulence factors. PMM/PGM is the product of the *algC* gene and is a monomeric protein with 463 residues (Zielinski et al., 1991). It catalyzes the reversible conversion of either glucose 6-phosphate (G6P) to glucose 1-phosphate (G1P), or mannose 6-phosphate (M6P) to mannose 1-phosphate (M1P), depending on the biosynthetic pathway in which it is operating. The active form of the protein is phosphorylated at S108, and the enzyme requires Mg^{2+} for full activity. The proposed reaction mechanism requires two phosphoryl transfer reactions: first from the enzyme to substrate, and second from the reaction intermediate back to the enzyme (Naught and

Tipton, 2001). The initial phosphoryl transfer is from phosphoserine 108 to bound substrate, creating a bisphosphorylated sugar intermediate (glucose 1,6-bisphosphate or mannose 1,6-bisphosphate). This intermediate must reorient and bind in an alternative position to permit transfer of a phosphoryl group back to the protein, forming product and regenerating the active form of the enzyme (Fig. 1A).

Although the chemistry of phosphoryl transfers has been studied in many systems, important questions remain regarding substrate recognition, binding specificity, and the role of conformational change during catalysis for the phosphohexomutase family. In the case of PMM/PGM, this includes the structural basis of its ability to utilize both mannose- and glucose-based phosphosugars as substrates. This dual substrate specificity allows the enzyme to function in multiple biosynthetic pathways in the bacterium, and also distinguishes it from the related eukaryotic enzyme, phosphoglucomutase (PGM), that exclusively utilizes phosphoglucose as a substrate (Ray et al., 1990). Even more intriguing is the ability of PMM/PGM to catalyze phosphoryl transfer with both the 1-phospho and 6-phospho forms of these two sugars. Because its phosphoryl transfer activity is fully reversible and utilizes the same catalytic phosphoserine residue, the active site of the enzyme must accommodate two completely different orientations of the phosphosugar, while maintaining high affinity and specificity of binding. This is a complex and challenging problem in ligand recognition for PMM/PGM and related phosphohexomutases, that has been previously unexplored.

Here we present four high-resolution crystal structures of *P. aeruginosa* PMM/PGM in complex with four biological ligands: G6P, M6P, G1P, and M1P. Because the PMM/PGM reaction is highly reversible (Naught and Tipton, 2001), all four

of these phosphosugars are efficient substrates for the enzyme, and it is equally correct to consider the structures presented here as enzyme-substrate or enzyme-product complexes. (For simplicity, we will use the former designation.) By utilizing a catalytically inactive form of the enzyme, we were able to trap each of these molecules bound in the active site, representing the state of the enzyme immediately prior to or following catalysis. These structures reveal for the first time the structural basis of diverse substrate recognition by PMM/PGM, and confirm a key role for conformational change of the enzyme in catalysis. They also allow a better understanding of the diverse biosynthetic roles of PMM/PGM in *P. aeruginosa* and serve as high quality templates for future efforts at inhibitor design.

Results and discussion

Overall structure and comparison with apo-protein

The overall protein fold and three-dimensional arrangement of the active site of *P. aeruginosa* PMM/PGM was previously described at 1.75 Å resolution by X-ray crystallographic studies of the wild-type protein and an active site mutant, S108A (Regni et al., 2002). These structures show that the protein has four domains, arranged in an overall "heart" shape (Fig. 1B). The first three domains share a similar tertiary fold and are bridged by extensive domain-domain interfaces. Domain 4 is structurally unrelated to the others, and has a less extensive interface with the remainder of the protein. Key residues in catalysis, including the catalytic phosphoserine and metal-binding loop, were found to cluster in a large active site cleft, formed by residues from all four domains of

PMM/PGM. Throughout this manuscript, we refer to the vicinity of the active site near S108 as the *phosphoryl transfer site*. Distinct from this is another area of the active site, which contains residues that interact with the phosphate group of the incoming substrate, that we call the *phosphate-binding site*.

The structures of the four PMM/PGM complexes are similar in overall structure to each other, and also to the apo-protein. The various pairs of enzyme-substrate complexes have C_{α} atom root-mean-square-deviations (rmsd) of 0.2 Å or less. Differences between the complexes associated with binding of the four different ligands are confined to the active site, and detailed in the following sections. Comparisons of the complexes with the apo-protein also show a high degree of structural similarity, with only minor differences in backbone conformation, and essentially no changes in secondary structure. However, superpositions of the enzyme-substrate complexes with the apo-protein (average rmsd for C_{α} atoms of 1.1 Å) indicate a rotation of domain 4 relative to the rest of the polypeptide by approximately 9°, resulting in the movement of individual residues by as much as 4.5 Å (Fig. 1B). This domain motion occurs primarily through a small change in the backbone angles of F367, which is located in a loop connecting domains 3 and 4. This results in a hinge movement that brings domain 4 in toward the active site, reducing its solvent accessible surface area and volume by 50% (Regni et al., 2002). The domain rotation also creates a new interface between domains 1 and 4 with a surface area of ~160 Å². Although the domain-domain contacts differ slightly in each complex, all four structures have a hydrogen bond between the side chains of Y17 and N424 (3.0 Å between the tyrosine hydroxyl and OD1 of N424). Two water-mediated hydrogen bonds bridging domains 1 and 4 are also conserved in all of the complexes.

The domain movement and new domain 1-4 interface changes the active site of the enzyme from a relatively open cleft to a deep pocket. The substrates in all four complexes are highly buried in this pocket, with only 5% of their total surface areas exposed to solvent.

The potential flexibility of domain 4 relative to the rest of the protein was predicted by the relatively small domain 3-domain 4 interface in apo-PMM/PGM (Regni et al., 2002). Small differences in the orientation of domain 4 are also seen between various structures of the related enzymes rabbit PGM (Liu et al., 1997) and parafusin (Muller et al., 2002). However, the relevance of this domain movement to substrate binding is demonstrated for the first time by these studies, since the interaction of the related enzymes with substrate has not been reported. (Two complexes of rabbit PGM with bound intermediate and inhibitor have been deposited in the PDB, but never described in a publication). We expect that rotation of domain 4 will be a common structural feature of this enzyme family, and that it may play a role at multiple points during catalysis. Movement of domain 4 would be required upon not only substrate binding and product release, but also presumably upon reorientation of the intermediate during the reaction. In addition, as described below, the rotation of domain 4 and its resulting interaction with domain 1 is critical for creating the high affinity substrate-binding site.

The invariant phosphate-binding site

Because the phosphate group is the most conserved structural feature of the four substrates, it seemed a likely site for critical interactions between substrate and enzyme.

In fact, a highly conserved phosphate-binding site is found in all four of the PMM/PGM complexes (Fig. 2A). Four residues (R421, S423, N424, and T425) in the same loop of domain 4 are within hydrogen bonding distance of the phosphate. The importance of one of these residues, R421, which makes a bidentate interaction with the phosphate group, was previously demonstrated by isolation of an R421C mutant that fails to produce alginate (Zielinski et al., 1991). Another conserved phosphate contact is made by Y17 from domain 1. These five residues are utilized in all four enzyme-ligand complexes in precisely the same fashion, with nearly identical bond lengths and angles between the contacting residues and phosphate group. In the G6P and M6P complexes, an additional contact to the phosphate is made by the side chain of K285. Two water molecules also interact with the phosphate (Table 2), which, together with the protein residues, completely fulfills the hydrogen bonding potential of this group.

The participation of Y17 in the invariant phosphate-binding site highlights the importance of protein conformational changes for creation of the substrate-binding site by PMM/PGM. In the apo-protein, for example, the distance between Y17 and R421 is 5.9 Å, while in the enzyme-substrate complexes it is 3.2 Å. Since Y17 is involved in the domain 1-4 interaction with N424, a direct link is made between binding of substrate and closure of the active site, via interactions with the phosphate group of the substrate. Thus, it appears that rotation of domain 4 is either required for, or induced by, binding of the phosphosugar substrates. This proposal is consistent with classical studies on rabbit PGM, which was used a model in early studies of substrate-induced conformational changes (Yankeelov and Koshland, 1965).

The extensive number of contacts between the enzyme and the phosphate group and their conservation across multiple structures implies that phosphate recognition plays an important role in binding of substrate by PMM/PGM. The phosphate group appears to function as a "handle" which the enzyme grabs to position the substrate in the correct orientation to accept a phosphoryl group from S108. This allows the enzyme to take advantage of the most structurally similar feature of the four ligands, regardless of the position of the phosphate (1 or 6) or the stereochemistry of the sugar (mannose or glucose). Phosphate is well suited for use as a potential determinant of binding, since it can participate in multiple hydrogen bonding and electrostatic interactions, both of which are seen in these structures. Thus, the invariant phosphate-binding site would appear to be one key to the problem of recognizing structurally diverse substrates in the same active site.

Recognition of 1- vs. 6-phosphosugars

The biggest challenge in substrate recognition for PMM/PGM arises during its utilization of the 1- and 6-phospho forms of its sugar substrates. Of course, these molecules are closely related, differing only in the position of their phosphate. However, as described above, the invariant phosphate-binding site anchors the incoming substrate via its phosphate group, regardless of the position of the substitution. Moreover, the enzyme mechanism requires that both the O1 and O6 hydroxyls of the substrate move into proximity with phosphoserine 108 at different points in the reaction. Within these constraints, perhaps the simplest way to complete the two phosphoryl transfers is to exchange the positions of the O1 and O6 hydroxyls, and let the rest of the ligand atoms

"come along for the ride". A superposition of G1P and G6P (Fig. 2B) as bound in the active site of PMM/PGM shows that this is essentially what happens. The sugar rings in these two complexes are related by a rotation of nearly 180° about an axis linking O5 and the midpoint of the C3-C4 bond. This nearly switches the positions of the O1 and O6 hydroxyls, with differences in oxygen atom positions of the overlaid substrates of less than 0.4 \AA at the phosphate-binding site and 1.2 \AA at the phosphoryl transfer site. A similar result is seen for M1P and M6P (data not shown).

The dramatic difference in the orientation of binding for the 1- and 6-phospho forms of the substrates greatly increases the complexity of the recognition problem faced by PMM/PGM. The different binding orientations transform these related sugars into two completely different ligands (except for the phosphate group) from the enzyme's point of view. Since the ligands lack two-fold symmetry, the 180° reorientation changes the position of every atom in the substrate, except for O5, which is near the rotation axis and stays within 0.3 \AA of its original position. The 6-membered sugar rings are offset by nearly half their width, and show distinct differences in their van der Waals surfaces (data not shown). The O2 hydroxyls occupy disparate positions in the superposition, and are separated by more than 6 \AA . The O3 and O4 hydroxyls of the two sugars exchange places with each other (differences of 0.5 to 0.9 \AA), in similar fashion to the O1 and O6 hydroxyls. The two different orientations of the substrates observed in the PMM/PGM complexes are consistent with ^{19}F NMR studies of the binding of fluorinated glucose analogs to rabbit PGM. This work indicated different binding environments for the fluorine substituents on pairs of fluoroglucose phosphate molecules, and led to the proposal of an "exchange mechanism" with two distinct, mutually exclusive binding sites

for this related enzyme (Percival and Withers, 1992). The exchange mechanism is consistent with the enzyme-substrate complexes of PMM/PGM, which show that the two predicted sugar-binding sites overlap in the active site.

Contacts between PMM/PGM and the sugar moiety of its four substrates are predominately mediated by hydrogen bonds to the hydroxyl groups, as is commonly seen in other protein-carbohydrate complexes. A discussion of the contacts to O1 and O6 in the phosphoryl transfer site is deferred to a later section, as is a description of contacts with the O2 hydroxyl, which differ in the glucose and mannose-based complexes. However, all four complexes share a set of conserved interactions with the O3 and O4 hydroxyls of the substrates. Three residues (H308, E325, and S327) hydrogen bond with these two hydroxyls (Fig. 2B). In the 1-phospho complexes, S327 contacts O3, H308 contacts O4, and E325 makes a bidentate interaction with both O3 and O4. In the 6-phospho complexes, the first two contacts are exactly reversed: H308 contacts O3, S327 contacts O4, while once again E325 contacts both. Only small conformational changes in these residues are required to adjust between the 1-phospho and 6-phospho complexes. We note that the K_m of PMM/PGM for G1P is 70-fold lower than for G6P (Naught and Tipton, 2001). While significant, this corresponds to a relatively small difference in stability (~ 2 kcal/mol), and structural comparisons did not reveal any obvious explanation for a difference in binding affinities.

To assess the importance of the O3-O4 contacts to the overall binding of the substrates, we characterized an E325A mutant of PMM/PGM. The mutant showed a somewhat reduced K_m of $7 \pm 2 \mu\text{M}$ and V_{\max} of $6.4 \pm 0.7 \text{ sec}^{-1}$ compared to the wild type enzyme ($K_m = 12.1 \mu\text{M}$, $V_{\max} = 22.2 \text{ sec}^{-1}$). Despite the conserved bidentate

interaction made by this residue, its contribution is not essential in the overall context of the active site. This is perhaps not surprising given the many other residues that interact with the O3, O4, and other sugar hydroxyls. Although additional mutants need to be evaluated to draw a firm conclusion, these data suggest that the PMM/PGM active site is highly robust and redundant, with individual residues making relatively small contributions to the binding of substrates. A similar picture has emerged from the analysis of other active site mutants of the enzyme (see (Naught et al., 2003) and Mechanistic Implications).

The ability of PMM/PGM to utilize a conserved set of contacting residues for O3 and O4 is a direct consequence of the stereochemistry of glucose and mannose. Because the O3 and O4 hydroxyls of these two sugars are both in equatorial positions, these atoms exchange places when the sugar ring is rotated by 180° as described above. A similar exchange would not occur for sugars where these hydroxyls are in axial positions, since they would occupy very different positions after rotation. It appears that these exchangeable contacts with O3 and O4 are another key to diverse substrate recognition by PMM/PGM, which could not be utilized for sugars with different stereochemistry at these positions.

To confirm this hypothesis, we tested the activity of wild-type PMM/PGM and the E325A mutant with two alternative substrates, allose 1-phosphate and galactose 1-phosphate, which are epimers of glucose at the O3 and O4 positions. In the reaction of the wild-type enzyme with allose 1-phosphate after 7 hours, only 3% of the substrate appeared as a product eluting at 10.7 minutes. No product could be detected in the reaction of the wild-type enzyme with galactose 1-phosphate, or for either substrate with

the E325A mutant. For comparison, a reaction containing 50 μM G1P and 0.14 μg PMM/PGM reached completion within 3 minutes. Galactose 1-phosphate and allose 1-phosphate were also tested as potential inhibitors of PMM/PGM, using a coupled spectrophotometric assay (Naught and Tipton, 2001). At a concentration of 0.2 mM, neither allose 1-phosphate nor galactose 1-phosphate inhibited the reaction with 10 μM G1P.

Notwithstanding the overall similarity of allose 1-P and galactose 1-P to its natural substrates, PMM/PGM is unable to effectively utilize them in catalysis. In addition, inhibition assays show that neither compound binds well to the enzyme. Although it is possible that the axial position of the O3 and O4 oxygens of these compounds interferes with binding due to steric conflicts, modeling in the active site (data not shown) indicates clashes with only a few side chains that can be rotated to avoid this. Therefore, it seems that the loss of all enzyme contacts with either O3 or O4 (in contrast with the loss of a single residue such as E325A) has serious consequences for enzyme recognition and activity. Other work has indicated that ribose 1-phosphate and 2-deoxy glucose 6-phosphate are also poor substrates for PMM/PGM (Ye et al., 1994). Despite its ability to accommodate differing orientations of its two phosphosugar substrates, PMM/PGM has impressive specificity for its biological ligands, and should not be considered a promiscuous enzyme.

The unique ability of PMM/PGM to recognize two different orientations of its substrates in the same active site has implications for the larger α -phosphohexomutase enzyme family, which includes both the dual specificity bacterial PMM/PGM enzymes, and the more specific eukaryotic PGM enzymes (Regni et al., 2002). Until now, no

structural explanation was available for any family member on how this two-step phosphoryl transfer could occur in a single active site. Because of the high sequence conservation of the catalytic serine and metal-binding loop, and overall similarity of the active sites of PMM/PGM and rabbit PGM (Regni et al., 2002), it seems likely that other members of the phosphohexomutase family will utilize a similar strategy for recognizing their 1- and 6-phosphosugar substrates.

Recognition of glucose and mannose phosphosugars

The dual substrate specificity of PMM/PGM for both glucose- and mannose-based phosphosugars allows this enzyme to participate in multiple biosynthetic pathways in *P. aeruginosa*. It is also the defining feature that distinguishes the bacterial enzymes from their eukaryotic PGM counterparts, which are highly specific for glucose. (Rabbit PGM shows a 6,000-fold preference for glucose phosphosugars over mannose (Lowry and Passonneau, 1969)). The structural difference between glucose and mannose is relatively minor, and, in principle, the ability to utilize both sugars as substrates could simply reflect a lack of specificity that allows the active site to accommodate both epimers at the C2 position of the sugar. Alternatively, specific contacts could be made with both possible positions of the O2 hydroxyl. In PMM/PGM, however, the situation is more complex because of the two different binding orientations of the 1- and 6-phospho sugars. In total, therefore, the sugar specificity of PMM/PGM must account for four different positions of the O2 hydroxyl in the active site.

The approach used by the enzyme to accomplish this task appears to be a combination of both specific and non-specific binding interactions. In the two

phosphoglucose complexes, specific contacts are made between the enzyme and O2 hydroxyls. In G1P, this contact is made by K285, which rotates slightly from its alternative role in the phosphate-binding site (Fig. 2A). In the G6P complex, two protein residues (S108 and H329) participate in hydrogen bonds with O2 (Fig. 2C). In the two phosphomannose complexes, however, no specific enzyme-O2 contacts are seen, although in both cases a water molecule makes hydrogen bonds with the O2 hydroxyl. It is easy to see how this arrangement, where specific enzyme contacts are made with O2 of G1P and G6P, but only water-mediated contacts are made with O2 of M1P and M6P, can result in the dual substrate specificity observed with PMM/PGM. However, it is not immediately obvious how it could be modified to create the highly specific PGM enzymes.

Mechanistic implications

Phosphoryl transfer reactions commonly proceed via general acid-base catalysis (Knowles, 1980). In the case of PMM/PGM, the reaction was proposed to begin with a general base, which would abstract a proton from the O1 or O6 hydroxyl of the phosphosugar, and activate it for nucleophilic attack on phosphoserine 108 (Naught and Tipton, 2001). After phosphoryl transfer, another residue would be expected to act as general acid to stabilize Ser108. Ionizable residues of PMM/PGM near the phosphoryl transfer site were examined to identify candidates for the general acid-base catalysts. For the 1-phospho complexes, the side chain of H329 makes a hydrogen bond with the O1 hydroxyl and seemed a likely choice for a general base; other possibilities based on their proximity to the phosphoryl transfer site are R20, H109, K118, R247, and H308.

However, site-directed mutagenesis of these residues (and a H109Q/K118L double mutant) did not produce the expected significant decrease in enzyme activity, although all of the mutants showed some decrease in activity (Naught et al., 2003). Based on this data, it appears that PMM/PGM may utilize the ensemble of residues in the active site, many of which are cationic, to create a positive electrostatic potential to stabilize the ionized hydroxyls of the substrate and S108 during catalysis. This unique mode for stabilizing the ionized substrate may allow the enzyme more freedom in positioning the reactive substrate hydroxyl in the active site, since a single specific residue is not required as a general base. This could potentially assist with the complex task of catalyzing phosphoryl transfer with both the 1- and 6-phospho forms of its substrates, the hydroxyls of which are separated by 1.2 Å in superpositions of the complexes (Fig. 2D).

The mechanism of a phosphoryl transfer by PMM/PGM, whether associative or dissociative, has not been determined. However, in either case, the substrate hydroxyl that accepts the phosphoryl group should be in proximity with phosphoserine 108. In the PMM/PGM complexes, each of the four substrates is bound with its O1 or O6 hydroxyl less than 2.7 Å from the O1P atom of phosphoserine 108 and within 3.5 Å of the phosphorus atom, and is therefore in a position appropriate for the initiation of catalysis. If phosphoryl transfer occurs through an associative pathway, it would be expected to have a trigonal bipyramidal transition state, formed through an in-line attack on the phosphorus by the incoming nucleophile (either the O1 or O6 hydroxyl of the substrate). In the PMM/PGM substrate complexes, the O6 hydroxyls of G1P and M1P are slightly closer to the phosphorus and more nearly colinear with the phosphorus-S108 O γ bond than the O1 hydroxyls of G6P and M6P (Fig. 2D & E). This placement, which

puts the O6 hydroxyls closer to the preferred 180° from the incipient leaving group, is consistent with the formation of the 6-phosphosugars being the faster direction of the reaction [$K_{eq}=17.3$ for the conversion of α -G1P to $(\alpha+\beta)$ -G6P (Atkinson et al., 1961)], assuming an associative pathway is used. The cluster of positively charged residues observed in the active site of PMM/PGM could also assist with stabilization of increased negative charge on the equatorial oxygen atoms in this pentacoordinate transition state.

Summary

It has been proposed that construction of a catalytic site is more difficult than a recognition site (Knowles, 1980). This hypothesis has particular relevance to phosphomutases such PMM/PGM, since the phosphoryl transfers catalyzed by these enzymes involve the same chemistry at two different positions of the ligand. In principle, this reaction could be catalyzed by two consecutive enzymes: one which would bind the substrate in a single orientation and transfer a phosphoryl group to create the bisphosphorylated intermediate; and another which would specifically bind the intermediate in the opposite orientation, and remove the original phosphate. The fact that these two reactions have been combined in a single active site demonstrates that it is indeed more efficient to produce a single enzyme that can accommodate multiple orientations of its substrates, rather than to produce two different, highly specific enzymes that catalyze the same reaction.

In summary, the four high-resolution PMM/PGM substrate complexes presented here reveal how the enzyme has solved the complex recognition problem presented by its intramolecular phosphoryl transfer reaction and dual-substrate specificity. First, it

maximizes interactions with the structurally conserved part of the ligands. Second, it utilizes several key residues that are precisely positioned to recognize two dramatically different orientations of the bound substrates. Third, its active site is sufficiently robust to make additional specific contacts with certain subsets of the complexes, such as the O2 hydroxyls of its glucose-based substrates. In all of three of these situations, conformational changes of the protein, either global or local, are involved. Thus, it appears that PMM/PGM is an outstanding example of the ability of proteins to create highly specific yet flexible binding sites. Similar recognition strategies may be used by other proteins, such as antibodies and receptors, which also have the task of recognizing structurally diverse ligands.

Experimental procedures

Complex formation and structure determination

G1P, G6P, M1P and M6P were purchased from Sigma. Purification and crystallization of apo-PMM/PGM was carried out as previously described (Regni et al., 2000). These crystals contain the phosphorylated form of the enzyme, but are catalytically inactive due to a substitution of Zn^{2+} in the Mg^{2+} binding site. Initial difficulties with complex formation due to the high salt conditions necessary for crystallization were overcome by transferring the crystals into polyethylene glycol (PEG). Briefly, crystals of apo-PMM/PGM grown from solutions of 50-60% saturated Na, K tartrate were transferred quickly into 79% (w/w) PEG 4000 and 25 mM ligand, and allowed to soak for one minute. Crystals were then flash-cooled without further

cryoprotection for data collection. All enzyme-substrate complexes were isomorphous with the apo-protein (space group $P2_12_12_1$) except for a reproducible reduction of the c axis by ~ 6 Å (Table 1). Datasets for the G1P, G6P and M6P complexes were collected at beam line 14-BMC at the Advanced Photon Source, Argonne National Laboratory. The M1P data set was collected on a Rigaku rotating anode generator and R-AXIS IV area detector. Diffraction data were processed with DENZO and merged with SCALEPACK (Otwinowski and Minor, 1997).

Structure solution and refinement

Due to the cell change relative to the apo-enzyme, phases for the G6P complex were determined by molecular replacement with CNS (Brünger et al., 1998) using wild-type PMM/PGM (1K35) as the search model. The partially refined G6P complex (without ligand) was used as a starting point for rigid-body refinement of the other complexes (G1P, M1P, M6P). Electron density for the ligands in each complex appeared as nearly continuous, positive peaks in F_o-F_c maps contoured at 3.0σ , allowing for unambiguous placement of the ligands (Fig. 2F). All structures were refined to convergence through iterative cycles of positional refinement using REFMAC 5.0 (Murshudov et al., 1999) and manual rebuilding with O (Jones et al., 1991). Progress of the refinement was monitored by following R_{free} . Five percent of each data set was set aside for cross-validation prior to refinement; the same reflections were flagged as the test set in all four enzyme complexes. Water molecules were placed automatically by WATPEAK (CCP4, 1994) in peaks $>3.0 \sigma$ in F_o-F_c maps and within hydrogen-bonding

distance of nitrogen or oxygen atoms; water molecules without electron density in $2F_o-F_c$ maps and B-factors above 60 \AA^2 were removed from the model.

The final models (Table 1) extend from residue 9 to 463, except for the M1P complex that begins at residue 6. Each model contains the following heteroatoms: phosphoserine 108, Zn^{+2} , phosphosugar, and waters. The G1P, G6P, and M1P structures have 12, 11, and 1 residues, respectively, modeled in two conformations. The individual complexes have from 12 to 16 residues whose side chains were truncated to alanine. All models were validated with the following programs: SFCHECK (Vaguine et al., 1999), and PROCHECK (Laskowski et al., 1993). The occupancy for all residues except those modeled in multiple conformations is 1.0.

For structural analyses, the following programs were used for calculations: pocket surface area and volumes were done by CAST (Liang et al., 1998); domain interface surface area by the protein-protein interaction server (Jones and Thornton, 1996); solvent accessible surface area of the ligands by AREAIMOL (CCP4, 1994); domain rotation by DYNDOM (Hayward and Berendsen, 1998); and C_α superpositions by TOP (Lu, 2000). These calculations were done using normalized structures, i.e., if one of the structures has a truncated residue at a position that could affect a calculation, that residue was truncated in all the structures. Enzyme-ligand hydrogen bonds as determined by CONTACT (CCP4, 1994) are compiled in Table 2. Figures were prepared with MOLSCRIPT (Esnouf, 1997) and PYMOL (DeLano, 2002).

Site-directed mutagenesis and kinetic assays

Site-directed mutagenesis was performed with the Quik Change mutagenesis kit from Stratagene using the expression plasmid described in (Naught et al., 2003) as the template DNA. The E325A mutant was confirmed by automated DNA sequencing.

Galactose 1-phosphate was obtained from Sigma and used without further purification. Allose 1-phosphate was synthesized following the general method for phosphorylation of hexoses (Warren and Jeanloz, 1973). Briefly, β -D-allose (0.25 g, 1.4 mmol) was dissolved in 1 mL freshly distilled pyridine and chilled on ice. Acetic anhydride (1.0 mL, 10.6 mmol) was added drop wise with stirring. After addition was complete, the reaction was allowed to warm to room temperature and stirred overnight. The solvent was removed by rotary evaporation and the residue was dissolved in 10 mL diethyl ether. The protected allose was transferred to a flask containing crystalline H_3PO_4 (0.8 g, 8.2 mmol) that had previously been dried *in vacuo* over P_2O_5 . The solvent was removed by rotary evaporation and the flask was evacuated and placed in an oil bath at 65° C. After 2 hours, the reaction mixture was removed from the oil bath and cooled, and the residue was dissolved in THF and cooled in an ice-salt water bath. The pH of the solution was adjusted to neutrality by the addition of 1.5 mL concentrated NH_4OH . Ammonium phosphate that precipitated from the solution was collected by filtration, washed with THF, and combined with the original filtrate. The solvent was removed by rotary evaporation to yield a brown oil. The oil was dissolved in a small volume of H_2O and extracted six times with CHCl_3 . A few drops of pyridine were added to the aqueous solution and the solvent was removed by rotary evaporation. The residue was resuspended in toluene and the solvent was again evaporated; resuspension in toluene and evaporation was repeated once more. The residue was dissolved in 10 mL methanol and

2-3 mL of sodium methoxide (25% w/w) was added drop wise. A white precipitate slowly formed; the solution was allowed to stand on ice for several hours, and the precipitate collected by centrifugation and washed with methanol. The solid was dissolved in H₂O and the pH of the solution quickly adjusted to 7.5 by the addition of 1 N HCl.

The crude product was purified by chromatography on DEAE Sephadex A-25 (1.5 x 6 cm) equilibrated in 10 mM triethylammonium bicarbonate. The column was developed with a gradient to 0.5 M triethylammonium bicarbonate over 200 mL. Fractions containing product were combined and the solvent was removed by rotary evaporation. ³¹P NMR analysis revealed peaks at -0.69 ppm and -1.13 ppm, present in a 3:1 ratio, representing the anomers of allose 1-P.

Galactose 1-phosphate and allose 1-phosphate were tested as substrates for wild-type PMM/PGM and the E325A mutant. Each compound was incubated at a concentration of 0.2 mM with 14 µg of enzyme, 2 µM glucose 1,6-bisphosphate, and 1.5 mM MgSO₄ in MOPS at pH 7.4 in a total volume of 1.0 mL. Aliquots were removed periodically, and after the enzyme was removed by vortexing with CHCl₃, analyzed by HPLC. Substrate depletion and product formation were evaluated directly by HPLC, using a Dionex Carbopac-1 column and pulsed amperometric detection (Dionex ED-40). The column was equilibrated in 0.1 M NaOH and operated at a flow rate of 1 mL/min; after injection of a 25 µl sample the column was washed for 1 minute in the starting solvent, and developed with a gradient over 15 minutes to solvent containing 0.1 M NaOH and 0.5 M NaOAc. Standard samples of G1P, galactose 1-phosphate, allose 1-phosphate, and G6P, eluted at 8.8 min, 8.2 min, 9.3 min, and 10.6 min, respectively.

Acknowledgements

We thank Wei Yang for suggesting crystal transfer into PEG to assist with complex formation. We acknowledge Keith Brister and the staff of beam line 14-BMC of the Advanced Photon Source of Argonne National Laboratory for synchrotron time and technical expertise. Use of the Advanced Photon Source was supported by the U.S. Department of Energy, Basic Energy Sciences, Office of Science. Use of the BioCARS Sector 14 was supported by the National Institutes of Health, National Center for Research Resources. This research was supported by a grant from NIH.

Coordinates: The G1P, G6P, M1P, and M6P coordinates and structure factors have been deposited in the PDB with ID codes of 1P5D, 1P5G, 1PCJ, 1PCM, respectively.

Table 1. Data collection and refinement statistics

	<u>G1P</u>	<u>G6P</u>	<u>M1P</u>	<u>M6P</u>
Data Collection *				
X-ray source	14-BMC	14-BMC	Home source	14-BMC
Space group	P2 ₁ 2 ₁ 2 ₁	P2 ₁ 2 ₁ 2 ₁	P2 ₁ 2 ₁ 2 ₁	P2 ₁ 2 ₁ 2 ₁
Cell, Å	a= 70.70 b= 74.19 c= 84.84	a= 70.59 b= 74.37 c= 85.99	a= 70.90 b= 74.31 c= 85.48	a= 70.65 b= 74.19 c= 85.40
λ , Å	0.900	0.900	1.54	0.900
Resolution, Å	25.0-1.60	25.0-1.60	100.0-2.0	25.0-1.90
Unique ref./redundancy	58633/8.2	59418/12.9	30357/4.8	35051/3.5
R _{merge} , %	7.4 (49.1)	6.2 (47.7)	4.5 (25.5)	6.0 (35.8)
I/ σ	32.1 (3.8)	41.8 (5.6)	29.2 (5.9)	21.9 (3.4)
Completeness, %	99.1 (98.3)	98.7 (87.7)	97.1 (96.4)	97.3 (97.8)
Refinement Statistics				
Resolution, Å	25.0-1.6	25.0-1.61	55.9-2.0	24.9-1.9
R _{work} /R _{free}	0.16/0.18	0.16/0.19	0.16/0.20	0.17/0.20
Non-H atoms	3536	3535	3455	3429
Waters	490	441	333	347
, Å ²				
protein atoms	16.42	15.3	29.03	20.09
waters	29.70	29.60	41.07	33.00
ligand	14.18	15.29	30.16	24.80
rmsd bonds Å/angles °	0.011/1.39	0.011/1.34	0.010/1.23	0.010/1.27
Ramachandran 1/2 [†] %	92.7/7.0	92.4/7.3	91.9/7.5	92.7/7.0

*Values for highest resolution shell are in parentheses. †1) Most favored and 2) additionally allowed regions.

Table 2. Enzyme-ligand hydrogen bond contacts in PMM/PGM complexes

	Ligand atom	Protein atom	G1P (Å)	M1P (Å)	1s*	G6P (Å)	M6P (Å)	6s [†]	ALL [‡]
Phosphate contacts	O1P	K285 NZ				2.77	3.01	✓	
		R421 NH1	2.78	2.74		2.72	2.67		✓
		Water	2.76	2.58	✓				
	O2P	S423 OG	2.64	2.71		2.62	2.61		✓
		T425 OG1	2.72	2.71		2.67	2.73		✓
		Water	2.77	2.68		2.79	2.86		✓
	O3P	Y17 OH	2.61	2.58		2.62	2.56		✓
		R421 NH2	2.95	2.94		2.94	3.00		✓
		N424 N	2.88	2.82		2.84	2.92		✓
Sugar ring contacts	O1	S108 O1P				2.53	2.60	✓	
		Water				3.26			
	O2	S108 O2P				3.11			
		K285 NZ	2.92						
		H329 NE2				3.03			
	O3	Water	3.17	2.55	✓				
		Water				2.92	2.86	✓	
		H308 N				2.83	2.78	✓	
		E325 OE1	2.56	2.55	✓				
	O4	E 325 OE2				2.59	2.70	✓	
		S327 OG	2.69	2.73	✓				
		Water	2.84	2.74	✓				
	O5	H308 N	2.93	3.07	✓				
		E325 OE1				2.53	2.67	✓	
		E325 OE2	2.73	2.79	✓				
S327 OG					2.80	2.69	✓		
O6	Water				3.18	3.06	✓		
	R247 NH2	3.24							
O6	S108 O1P	2.66	2.59	✓					
	H329 NE2	2.75	2.85	✓					

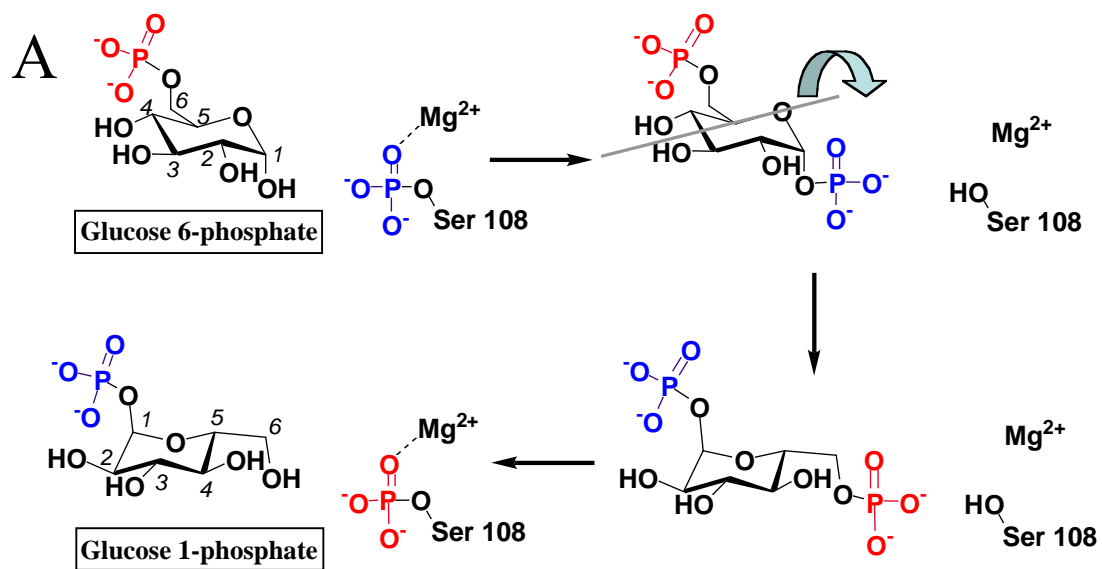
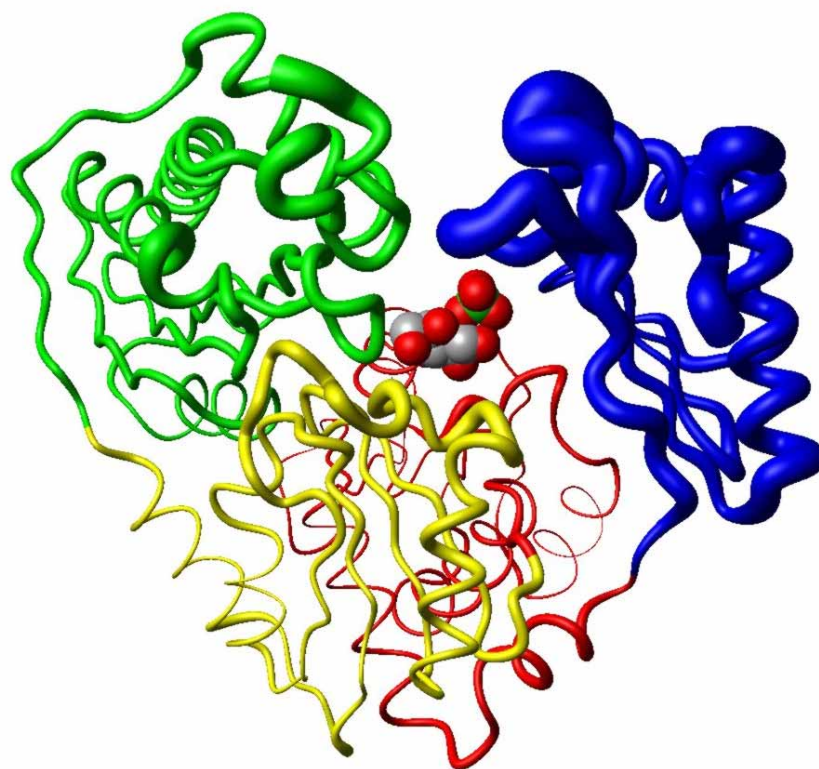
All hydrogen bonds are < 3.3 Å with favorable geometry. *1s: contacts specific to G1P and M1P complexes. †6s: contacts specific to G6P and M6P complexes. ‡Contacts conserved in all four enzyme-substrate complexes.

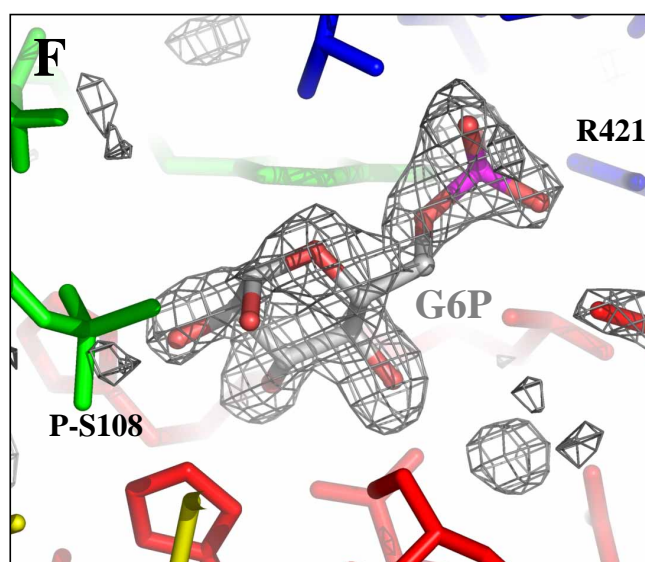
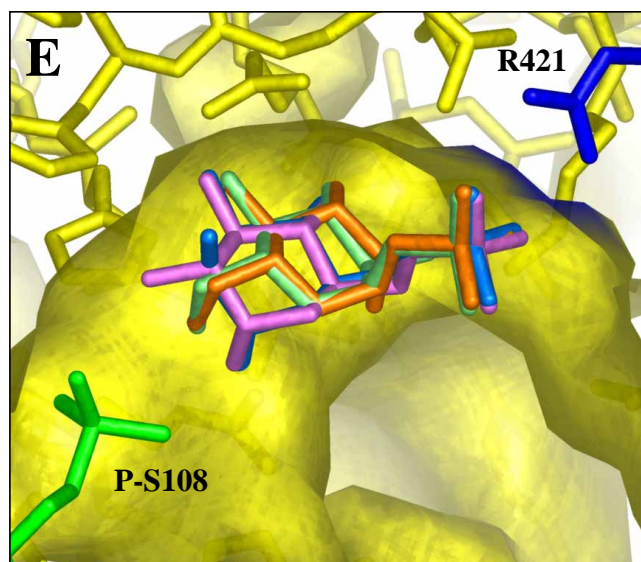
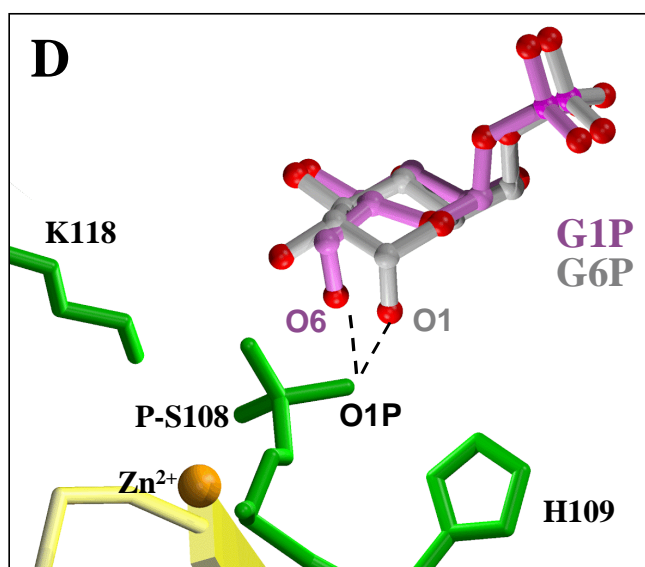
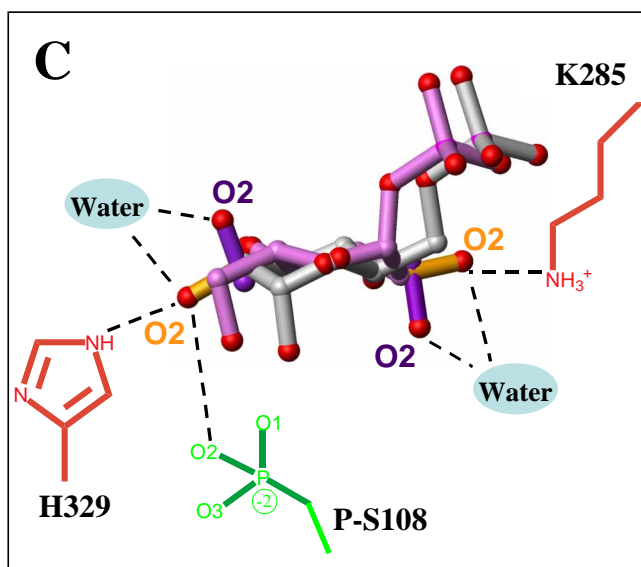
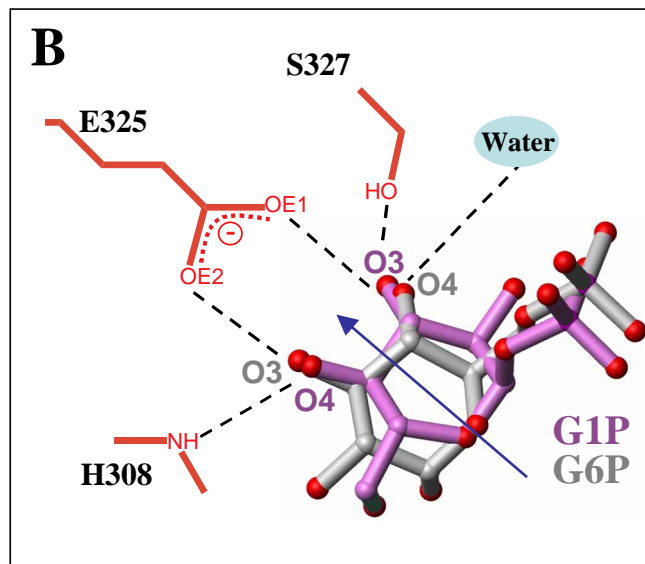
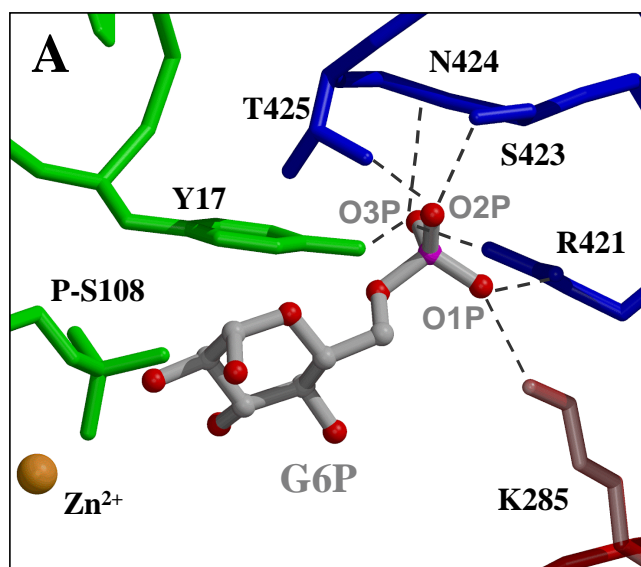
Figure Legends

Fig. 1. (A) Mechanism of PMM/PGM shown in the biosynthetic direction of the reaction with G6P as the substrate. (B) Tube rendering of PMM/PGM and the G1P complex. The apo-protein and G1P complex were superimposed and the areas differing between the two protein backbones are shown as a tube of varying diameter, proportional to the differences between the two structures. Domains 1 to 4 are shown in green (residues 1-153), yellow (residues 154-256), red (residues 257-368) and blue (residues 369-463), respectively.

Fig. 2. A close-up view of interactions between PMM/PGM and its phosphosugar substrates. Protein side chains are shown using the same color scheme as in Fig. 1B. (A) The invariant phosphate-binding site illustrated with G6P. (B) Superposition of G1P and G6P with critical contacts to the O3 and O4 hydroxyls highlighted. (C) Schematic of contacts made with the four different positions of the O2 hydroxyl. The full structures of G1P and G6P are shown (with the C2-O2 bond in orange). For M1P and M6P, only the C2-O2 bond of the sugar is shown (in purple). (D) Close-up view of the O1 and O6 hydroxyls of G6P and G1P in the phosphoryl transfer site. (E) Superposition of the four phosphosugar substrates in the active site of PMM/PGM. G1P is lime green, G6P is purple, M1P is orange, and M6P is light blue. The protein surface is colored yellow; protein interior is white. (F) An $F_o - F_c$ difference Fourier map (contoured at 3σ) showing electron density (gray) for G6P in the active site. Phases for the map are from the

beginning of the refinement process, immediately after the first round of rigid-body and positional refinement, and prior to extensive manual rebuilding. Substrate and solvent were not included in the model.

Fig. 1**B**



References

1. Atkinson, M. R., Johnson, E., and Morton, R. K. (1961). Equilibrium constants of phosphoryl transfer from C-1 to C-6 of alpha-D-glucose 1-phosphate and from glucose 6-phosphate to water. *Biochem J* 79, 12-15.
2. Brünger, A. T., Adams, P. D., Clore, G. M., DeLano, W. L., Gros, P., Grosse-Kunstleve, R. W., Jiang, J. S., Kuszewski, J., Nilges, M., Pannu, N. S., *et al.* (1998). Crystallography & NMR system: A new software suite for macromolecular structure determination. *Acta Crystallogr. D* 54, 905-921.
3. DeLano, W. L. (2002). The PyMOL Molecular Graphics System (San Carlos, CA, DeLano Scientific).
4. Esnouf, R. M. (1997). An extensively modified version of MolScript that includes greatly enhanced coloring capabilities. *J. Mol. Graph. Model.* 15, 132-134, 112-133.
5. Govan, J. R. W., and Deretic, V. (1996). Microbial pathogenesis in cystic fibrosis - Mucoid *Pseudomonas aeruginosa* and *Burkholderia cepacia*. *Microbiol. Rev.* 60, 539-574.
6. Hayward, S., and Berendsen, H. J. (1998). Systematic analysis of domain motions in proteins from conformational change: new results on citrate synthase and T4 lysozyme. *Proteins* 30, 144-154.
7. Jones, S., and Thornton, J. M. (1996). Principles of protein-protein interactions. *Proc. Natl. Acad. Sci. USA* 93, 13-20.

8. Jones, T. A., Zou, J. Y., Cowan, S. W., and Kjeldgaard, M. (1991). Improved methods for building protein models in electron density maps and the location of errors in these models. *Acta Crystallogr. A* 47, 110-119.
9. Knowles, J. R. (1980). Enzyme-catalyzed phosphoryl transfer reactions. *Annu Rev Biochem* 49, 877-919.
10. Laskowski, R. A., McArthur, M. W., Moss, D. S., and Thornton, J. M. (1993). PROCHECK: A program to check the stereochemical quality of protein structures. *J. Appl. Crystallogr.* 26, 283-291.
11. Liang, J., Edelsbrunner, H., and Woodward, C. (1998). Anatomy of protein pockets and cavities: measurement of binding site geometry and implications for ligand design. *Protein Sci.* 7, 1884-1897.
12. Liu, Y., Ray, W., and Baranidharan, S. (1997). Structure of rabbit muscle phosphoglucomutase refined at 2.4 Å resolution. *Acta Crystallogr. D* 53, 392-405.
13. Lowry, O. H., and Passonneau, J. V. (1969). Phosphoglucomutase kinetics with the phosphates of fructose, glucose, mannose, ribose, and galactose. *J. Biol. Chem.* 244, 910-916.
14. Lu, G. (2000). TOP: A new method for protein structure comparison and similarity searches. *J. Appl. Crystallogr.* 33, 176-183.
15. Lyczak, J. B., Cannon, C. L., and Pier, G. B. (2000). Establishment of *Pseudomonas aeruginosa* infection: lessons from a versatile opportunist. *Microbes Infect.* 2, 1051-1060.

16. Muller, S., Diederichs, K., Breed, J., Kissmehl, R., Hauser, K., Plattner, H., and Welte, W. (2002). Crystal structure analysis of the exocytosis-sensitive phosphoprotein, pp63/parafusin (phosphoglucomutase), from *Paramecium* reveals significant conformational variability. *J. Mol. Biol.* *315*, 141-153.
17. Murshudov, G. N., Vagin, A. A., Lebedev, A., Wilson, K. S., and Dodson, E. J. (1999). Efficient anisotropic refinement of macromolecular structures using FFT. *Acta Crystallogr. D* *55*, 247-255.
18. Naught, L. E., Regni, C., Beamer, L. J., and Tipton, P. A. (2003). Roles of active site residues in *P. aeruginosa* phosphomannomutase/phosphoglucomutase. *Biochemistry* *42*, 9946-9951.
19. Naught, L. E., and Tipton, P. A. (2001). Kinetic Mechanism and pH Dependence of the Kinetic Parameters of *Pseudomonas aeruginosa* Phosphomannomutase/Phosphoglucomutase. *Arch Biochem Biophys* *396*, 111-118.
20. CCP4 Collaborative Computational Project No. 4 (1994). The CCP4 suite: Programs for Protein Crystallography. *Acta Crystallogr. D* *50*, 760.
21. Olvera, C., Goldberg, J. B., Sanchez, R., and Soberon-Chavez, G. (1999). The *Pseudomonas aeruginosa* algC gene product participates in rhamnolipid biosynthesis. *FEMS Microbiol. Lett.* *179*, 85-90.
22. Otwinowski, Z., and Minor, W. (1997). Processing of X-ray diffraction data collected in oscillation mode. *Methods Enzymol.* *276*, 307-326.

23. Percival, M. D., and Withers, S. G. (1992). ^{19}F NMR investigations of the catalytic mechanism of phosphoglucomutase using fluorinated substrates and inhibitors. *Biochemistry* *31*, 505-512.
24. Ray, W. J., Jr., Burgner, J. W., 2nd, and Post, C. B. (1990). Characterization of vanadate-based transition-state-analogue complexes of phosphoglucomutase by spectral and NMR techniques. *Biochemistry* *29*, 2770-2778.
25. Regni, C., Tipton, P. A., and Beamer, L. J. (2002). Crystal structure of PMM/PGM: an enzyme in the biosynthetic pathway of *P. aeruginosa* virulence factors. *Structure* *10*, 269-279.
26. Regni, C. A., Tipton, P. A., and Beamer, L. J. (2000). Crystallization and initial crystallographic analysis of phosphomannomutase/phosphoglucomutase from *Pseudomonas aeruginosa*. *Acta Crystallogr. D* *56*, 761-762.
27. Rocchetta, H. L., Burrows, L. L., and Lam, J. S. (1999). Genetics of O-antigen biosynthesis in *Pseudomonas aeruginosa*. *Microbiol. Mol. Biol. R.* *63*, 523-553.
28. Vaguine, A. A., Richelle, J., and Wodak, S. J. (1999). SFCHECK: a unified set of procedures for evaluating the quality of macromolecular structure-factor data and their agreement with the atomic model. *Acta Crystallogr. D* *55*, 191-205.
29. Warren, C. D., and Jeanloz, R. W. (1973). Chemical synthesis of ficaprenyl alpha-D-mannopyranosyl phosphate. *Biochemistry* *12*, 5031-5037.

30. Yankeelov, J. A., and Koshland, D. E. (1965). Evidence for conformation changes induced by substrates of phosphoglucomutase. *J. Biol. Chem.* *240*, 1593-1602.

31. Ye, R. W., Zielinski, N. A., and Chakrabarty, A. M. (1994). Purification and characterization of phosphomannomutase/phosphoglucomutase from *Pseudomonas aeruginosa* involved in biosynthesis of both alginate and lipopolysaccharide. *J. Bacteriol.* *176*, 4851-4857.

32. Zielinski, N. A., Chakrabarty, A. M., and Berry, A. (1991). Characterization and regulation of the *Pseudomonas aeruginosa* algC gene encoding phosphomannomutase. *J. Biol. Chem.* *266*, 9754-9763.

CHAPTER 5

ROLES OF ACTIVE SITE RESIDUES IN *PSEUDOMONAS AERUGINOSA* PHOSPHOMANNOMUTASE/PHOSPHOGLUCOMUTASE

Reproduced with permission from Naught, L.E., Regni, C.A., Beamer, L.J., and P.A. Tipton, *Roles of active site residues in Pseudomonas aeruginosa Phosphomannomutase/Phosphoglucomutase*. *Biochemistry*, 2003. **42**(33): p. 9946-51. Copyright 2003 American Chemical Society.

Abstract

In *Pseudomonas aeruginosa* the dual specificity enzyme phosphomannomutase/phosphoglucomutase catalyzes the transfer of a phosphoryl group from serine 108 to the hydroxyl group at the 1-position of the substrate, either mannose 6-P or glucose 6-P. The enzyme must then catalyze transfer of the phosphoryl group on the 6-position of the substrate back to the enzyme. Each phosphoryl transfer is expected to require general acid-base catalysis, provided by amino acid residues at the enzyme active site. An extensive survey of the active site residues by site-directed mutagenesis failed to identify a single key residue that mediates the proton transfers. Mutagenesis of the active site residues Arg 20, Lys 118, Arg 247, His 308, and His 329 to residues that do not contain ionizable groups produced proteins in which V_{\max} was reduced to 4-12% that of wild type. The fact that no single residue decreased catalytic activity more significantly, and that several residues had similar effects on V_{\max} , suggested that the ensemble of active site amino acids act by creating positive electrostatic potential, which serves to depress the pK of the substrate hydroxyl group so that it binds in ionized form at the active site. In this way the necessity of positioning the reactive hydroxyl group near a specific amino acid residue is avoided, which may explain how the enzyme is able to promote catalysis of both phosphoryl transfers, even though the 1- and 6-positions do not occupy precisely the same position when the substrate binds in the two different orientations in the active site. When Ser 108 is mutated, the enzyme retains a surprising amount of activity, which has led to the suggestion that an alternative residue becomes phosphorylated in the absence of Ser 108. ^{31}P NMR spectra of the S108A protein confirm that it is phosphorylated. Although the S108A/H329N protein had no detectable catalytic activity, the ^{31}P NMR spectra were not consistent with a phospho-histidine residue.

In the bacterium *Pseudomonas aeruginosa* the *algC* gene encodes the dual specificity enzyme phosphomannomutase/phosphoglucomutase, which catalyzes the interconversion of mannose 6-P and mannose 1-P, as well as the interconversion of glucose 6-P and glucose 1-P. Genetic studies have established that the PMM¹ activity is required for both alginate and lipopolysaccharide biosynthesis, and that the PGM activity is required for LPS biosynthesis (1). Recently it has been shown that *algC* is also required for rhamnolipid biosynthesis (2), and that rhamnolipids are required for mature biofilm formation (3). Since alginate, LPS, and rhamnolipid are all important virulence factors, PMM/PGM may be a useful target for pharmaceutical intervention to combat *P. aeruginosa* infections, and detailed characterization of PMM/PGM should facilitate the development of useful inhibitors.

Steady-state kinetic characterization of the PMM and PGM activities in the biosynthetically relevant direction established that mannose 6-P and glucose 6-P are accepted by PMM/PGM as substrates with equal efficiency (4). The active site has been identified through structural studies (5); Ser 108 is phosphorylated in the resting enzyme, and the catalytic mechanism is believed to involve initial transfer of the phosphoryl group from Ser 108 to the substrate to generate a bis-phosphorylated intermediate. To complete the catalytic cycle the intermediate must reorient and then rephosphorylate Ser 108 using the phosphoryl group that was on the substrate originally. The net effect of these group transfers is to move a phosphoryl group from the 6-position to the 1-position of the substrate and regenerate active, phosphorylated enzyme. Each phosphoryl transfer is expected to require general base catalysis to increase the nucleophilicity of the hydroxyl group to be phosphorylated, and general acid catalysis to stabilize the group from which the phosphoryl group was transferred. With a structure of PMM/PGM containing ligands bound at the active site in hand, we have applied site-directed mutagenesis and kinetic studies to

identify the residues that serve as general acid/general base residues in the catalytic reaction. Surprisingly, we found that no single residue could be identified as playing a critical role in the catalytic reaction; rather, mutation of each of several residues led to significant decreases in V_{\max} , but did not abolish activity. We also have investigated further the surprising observation we reported earlier (4), that mutation of Ser 108 to alanine led to only a 20-fold reduction in V_{\max} . We now provide direct spectroscopic evidence that the S108A mutant protein is phosphorylated, although the site of phosphorylation remains obscure. The picture that emerges from these mutational studies is of an unusually plastic active site in which the reactivity of the substrate is modulated by an ensemble of amino acids, rather than one in which individual amino acids play unique, easily identifiable roles.

Materials and Methods

Glucose 1-P, glucose 1,6-P₂, and glucose 6-P dehydrogenase from *Leuconostoc mesenteroides* were obtained from Sigma.

The *algC* gene, encoding PMM/PGM, was subcloned into the pET-14b vector (Novagen), to allow for the production of PMM/PGM containing a (His)₆-tag at the N-terminus. *E. coli* BL21(DE3) cells were transformed with the expression plasmid; cell growth, preparation and treatment of the cell free extract with protamine sulfate and ammonium sulfate was performed as described previously (4). The ammonium sulfate pellet containing PMM/PGM was dissolved in 20 mM sodium phosphate buffer, pH 7.4, containing 10 mM imidazole and 0.5 M NaCl (buffer A). The sample was applied to a Chelating Sepharose (Pharmacia) column charged with Ni²⁺ and equilibrated in buffer A. The column was washed with buffer A until the absorbance of the eluate at 280 nm returned to baseline. PMM/PGM was eluted from the column by washing with

buffer A supplemented with 140 mM imidazole. Fractions containing PMM/PGM were identified by enzymatic activity or by SDS-PAGE. The desired fractions were pooled, concentrated by ultrafiltration, supplemented with glycerol to 10% (v/v) and stored at -80 °C.

Site-directed mutants of PMM/PGM were constructed using the QuikChange mutagenesis kit (Stratagene); the integrity of each mutated *algC* gene was verified by automated DNA sequencing. Mutants were purified in the same manner as the wildtype protein. Purified proteins were characterized by CD spectroscopy to determine whether gross changes in secondary structure had been incurred by the mutations.

Wild type PMM/PGM and the S108A mutant were characterized by MALDI-TOF mass spectrometry, after in-gel trypsin digestion, at the University of Missouri Proteomics Center. The expected peptides and the masses were calculated with the Peptide-Mass algorithm at the ExPASy website (<http://us.expasy.org/cgi-bin/peptide-mass.p1>). The mass spectrometry analysis was conducted with approximately 10 µg of each protein sample.

³¹P NMR spectra of PMM/PGM S108A were acquired using a Bruker DMX500 spectrometer operating at 203 MHz. The sample was dialyzed exhaustively to remove the phosphate buffer from the metal affinity chromatography step, and the protein was concentrated to 1 mM. The sample was prepared in H₂O in 50 mM MOPS, pH 7.4 containing 0.5 mM DTT; 50 µl d₆-DMSO was added to the 0.6 mL sample to provide a lock signal. Spectra were obtained using a 0.5 s acquisition time, 0.5 s relaxation delay, and approximately 50,000 scans. After the spectrum of the native protein was acquired, NaOH was added to raise the pH to 12, and a spectrum of the denatured protein was obtained.

The activity of each mutant protein was quantitated by measuring the PGM activity in the direction of glucose 6-P formation, using a coupled assay with glucose 6-P dehydrogenase.

Glucose 1-P was varied from 1-200 μM , NAD^+ was present at 0.9 mM, glucose 1,6- P_2 was at 0.5 μM , and MgSO_4 was at 1.5 mM. Reactions were run in 50 mM MOPS, pH 7.4, containing 1 mM DTT. The reaction was monitored by measuring the rate of production of NADH, based on its fluorescence at 430 nm when excited at 340 nm. Changes in fluorescence signal per unit time were converted to concentration units by constructing a standard curve with authentic NADH. The kinetic data were fitted to either the Michaelis-Menten equation or to equation 1 when substrate inhibition was observed.

$$v = \frac{VA}{K_a + A + A^2 / K_I} \quad (1)$$

Results

For the studies reported here PMM/PGM was produced with a His-tag, in order to ensure that the activity that was measured arose from PMM/PGM and not from contaminating *E. coli* PGM. All of the mutants were soluble and their CD spectra were identical with the wild type protein, suggesting that the mutations that were introduced did not cause dramatic changes in structure. A comparison of wild type PMM/PGM with and without the His-tag demonstrated that it did not affect the kinetic properties of the enzyme (data not shown). All of the proteins produced for this study were >95% pure after metal affinity chromatography, based on Coomassie Blue-stained SDS-PAGE gels.

The kinetic properties of the mutant proteins that were produced in order to examine the roles of potential acid-base catalytic residues are listed in Table 1. It can be seen that the H109Q, H329N, K118L, R20A, and R247A proteins have similar kinetic properties. In each instance

V_{\max} and V/K are reduced to 5-10% of the values of the wild type enzyme. The H308N protein has kinetic properties quite similar to that of wild type enzyme.

A second group of mutant enzymes was prepared in an attempt to identify the putative alternative phosphorylation site, that is, the residue that is phosphorylated in the absence of Ser 108 (Table 2). The S108A protein exhibited V_{\max} that was greater than 10% the value of wild type enzyme; V/K was unchanged from the wild type. When Ser 108 was replaced by a charged residue (aspartate), V_{\max} decreased 10-fold as in the S108A protein, and V/K decreased four-fold relative to wild type. Replacement of Ser 108 by valine had a more dramatic effect on V_{\max} , which decreased to 1% of the wild type value; V/K also decreased approximately 100-fold. The three active site histidine residues were each mutated in the S108A mutant protein, to create three double mutants. The S108A/H109Q and S108A/H308N proteins showed kinetic properties similar to the S108A and H109Q single mutants. However, the S108A/H329N double mutant exhibited no detectable kinetic activity.

We confirmed that the S108A protein was phosphorylated by ^{31}P NMR. The spectrum of the native protein exhibited a broadened peak at -0.80 ppm, which we attribute to the phosphorylated protein, as well as a peak at 2.2 ppm that we attribute to inorganic phosphate, and a peak at 5.4 ppm, whose origin is unknown. Upon denaturation of the enzyme by addition of NaOH to raise the pH to 12, the peak at -0.80 ppm disappeared, and was replaced by a 47 Hz wide peak at 3.9 ppm.

We explored the possibility of determining the site of phosphorylation in the S108A mutant directly by mass spectrometry. Preliminary measurements of the mass of PMM/PGM and various mutants strongly suggested that the proteins were phosphorylated (data not shown). However, ambiguities arising from methionine oxidation and matrix effects led us to seek

improved precision by characterizing tryptic peptides rather than the entire protein. The wild type protein yielded a peptide of mass 2000.17 Da, which corresponds to the Ser 108-containing peptide that extends from residues 101-118. The calculated mass of the phosphorylated peptide is 2000.10 Da, consistent with our expectation that Ser 108 is phosphorylated. In the S108A protein the 101-118 peptide, which was not expected to be phosphorylated, had an observed mass of 1903.22 Da, which compares well with the calculated mass of 1902.88 Da. Based on the kinetic analysis of the double mutants, we sought to determine whether His 329 was phosphorylated in the S108A protein. His 329 is contained in the 317-333 peptide that is generated by trypsin digestion. In the wild type and S108A mutant proteins the observed masses for the 317-333 peptide were 1791.91 Da and 1792.12 Da, respectively. The calculated mass for the non-phosphorylated peptide is 1791.87 Da. Thus, the mass spectrometry analysis provided no evidence that His 329 is phosphorylated in the S108A mutant.

Discussion

In each catalytic cycle PMM/PGM must catalyze two chemical events, the first a phosphoryl transfer from the enzyme to the substrate, the second a phosphoryl transfer from the intermediate back to the enzyme. The chemistry of phosphoryl transfers has been studied extensively (6). Regardless of whether the group transfer proceeds via an associative or a dissociative mechanism, the hydroxyl group that is being phosphorylated must be deprotonated, so one would expect the reaction to be facilitated by an amino acid residue acting as a general base. For example, the crystal structure of brain hexokinase I establishes that Asp 657 is within 3 Å of the 6-OH group of glucose bound at the active site (7). The hydroxyl group must be deprotonated to allow phosphorylation of glucose by MgATP, and the activity of the D657A mutant protein is

too low to characterize (8), suggesting that Asp 657 serves as the general base in the hexokinase reaction. Phosphoryl group transfer should also be facilitated by general acid catalysis, to stabilize via protonation the alkoxide formed at the position from which the phosphoryl group departs. In the first half of the reaction catalyzed by PMM/PGM, the leaving group is the sidechain of Ser 108. An analogous reaction is that catalyzed by calcineurin, which catalyzes the dephosphorylation of phosphoserine and phosphothreonine residues; it has been proposed that His 151 functions as a general acid to protonate the leaving serine or threonine residue (9).

Examination of the active site of PMM/PGM with substrate bound reveals a rich array of amino acid residues that could potentially serve as general acid-base catalysts (Scheme 1). Arg 20, His 109, and Lys 118 are all located appropriately to act as a general acid to stabilize Ser 108 during phosphorylation of the substrate, and to deprotonate the Ser 108 sidechain when it is being rephosphorylated by the reaction intermediate. His 308 is 4 Å from the hydroxyl at the 6-position of the substrate, and appeared to be a likely candidate to act as a general base. Arg 247 and His 329 are 5-7 Å from the phosphorylation site, and were considered as potential candidates as well. The disordered electron density for Arg 20 and Arg 247 indicates that those residues may be mobile, and therefore we considered the possibility that dynamic motions during the catalytic cycle could bring one of them, or another residue, into closer proximity to the substrate.

Surprisingly, mutagenesis of either Arg 20, His 109, Lys 118, Arg 247, or His 329 to a residue that could not participate in general acid-base catalysis resulted in a substantial loss of catalytic activity, as reflected in V_{\max} ; however, none of the mutants lost so much activity that the mutated residue could be considered to be absolutely critical for catalysis. Of all the mutant proteins generated, only H308N was unchanged in its kinetic parameters from the wild type enzyme. The V_{\max} values in the other mutants varied from 4% to 12% of the wild type enzyme;

such changes are clearly within the limits of the accuracy of the kinetic experiments, yet are far smaller than what would be expected for loss of a residue that played a unique, required role in the reaction. For example, mutation of Glu 165, which acts as the general base in the triose phosphate isomerase reaction, to an aspartate residue, resulted in a decrease in V_{\max} of 1000-fold (10), and mutation of His 95, which acts as the general acid, caused a 400-fold decrease in V_{\max} (11). A trivial explanation for the residual activity that was measured with PMM/PGM is that it arises from contaminating *E. coli* PGM, but we consider that unlikely since each mutant protein was purified by metal-affinity chromatography and appeared pure by SDS-PAGE.

Since no single residue could be identified as the expected general base or general acid, but rather several residues appeared to be important for full activity, we considered what the effect of the ensemble of amino acids would be. Figure 1 shows how Arg 20, His 109, Lys 118, Arg 247, and His 329 are arranged at the active site. Figure 2 shows the electrostatic potential generated by the amino acid residues at the active site, and it can be seen that the phosphorylated serine residue and the reactive hydroxyl group on the substrate lie between two regions of positive electrostatic potential. This arrangement suggests a possible explanation for the kinetic data and a mechanism for facilitating phosphoryl transfer. In the presence of a positive electrostatic field the pK of the substrate hydroxyl group should be decreased. If the effect is substantial enough the hydroxyl group may ionize "spontaneously", i.e., the substrate may be present as the alkoxide at the active site, so no general base is necessary for phosphorylation. Similarly, the Ser 108 alkoxide arising from phosphorylation of the substrate should be stabilized by the positive electrostatic field, so general acid catalysis would not be necessary. In this manner the enzyme can enhance the nucleophilicity of the phosphorylation acceptor group and stabilize the leaving group, but without utilizing classic general acid-base catalysis. The catalytic function of the

ensemble of amino acids would account for the substantial, but incomplete, loss of activity in each of the single mutants. The active site of PMM lies in a deep cleft, and only 5% of the surface of the substrate is solvent exposed; by sequestering the substrate from solvent, electrostatic effects arising from the protein should be enhanced.

An alternative explanation of the mutagenesis data is that the active site is constructed in a highly redundant fashion, so that if one residue is removed, another assumes its function. In order to evaluate that possibility the K118L/H109Q double mutant was constructed. Lys 118 and His 109 are each appropriately located to act as the general acid to stabilize the Ser 108 alkoxide formed by phosphorylation of the substrate. *A priori*, it seemed quite reasonable to suppose that either Lys 118 or His 109 could be the expected general acid. However, removal of either residue by mutagenesis did not decrease catalytic activity as much as we expected. To explain these data we hypothesized that in the artificial situation created by mutagenesis where one residue is absent, the other would substitute. However, the kinetic properties of the double mutant were quite similar to those of the two single mutants, demonstrating that the enzyme could capably function without either residue. Obviously, many other pairwise mutant possibilities are possible, and we have not explored them all, so it is formally possible that each mutation induces a different residue to function as a general acid-base catalyst. Such a scenario does not really explain why each individual mutation causes a significant diminution in V_{\max} , however, and therefore we do not favor this explanation.

A potential rationale for the strategy of utilizing electrostatic forces to ionize the substrate is that the enzyme must bind each of its substrates in two orientations, and it must accommodate two different substrates, mannose 6-P and glucose 6-P. Perhaps by utilizing electrostatic forces to favor the ionization of the substrate hydroxyls, the necessity of precise positioning of each

reactive hydroxyl within reach of a general base is avoided. Comparison of the structures of PMM/PGM with ligands bound shows that mannose 6-P and glucose 6-P do not place their reactive hydroxyl (at the 1-position) at the same position as do mannose 1-P and glucose 1-P (in which the reactive hydroxyl is at the 6-position)². However, in either orientation the reactive hydroxyl group is placed within the electrostatic field created by the electropositive active site residues. The N-terminal end of the α -helix extending between residues His 308 and Thr 318 also points into the active site, and the positive dipole moment arising from the helix could reinforce the effect caused by the active site residues.

Rabbit muscle phosphoglucomutase (PDB accession code 1C47) has a similar constellation of amino acid residues arranged in a manner like that seen in PMM/PGM; the proximal phosphoryl group is encircled by Arg 22, His 117, Lys 129, Arg 292, and Lys 388. A BLAST comparison of *P. aeruginosa* PMM/PGM with the 50 most closely related sequences reveals that Arg 20, His 109, Lys 118, Arg 247, and His 329 (*P. aeruginosa* numbering) are conserved with only two or three exceptions. Since all of these enzymes, and rabbit muscle PGM, face the same task as PMM/PGM, the positive electrostatic ring around the phosphoryl group may be a general strategy adopted to enhance the nucleophilicity of the reactive hydroxyl groups.

It is interesting to note that the K_m for glucose 1-P did not change significantly in any of the mutant proteins. The values that were measured when H109, K118, H308, H329, and R247 were mutated were within experimental error of the value observed with the wild type protein. The K_m in the R20A protein was lower than that observed in the wild type protein. These results suggest that the determinants for binding are other amino acid residues at the active site.

Mutation of His 109, Arg 20, and Arg 247 relieved the weak substrate inhibition that is observed with the wild type enzyme. Since substrate inhibition arises from the competition

between substrate and the bis-phosphorylated intermediate for binding to the dephospho-enzyme, the loss of substrate inhibition in these mutants suggests that, in addition to their role in promoting phosphoryl transfer, these residues are important in the binding of the intermediate to the enzyme.

Another surprising feature of *P. aeruginosa* PMM/PGM is the extensive activity of the proteins in which Ser 108 is mutated. The kinetic behavior of the enzyme strongly supports the proposed role of phosphoserine in the catalytic reaction (4), and the crystal structure of the enzyme demonstrates that Ser 108 is phosphorylated (5). However, the S108A mutant retained a value of V_{\max} that was 12% that of wild-type and the S108D mutant had a V_{\max} 7% that of wild type. We reported these observations earlier and suggested that in the absence of Ser 108 another residue at the active site became phosphorylated (4). Examination of the active site suggests that one of several histidine residues might be appropriately positioned to act as a surrogate for Ser 108. To further investigate the origin of the activity in the absence of Ser 108 we have constructed a series of double mutants, whose kinetic properties are listed in Table 2. While the S108A/H109Q and S108A/H308N double mutants did not differ substantially in their kinetic properties from either the S108A or H109Q single mutants,, the S108A/H329N double mutant had no detectable catalytic activity. Its CD spectrum was identical to that of the wild type protein, so it appears that its lack of catalytic activity is not a consequence of misfolding. Therefore, these data suggested that His 329 is the alternative site of phosphorylation in PMM/PGM.

However, the ^{31}P NMR data allow us to rule out phosphorylation of His 329, because the signal arising from the phosphorylated residue appears too far downfield. 3-*N*-Phosphohistidine and 1-*N*-phosphohistidine resonate at -3.9 ppm and -4.7 ppm, respectively.(12). Pyruvate

phosphate dikinase is a well-characterized enzyme that has a phosphohistidine residue. The native protein is characterized by a ^{31}P NMR peak at -4.0 ppm, which shifts to -3.9 ppm when the protein is denatured in 5 M urea (13). In comparison, the ^{31}P NMR signal for PMM/PGM S108A shifts from -0.8 ppm in the native protein downfield to 3.9 ppm in the denatured protein. Clearly, His 329 plays a critical role in the reaction catalyzed by the S108A mutant, but it does not appear to be the site of phosphorylation.

In summary, the results of the mutagenesis experiments described here yield a picture of PMM/PGM as a surprisingly elastic and resilient enzyme. The alternative phosphorylation site is probably a quirk of the enzyme, with no mechanistic or physiological significance. The strategy that is utilized for the required proton transfers is, however, probably of mechanistic significance. By constructing an active site in which substrate ionization can occur without precise positioning of the reactive hydroxyl near one particular residue, the enzyme has developed the means to accommodate the distinct geometrical orientations of the substrate that occur during the catalytic cycle.

Table 1. Kinetic parameters for PMM/PGM site-directed mutants in the conversion of glucose 1-P to glucose 6-P.

protein	V_{\max} (s^{-1})	V/K ($s^{-1}\mu M^{-1}$)	K_m (μM)	K_i (μM)
wild type	22±1	1.8±0.2	12±1	110 ± 10
H109Q	1.3±0.1	0.15±0.06	8±3	-- ^a
H308N	22±2	2.1±0.4	10±2	160 ± 30
H329N	1.4±0.3	0.09±0.04	16±6	170 ± 80
K118L	0.9±0.2	0.12±0.05	8±3	170 ± 80
R20A ^a	2.6±0.1	0.9±0.2	2.8±0.7	-- ^a
R247A ^a	1.9±0.1	0.22±0.06	9±2	-- ^a
H308N/H329N ^a	1.02±0.01	0.8±0.4	1.3±0.7	-- ^a
K118L/H109Q ^a	1.1±0.1	0.4±0.1	2.7±0.8	-- ^a

^ano substrate inhibition observed.

Table 2. Kinetic parameters for PMM/PGM Ser 108 mutants in the conversion of glucose 1-P to glucose 6-P.

protein	V_{\max} (s^{-1})	V/K ($s^{-1}\mu M^{-1}$)	K_m (μM)	K_i (μM)
wild type	22±1	1.8±0.2	12±1	110 ± 10
S108A	2.6±0.1	2.0±0.5	1.3±0.3	500 ±190
S108V	0.22±0.03	.022±0.006	10±2	280 ±100
S108D	1.52±0.08	0.44±0.09	3.4±0.6	-- ^a
S108A/H109Q	1.38±0.06	0.6±0.1	2.4±0.4	-- ^a
S108A/H308N	0.62±0.07	0.12±0.05	5±2	160 ± 10
S108A/H329N	n.d. ^b	n.d.	n.d.	-- ^a

^aSubstrate inhibition was not observed in these reactions. ^bn.d., not detectable.

Figure Legends

Figure 1. Closeup view of the PMM/PGM active site with glucose 1-P bound. Residues that are believed to play roles in the catalytic reaction are indicated.

Figure 2. Electrostatic potential in the active site of PMM/PGM. The potentials from coulombic interactions between the amino acid residues shown were calculated in DeepView and are contoured at +/- 2.55 kT/e; blue is positive potential and red is negative potential.

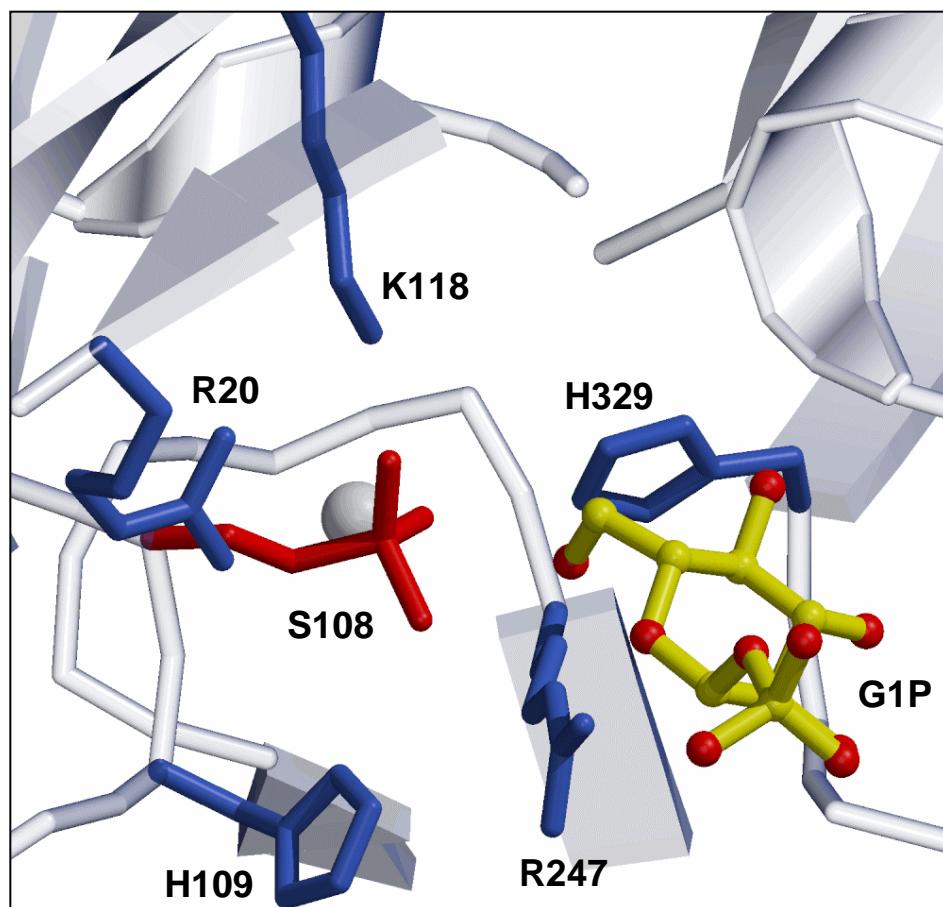


Figure 1

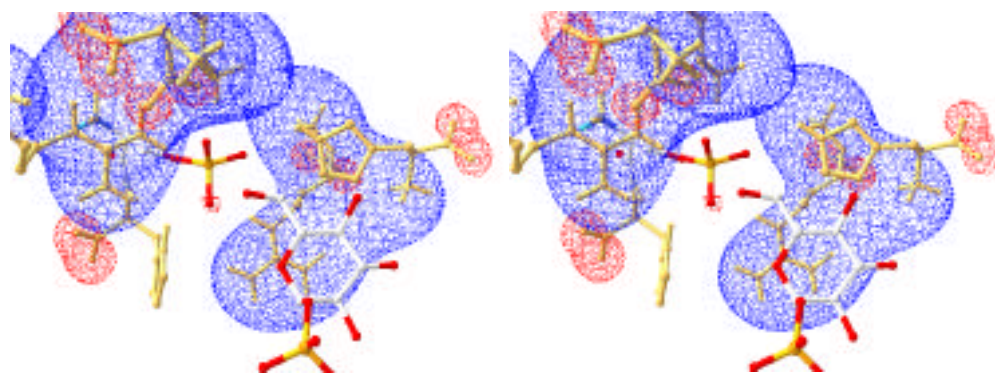
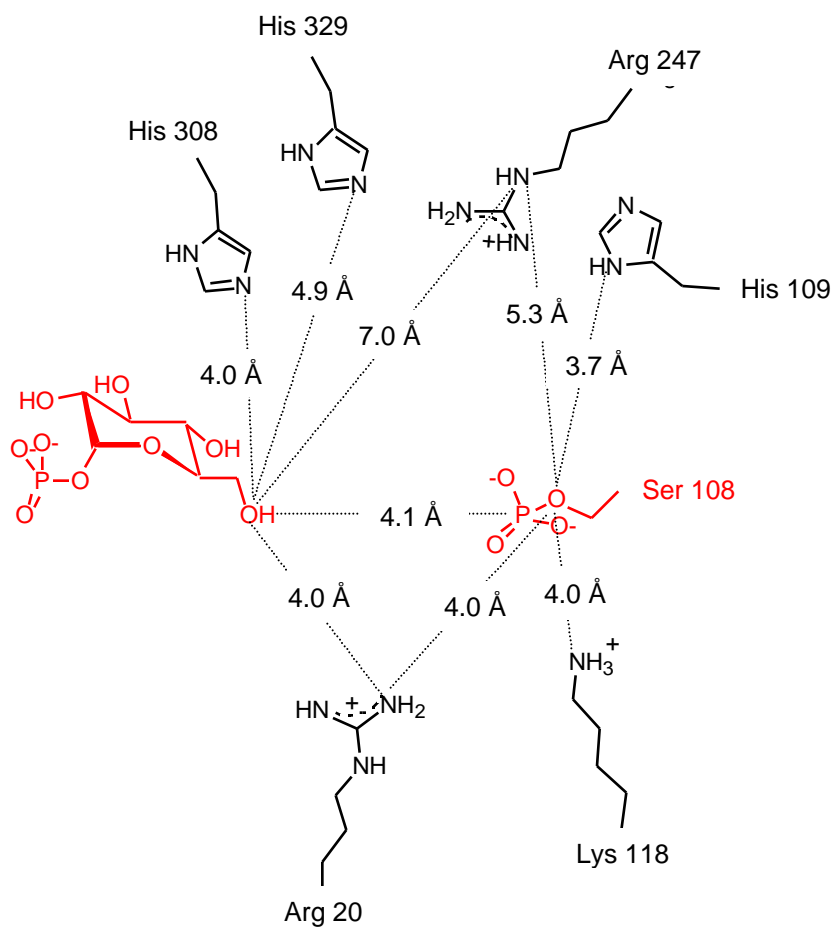


Figure 2

**Scheme 1**

References

1. Ye, R. W., Zielinski, N. A., and Chakrabarty, A. M. (1994) *Journal of Bacteriology* **176**(16), 4851-4857
2. Olvera, C., Goldberg, J. B., Sanchez, R., and Soberon-Chavez, G. (1999) *FEMS Microbiol. Lett.* **179**, 85-90.
3. Davey, M. E., Caiazza, N. C., and O'Toole, G. A. (2003) *J. Bacteriol.* **185**(3), 1027-1036.
4. Naught, N. E., and Tipton, P. A. (2001) *Arch. Biochem. Biophys.* **396**, 111-118.
5. Regni, C., Tipton, P. A., and Beamer, L. J. (2002) *Structure* **10**, 269-279.
6. Cleland, W. W., and Hengge, A. C. (1995) *FASEB J.* **9**, 1585-1594.
7. Aleshin, A. E., Kirby, C., Liu, X., Bourenkov, G. P., Bartunik, H. D., Fromm, H. J., and Honzatko, R. B. (2000) *J. Mol. Biol.* **296**, 1001-1015.
8. Arora, K. K., Filburn, C. R., and Petersen, P. L. (1991) *J. Biol. Chem.* **266**(9), 5359-5362.
9. Rusnak, F., and Mertz, P. (2000) *Physiol. Rev.* **80**(4), 1483-1521.
10. Straus, D., Raines, R., Kawashima, E., Knowles, J. R., and Gilbert, W. (1985) *Proc. Nat. Acad. Sci. U. S. A.* **82**, 2272-2276.
11. Nickbarg, E. B., Davenport, R. C., Petsko, G. A., and Knowles, J. R. (1988) *Biochemistry* **27**, 5948-5960.
12. Gassner, M., Stehlik, D., Schrecker, O., Hengstenberg, W., Maurer, W., and Ruterjans, H. (1977) *Eur. J. Biochem.* **75**, 287-296.
13. Thrall, S. H., Mehl, A. F., Carroll, L. J., and Dunaway-Mariano, D. (1993) *Biochemistry* **32**, 1803-1809.

CHAPTER 6 STRUCTURAL ANALYSIS OF INTERMEDIATE COMPLEXES IN PMM/PGM

The enzyme PMM/PGM from *P. aeruginosa* is part of the α -D-phosphohexomutase enzyme superfamily, members of which are found in all organisms from *E. coli* to humans. Enzymes in this family catalyze an intramolecular phosphoryl transfer utilizing a phosphoserine residue. In the course of the reaction, the phosphoryl group on the enzyme is transferred to the substrate, forming a bisphosphorylated sugar intermediate. The intermediate must then reorient to donate a phosphoryl group originally on the substrate back to the enzyme, which is then competent for another round of catalysis. In vivo, PMM/PGM converts mannose 6-phosphate (M6P) to mannose 1-phosphate (M1P), or glucose 6-phosphate (G6P) to glucose 1-phosphate (G1P).

To complete our structural analysis of the catalytic steps of the PMM/PGM reaction, a complex of the dephospho-enzyme with the intermediate, glucose 1,6 bisphosphate (G16P), was sought. During efforts at complex formation, an unexpected result was obtained: a second, distinct complex of PMM/PGM with intermediate, bound to the *phosphorylated* form of the enzyme. Here we present a structural analysis of two PMM/PGM complexes with its reaction intermediate G16P. One of these, produced with dephosphorylated enzyme, provides a picture of the enzyme immediately after the initial phosphoryl transfer, or, equivalently, prior to the second phosphoryl transfer. The second complex, with phosphorylated enzyme, shows an unexpected but fortuitous “non-productive” mode of intermediate binding, which is distinct in enzyme conformation, in

the type of enzyme-intermediate interactions, and in the position/location of ligand binding in the active site. This work has implications for an understanding of the many biosynthetic reactions catalyzed by members of the α -D-phosphohexomutase superfamily. Unexpectedly, it has also shed light on other enzymatic systems that undergo multiple cycles of catalysis without release of substrate, such as processive enzymes.

Materials and Methods

Complex formation and structure determination

Initially, formation of the dephospho-PMM/PGM complex was attempted using the site-directed mutant S108A, since this substitution prevents phosphorylation at position 108. In the wild-type apo structure (1K35), a terminal oxygen from the phosphoserine provides a ligand for the bound metal ion. In the S108A structure, a tartrate molecule from the crystallization buffer was observed acting as a ligand, replacing the missing oxygen from the serine [1]. All efforts to remove this tartrate were unsuccessful (data not shown); therefore, formation of the dephospho-PMM/PGM complex was accomplished using the site-directed mutant S108D. As described below, the carboxylate side chain of aspartate substitutes as a ligand for the metal ion while simultaneously preventing phosphorylation at position 108. Initial production of the phospho-PMM/PGM complex was inadvertent, due to incomplete dephosphorylation of the protein sample used for crystallization. Purification and crystallization of apo-PMM/PGM and the S108D mutant was carried out as previously described [2] and crystallized in the space group space group $P2_12_12_1$, with small differences in the unit cell axes, described below. G16P was purchased from Sigma. Complex formation for PMM/PGM and S108D was done by soaking G16P into crystals of catalytically inactive enzyme that contain Zn^{2+}

rather than the Mg^{2+} ion required for activity, following the approach used for forming enzyme-substrate complexes [3]. Briefly, crystals of PMM/PGM or S108D grown from solutions of 50-60% saturated Na, K tartrate were transferred quickly into 70% (w/w) PEG 4000 and 50 mM ligand, and allowed to soak for 10-15 minutes. Crystals were flash-cooled without further cryoprotection for data collection. The phospho-PMM/PGM complex had a reproducible reduction of the c axis by ~ 6 Å compared with apo enzyme (Table 1). Diffraction data were collected at beam line SBC 19-ID at the Advanced Photon Source, Argonne National Laboratory and processed with DENZO and merged with SCALEPACK [4]. The phospho-PMM/PGM complex showed a reduction along the b axis of ~ 2 Å (Table 1) compared to the enzyme-substrate complexes. Diffraction data were collected at beam line MBC 4.2.2 at the Advanced Light Source, Lawrence Berkeley National Laboratory. Data were processed and merged with D*TREK [5].

Structure solution and refinement

- *Dephospho-PMM/PGM complex.*

Due to the cell change relative to the apo-enzyme, phases for the S108D complex were determined by molecular replacement with CNS [6] using the PMM/PGM-glucose 1-phosphate complex (1P5D) as the search model. The structure was refined to convergence through iterative cycles of positional refinement using REFMAC 5.0 [7] and manual rebuilding with COOT [8]. Five percent of the data set was set aside for cross-validation prior to refinement. Water molecules were placed automatically by WATPEAK [9] in peaks $>3.0 \sigma$ in F_o-F_c maps and within hydrogen-bonding distance of nitrogen or oxygen atoms; water molecules without electron density in $2F_o-F_c$ maps and B-factors above 60 \AA^2 were removed from the model.

The final model (Table 1) extends from residue 10 to 463, and contains the following heteroatoms: Zn^{+2} , G16P, and waters. The structure has 1 residue modeled in two conformations. The side chains of 26 residues were truncated to alanine. The model was validated with the following programs: SFCHECK [10], and PROCHECK [11]. The occupancy for all residues except those modeled in multiple conformations is 1.0.

- *Phospho-PMM/PGM complex.*

The phospho-PMM/PGM complex was determined by regular refinement against apo-PMM/PGM. Electron density for the intermediate appeared as a nearly continuous, 3.0σ peak in F_o-F_c maps allowing for unambiguous placement of the ligand (Fig. XX). The structure was refined to convergence through iterative cycles of positional refinement using REFMAC 5.0 [7] and manual rebuilding with COOT [8]. Five percent of the data set was set aside for cross-validation prior to refinement; the same reflections were flagged as the test set. Water molecules were placed as described above. The final model (Table 1) extends from residue 9 to 463, and contains the following heteroatoms: phosphoserine 108, Zn^{+2} , G16P, and waters. The structure has three residues modeled in two conformations. The side chains of 33 residues were truncated to alanine. The occupancy for all residues except those modeled in multiple conformations is 1.0.

For structural analyses, the following programs were used for calculations: pocket surface area and volumes were done by CAST [12]; domain interface surface area by the protein-protein interaction server [13]; solvent accessible surface area of the ligands by AREAIMOL [9]; domain rotation by DYNDOM [14]; and C_α superpositions by MultiProt [15] and Superpose Version 1.0 [16]. Enzyme-ligand hydrogen bonds as

determined by CONTACT [9] are compiled in Table 4. Figures were prepared with MOLSCRIPT [17] and PYMOL [18].

Results

Two complexes of PMM/PGM with its reaction intermediate, G16P, have been refined at 1.9 and 2.0 Å (Table 1). The only difference between the proteins in these two structures is the residue at position 108. The *dephospho*-PMM/PGM complex is the site-directed mutant S108D, as described in Materials and Methods, bound to G16P. The *phospho*-PMM/PGM complex is wild-type enzyme (i.e., phosphorylated at Ser108) bound to G16P. These structures are most informative in the context of other PMM/PGM structures (Chapters 3-4), so throughout this chapter, the intermediate structures will be compared to those described previously. Discussion of “apo” enzyme refers to the ligand-free structures, wild-type PMM/PGM or the S108A mutant (PDB ID 1K35 and 1K2Y, respectively; refer to Chapter 3), and discussion of “enzyme-substrate complexes” refers to the structure of PMM/PGM bound to G1P, G6P, M1P or M6P (PDB ID 1P5D, 1P5G, 1PCJ and 1PCM, respectively; refer to Chapter 4).

The three-dimensional structure of PMM/PGM from *P. aeruginosa* was previously described by X-ray crystallographic studies of the wild-type protein and an active site mutant, S108A. The protein consists of four domains, arranged in an overall “heart” shape. The active site is located in the central cleft of the “heart”, and is composed of residues from all four domains. Key residues in catalysis, including the phosphoserine, metal binding loop and sugar binding residues cluster in this cleft [1].

Structures of PMM/PGM bound to its substrates/products revealed that each ligand is anchored by its phosphate group in a conserved network of hydrogen bonds with the protein. The residues participating in these contacts, mostly from domain 4, form the

phosphate-binding site. This area of the active site is distinct from the region near S108, or the *phosphoryl transfer site*, where the chemistry of the reaction occurs. (These regions are described in Chapter 4 and will be referred to as such throughout this chapter, see Fig. 2) [3].

Overall Structures

The protein structures in the two PMM/PGM intermediate complexes are quite similar to the apo-protein and enzyme-substrate complexes. When all eight structures are superimposed, the CA rms deviation is 0.78 Å. Figure 1 shows a CA superposition for the apo-protein, enzyme-substrate, and intermediate complexes. The largest differences between the backbones are confined to domain 4. Table 2 lists pair wise superposition data for the intermediate complexes compared to the apo-protein and enzyme-substrate forms, over the entire protein and by regions important for catalysis or ligand binding. The larger values for the overall CA rms deviations for some of the structures reflect differences in the conformation of domain 4 between structures. The CA rms deviations by protein region show that only minor changes in the backbone are observed in the metal-binding loop and sugar-binding loop relative to the apo enzyme. Most differences in these regions are confined to side chain conformations.

As in previous structures, different conformations of domain 4 are observed in the two PMM/PGM intermediate complexes. The enzyme-substrate complexes show that upon binding of ligand, the open active site of PMM/PGM closes to become a deep pocket, through a rotation of domain 4 by 9° relative to the apo-enzyme [3]. In the enzyme-intermediate complexes, two distinct conformations of domain 4 are seen: an essentially closed form (dephospho complex) and a novel, “half open” conformation (phospho complex). In Table 3, the rotation of domain 4 and the associated changes in solvent accessible surface area and volume of the active site, and several domain interfaces are shown and compared with the previous structures. These data show that

the structural changes associated with intermediate binding to dephosphorylated enzyme are similar to those seen in the enzyme-substrate complexes. In contrast, when the intermediate binds to phosphorylated enzyme, the protein assumes a conformation almost midway between “open” and “closed”.

The rotation of domain four of PMM/PGM has profound effects on the solvent accessibility of the intermediate in the two complexes. In the dephospho-complex, which structurally resembles the enzyme-substrate forms, the solvent accessible surface area and volume of the active site is reduced by 50% compared with the apo protein, and buries 90% of the surface area of G16P. In the phospho-complex, the solvent accessible surface area and volume of the active site cleft is 10% larger than the enzyme-substrate complexes, and buries only 73% of the surface area of G16P.

Enzyme-intermediate interactions

The two enzyme-intermediate complexes show differences in the binding location, orientation, and conformation of the intermediate. In the dephospho-PMM/PGM complex G16P is positioned deep within the active site, while in the phospho-complex G16P is “suspended” by its phosphate groups in a more exposed position. In the dephospho-complex, the 6-phosphate of G16P is in the phosphate-binding site, while the 1-phosphate is near the phosphoryl transfer site. The opposite orientation of the intermediate is observed in the phospho-complex. In the dephospho-complex, G16P adopts an extended conformation, placing the two phosphorus atoms 7.7 Å from each other. However, in the phospho-complex a rotation about the C6-O6 bond of G16P produces a compact conformation with the two phosphorus atoms 6.9 Å from each other. Differences are also seen in the contacting residues and interactions with solvent. Detailed descriptions of the interactions in each complex are below.

- *Dephospho-PMM/PGM complex.*

As noted above, G16P has an extended conformation and spans the active site in the dephospho-PMM/PGM complex. The 6-phosphate is positioned within the phosphate-binding site, while the 1-phosphate group is near D108 (Fig. 2). Structurally, it is unclear why the orientation observed for G16P is preferred, and the mechanism of the reaction requires the enzyme to bind the intermediate in two orientations to complete the catalytic cycle. However, both the initial Fo-Fc (Fig. 3) and final 2Fo-Fc electron density maps support modeling G16P in a single orientation in this complex.

Many specific interactions between the protein and intermediate are observed in the dephospho-enzyme complex (see Table 4). Indeed, residues from all four domains contact G16P. The 6-phosphate is anchored in the phosphate-binding site via an extended network of hydrogen bonds with both side chain and backbone atoms of the protein. The 1-phosphate is found near the phosphoryl transfer site, and forms contacts with a number of side chains, including several ionizable residues (Lys118, His308, His329 and Arg247). This places the 1-phosphate of G16P in a position that appears favorable for phosphoryl transfer to residue 108 of the enzyme. The sugar ring of the intermediate is positioned by hydrogen bonds to its hydroxyls contributed by residues in domains 1-3, including residues Glu325 and Ser327, which make similar contacts in the enzyme-substrate complexes.

Solvent molecules that bridge between protein atoms and G16P atoms are also observed in the dephospho-PMM/PGM structure. Of the four water molecules that contact G16P, two make bridging interactions with side chain atoms of the protein. Some of these side chains are in key regions of the active site, including the phosphate-binding site. Other side chains, such as Lys 285 and Asp 283, are on the periphery of the active

site. Hence, these bridging contacts from solvent to G16P extend interactions with the intermediate both within and to the edges of the active site.

In many ways, the dephospho-PMM/PGM complex resembles the enzyme-substrate complexes described in Chapter 4. First, the position of the intermediate within the active site is similar. In a superposition of the dephospho complex with the enzyme-substrate complexes, the phosphate groups of the ligands occupy essentially the same position in the phosphate-binding site: the four oxygen atoms of the phosphate groups are all within 0.5 Å of each other. Also, the sugar rings of the intermediate and substrate overlap to a large degree, although not as closely as the phosphate group. Therefore, almost all of the residues that contact the intermediate were previously observed contacting the substrates in the enzyme-substrate structures. However, a new contact is observed near the phosphoryl transfer site, between Lys 118 and the 1-phosphate of G16P.

- *Phospho-PMM/PGM complex*

As described in Materials and Methods, a second PMM/PGM-intermediate complex, with phosphorylated enzyme, was produced during our initial efforts at complex formation. This complex represents an “off pathway” or “non-productive” binding event, since in the normal course of the reaction the intermediate is produced by dephosphorylation of the enzyme. Nonetheless, a distinct binding site for G16P in the active site of phospho-PMM/PGM was observed (Fig. 2). In this complex, G16P appears “suspended” within the active site by its phosphate groups, and adopts a compact conformation. This conformation appears necessary given the position of G16P, which is sandwiched between domains 1 and 4. This location, which is more exposed than that

seen in the dephospho complex, avoids unfavorable steric and electrostatic interactions between the bisphosphorylated intermediate and phosphoserine 108. Electron density maps (Fig. 4) of this complex indicate that G16P is also primarily bound in one orientation, with its 1-phosphate close to the phosphate-binding site, and its 6-phosphate adjacent to the phosphoryl transfer site.

Despite its unexpected binding position, a number of specific protein-ligand interactions are observed in the phospho-PMM/PGM complex. The most extensive protein-ligand interactions are with the two phosphate groups of G16P, and many of the contacting residues are basic, such as Arg15, Arg20, His109, and Arg421. The 1-phosphate of G16P is positioned within a perturbed version of the phosphate-binding site, which differs in the number of contacting residues and geometry of the interactions relative to the enzyme-substrate and dephospho-intermediate complexes. Only a single contact is made to the sugar moiety of G16P, by residue Ser327. Instead, the majority of contacts to the G16P sugar ring are with water molecules (see Table 4). Of the ten water molecules in the complex, eight contact the hydroxyl groups of the sugar ring. Four of these waters bridge between G16P and protein side chain atoms from domains 1 and 3. Overall, this complex has more extensive solvent contacts to G16P than seen in the dephospho-complex. This observation is consistent with the fact that phosphorylated PMM/PGM has a lower affinity for the bisphosphorylated sugar intermediate than the substrate [19].

Many of the enzyme-intermediate interactions in the phospho-PMM/PGM complex are unique. Of the contacting residues, Arg15, Arg20, His109 and Asn110 (highlighted on Table 4) were *not* observed to make contacts in any of the enzyme-substrate

complexes, or the dephospho-PMM/PGM intermediate complex. These four residues cluster in domain 1 and form a phosphate-binding “sub-site”, which surrounds the 6-phosphate of G16P. Three of these residues, Arg20, His109, and Asn110, are conserved throughout the α -D-phosphohexomutase family, suggesting a key role in enzyme function [20].

Discussion

In this study we have presented structures of dephosphorylated and phosphorylated PMM/PGM bound to G16P. The dephospho-complex represents a snapshot of the catalytic reaction: either immediately after phosphoryl transfer from the enzyme to the substrate, or prior to phosphoryl transfer from the intermediate back to the enzyme. Overall, the dephospho-complex is structurally similar to the enzyme-substrate complexes, including most notably the closed conformation of domain 4 (refer to superposition data in Results). In addition, many of the same protein-ligand interactions are observed in the phosphate-binding site and to the sugar ring. The G16P intermediate appears to bind in one orientation, with its 1-phosphate group surrounded by ionizable residues and in an appropriate position for transfer of the phosphoryl group to residue 108. Nearly all of the residues that contact the 1-phosphate of G16P were also involved in contacts in the enzyme-substrate structures (Chapter 4), but the interactions were with different functional groups of the ligand, namely the sugar hydroxyls. Thus, one theme that emerges from this complex is the ability of residues in the active site of PMM/PGM to play more than one role (i.e., to make different contacts in different complexes). Such robustness and redundancy of design was previously noted in the ability of the active site

of PMM/PGM to bind both the 1-phospho and 6-phospho forms of the substrates in different orientations (Chapter 4).

Formation and characterization of the second PMM/PGM intermediate complex, with phosphorylated enzyme, has revealed several intriguing structural features. First, a partly “open” conformation of domain 4 was observed, adding weight to the proposed role for flexibility of the enzyme in catalysis. Second, the location and solvent accessibility of the ligand distinguishes this complex from the enzyme-substrate and dephospho- forms. Third, a novel phosphate-binding “sub-site” was identified surrounding the 6-phosphate group of the intermediate, which utilizes several residues not previously observed to participate in enzyme-ligand interactions.

The newly identified “sub-site” in the phospho-complex suggests for the first time a function for these residues that could not be deduced from the other PMM/PGM structures. Three of the four residues (Arg20, His109, Asn110) are conserved throughout the superfamily, yet none of them had been observed to contact the substrates or participate in contacts with G16P in the “productive” dephospho-complex. Furthermore, the preponderance of basic charge and flexible nature of the side chains piqued our curiosity. One possibility is that this complex might represent a “snap shot” of the intermediate at a quasi-stable point during its 180° reorientation, a required step in the catalytic reaction. If this is indeed the case, a potential role for residues in the phosphate-binding sub-site could be in the reorientation of the G16P during catalysis.

As mentioned in the introduction, the PMM/PGM reaction entails two phosphoryl transfers, first from enzyme to substrate, and second, from intermediate to enzyme. This mechanism necessitates a 180° reorientation of the bisphosphorylated sugar intermediate

in between the two phosphoryl transfer steps. Our enzyme-substrate complexes confirmed this model for the first time, demonstrating that 1- and 6- phosphosugars bind in two distinct orientations, with the sugar rings flipped relative to one another while the phosphate groups are held in one place [3] (Refer to Chapter 4). Although dynamic processes, such as conformational changes, are important to many enzymes, the reorientation of the bisphosphorylated sugar intermediate as a required step in the catalytic reaction of PMM/PGM and related enzymes is unique and not well understood.

Therefore, we formulated a hypothesis that residues in the sub-site were important for reorientation of G16P during catalysis. Specifically, we chose to investigate whether they are involved in maintaining association of G16P with the enzyme during the reorientation step. This question can be directly addressed because it has been demonstrated that reorientation of the G16P intermediate occurs *without* dissociation from wild-type PMM/PGM. Isotope trapping experiments, which measured the frequency of dissociation of G16P from the active site during turnover [21], showed that it remains associated in 14 out of 15 catalytic cycles.

Site-directed mutants of residues in the phosphate-binding sub-site (R15, N110, R20) and other areas of the active site (R247, and R421) to alanine are being characterized in the isotope trapping experiment (data not shown). Preliminary results indicate generally modest changes in steady state parameters of these mutants. However, R15A and N110A both show significant increases in the frequency of dissociation of G16P from the enzyme during catalysis. In fact, the R15A mutant appears to lose the intermediate nearly every other catalytic cycle, an increase of nearly 7-fold, supporting

our hypothesis that these residues are important for maintaining association of the intermediate with the enzyme during catalysis.

Although these studies are not yet complete, we have chosen to discuss them herein due to their exciting potential significance for understanding the reaction catalyzed by PMM/PGM and other members of the α -D-phosphohexomutase family. Based on a sequence-structure (ET) analysis of α -D-phosphohexomutases, it appears that all members of this ubiquitous enzyme superfamily utilize a common reaction mechanism, including the dramatic reorientation of the reaction intermediate [20]. The isotope trapping studies of the PMM/PGM mutants demonstrate for the first time that residues in the active site of the enzyme have a specific role in the reorientation process. Since several of the residues in the phosphate-binding sub-site are conserved in the enzyme superfamily, studies of other members of this protein family may reveal further insights into the role of residues in the reorientation of the intermediate.

Furthermore, this work has implications for structure-function studies of enzymes in general. It is important to note that residues of the sub-site were not observed to participate in the PMM/PGM-substrate complexes. These structures are representative of high-affinity enzyme-ligand complexes typically sought and characterized by X-ray crystallography, and which, in this case, failed to identify residues with significant functional importance. This raises questions about whether many enzymes could have residues with “invisible” roles in catalysis that are not easily identified by classical structure-function analyses.

One class of enzymes on which our studies may provide insights is processive enzymes. We suggest that PMM/PGM can be thought of as a simple version of a

processive enzyme. Due to the novel reorientation of the intermediate, which occurs after the first phosphoryl transfer and before the second during catalysis, the PMM/PGM reaction fulfills the definition of processivity, which is multiple cycles of catalysis on a single substrate molecule without dissociation from the enzyme [22]. Thus, the residues of PMM/PGM identified to play a role in maintaining association with G16P may also have counterparts in the many processive enzymes that have been characterized. These include the DNA and RNA polymerases; some of these enzymes are estimated to catalyze thousands of reactions before the nucleic acid substrate and enzyme dissociate from one another [22].

General comparisons of structural features of PMM/PGM with processive enzymes reveal a number of similarities. First, large binding grooves are commonly noted in structurally characterized processive enzymes. These grooves allow the enzyme to accommodate movement of the substrate without compromising affinity or specificity, by providing a large interaction surface for the substrate. In the case of PMM/PGM, the large, active site cleft is sufficient to capture and enclose the substrate, *and* also accommodate the 180° reorientation of the intermediate through rotation of domain 4. Overall, the surface of PMM/PGM is negatively charged, but the active site cleft is positively charged and this may also help to “trap” its anionic substrates. Positively charged surfaces have also been observed in structurally characterized processive enzymes, some of which bind double-stranded DNA, such as processivity factor UL42 from herpes simplex virus [22]. Clearly, there are also significant differences between PMM/PGM and other processive enzymes. For example, most of them have large, oligomeric substrates, while PMM/PGM uses a small phosphosugar. However, broad structural comparisons indicate that PMM/PGM may utilize similar strategies to accomplish processive catalysis as its more complex counterparts, and our studies may help lead the way to a better understanding of the structural basis of processivity.

In summary, structural analyses of the two PMM/PGM intermediate complexes described herein have provided new insights into the enzyme and its unique reaction. The dephospho-intermediate complex has filled in a missing piece of our structural characterization of catalysis by PMM/PGM. This structure shows a closed enzyme complex, with many direct enzyme-intermediate interactions. In contrast, the phospho-complex reveals a partly open complex, where flexible, positively charged residues makes contacts primarily to the phosphate groups of the intermediate. Investigation into the potential roles of these residues in maintaining association with G16P during reorientation is ongoing, but has already provided some important new clues about how enzymes can adapt to accommodate structural diversity and movement of ligands.

Table 1. Data collection and refinement statistics.

	<u>Phospho-</u> <u>PMM/PGM</u>	<u>Dephospho-</u> <u>PMM/PGM</u>
Data Collection*		
X-ray source	SBC 19ID	MBC 4.2.2
Space group	P2 ₁ 2 ₁ 2 ₁	P2 ₁ 2 ₁ 2 ₁
Cell, Å	a= 70.87 b= 72.85 c= 91.26	a= 70.22 b= 70.36 c= 84.39
λ , Å	0.97934	0.97909
Resolution, Å	50.0-1.9	50.0-1.9
Unique ref./redundancy	38,037/8.1	33,583/6.5
R _{merge} , %	8.2 (68.9)	7.5 (34.6)
I/ σ	28.4 (2.7)	13.9 (4.0)
Completeness, %	99.7 (99.3)	99.9 (99.4)
Refinement Statistics		
Resolution, Å	50.00-2.00	50.00-1.90
R _{work} /R _{free}	17.6/23.5	19.4/25.0
Non-H atoms	3727	3636
Waters	305	238
$\langle B \rangle$, Å ²		
protein atoms	37.54	31.88
waters	42.72	35.16
ligand	37.24	38.51
rmsd bonds Å/angles °	0.012/1.357	0.014/1.502
Ramachandran 1/2 [†] %	90.4/9.1	91.4/8.1

Table 2. Pairwise superpositions to Apo-PMM/PGM (1K35) using Superpose Version 1.0. Superpositions of CA and all atoms, over the entire chain and by protein region.

RMSD, Å	Overall CA	Metal Binding (aa 240-250)		Sugar Binding (aa 320-330)		Phosphate Binding (aa 415-430)	
		CA	All	CA	All	CA	All
Enzyme-Substrate (1P5D)	1.26	0.14	0.76	0.20	0.64	0.53	0.78
Dephospho-PMM/PGM	1.05	0.17	0.74	0.21	0.46	0.44	0.68
Phospho-PMM/PGM	0.46	0.09	0.44	0.11	0.56	0.21	0.32

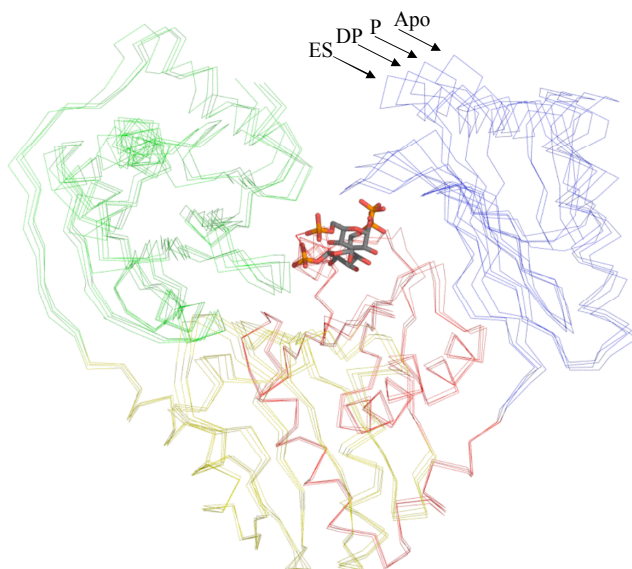
Table 3. Comparison of all PMM/PGM structures.

	Volume Active Site (Å³)	Solvent Accessible Surface Area Active Site (Å²)	Rotation Domain 4 (°)	Domain 1-4 Interface (Å²)	Domain 1-3 Interface (Å²)	Burial of ligand (%)
“Apo” (1K2Y, 1K35)	1400	1603	--	--	380	--
“Enzyme-Substrate” (1P5D, 1P5G, 1PCM, 1PCJ)	466±45	735 ±55	9±.6	170±26	570±8	97.4±.8
Phospho-PMM/PGM	927	946	3.4	67	530	73.4
Dephospho-PMM/PGM	551	770	7.8	139	567	90.2

Table 4: Enzyme-ligand hydrogen bond contacts in PMM/PGM complexes. All contacts are within 3.5 Å and have favorable geometry. In red, contacts unique to phospho-PMM/PGM complex.

Ligand atom	Residue/Atom	Phospho-PMM/PGM (Å)	Bridging Residue/Atom (s)	Residue/Atom	Dephospho-PMM/PGM (Å)	Bridging Residue/Atom(s)
1-phosphate						
*O1P	R421 NH1	3.02		Wat 191	3.38	
	R421 NH2	3.14				
	N424 N	3.02				
	Wat 165	3.04	T306 OG1			
*O2P	T425 N	3.21		K118 NZ	3.16	
	T425 OG1	2.72		H308 NE2	3.37	
	Wat 148	2.69		H329 NE2	3.21	
*O3P	S423 OG	2.57		D108 OD2	3.06	
	Wat 103	2.69		R247 NH2	3.45	
	Wat 136	2.63		Wat 191	2.77	
Sugar hydroxyls						
O1	Wat 136	3.37				
	Wat 165	3.38	T306 OG1			
	Wat 294	3.36				
O2	S327 OG A	3.26		H308 N	3.02	
	Wat 177	3.35	S327 OG A	E325 OE1	3.49	
	Wat 294	2.53	K285 NZ	E325 OE2	2.66	
O3	S327 OG A	2.83		E325 OE1	2.48	
	Wat 293	2.59	E325 OE1	E325 OE2	3.13	
			S327 OG B	S327 OG	2.67	
			G307 O A	Wat 37	2.86	E325 OE1 S327 N K285 NZ D283 OD2
O4			K285 NZ	3.47		
O5	Wat 103	3.23				
	Wat 295	2.69		R247 NH2	2.96	
O6	Wat 295	2.84		Wat 191	3.16	
	Wat 296	3.06		Y17 OH	3.50	
6-phosphate						
O1P	R15 NH2	3.15		Y17 OH	2.52	
	R20 NH1	2.98		R421 NH2	2.99	
				N424 N	2.74	
O2P	R15 NH1	2.90		R421 NH1	2.71	
	Wat 51	2.83	N110 OD1	Wat 179	2.44	K285 NZ R421 NH1
				Wat 217	3.01	
O3P	N110 ND2	2.99		S423 OG	2.43	
	H109 NE2	3.25		T425 OG1	2.51	
	Wat 296	2.87		Wat 217	2.72	

Figure 1. Superposition of PMM/PGM structures: ES, enzyme-substrate; DP, dephospho-PMM/PGM; P, phospho-PMM/PGM, and Apo. Domains 1-4 are green, yellow, red and blue, respectively. G16P is depicted as gray sticks.



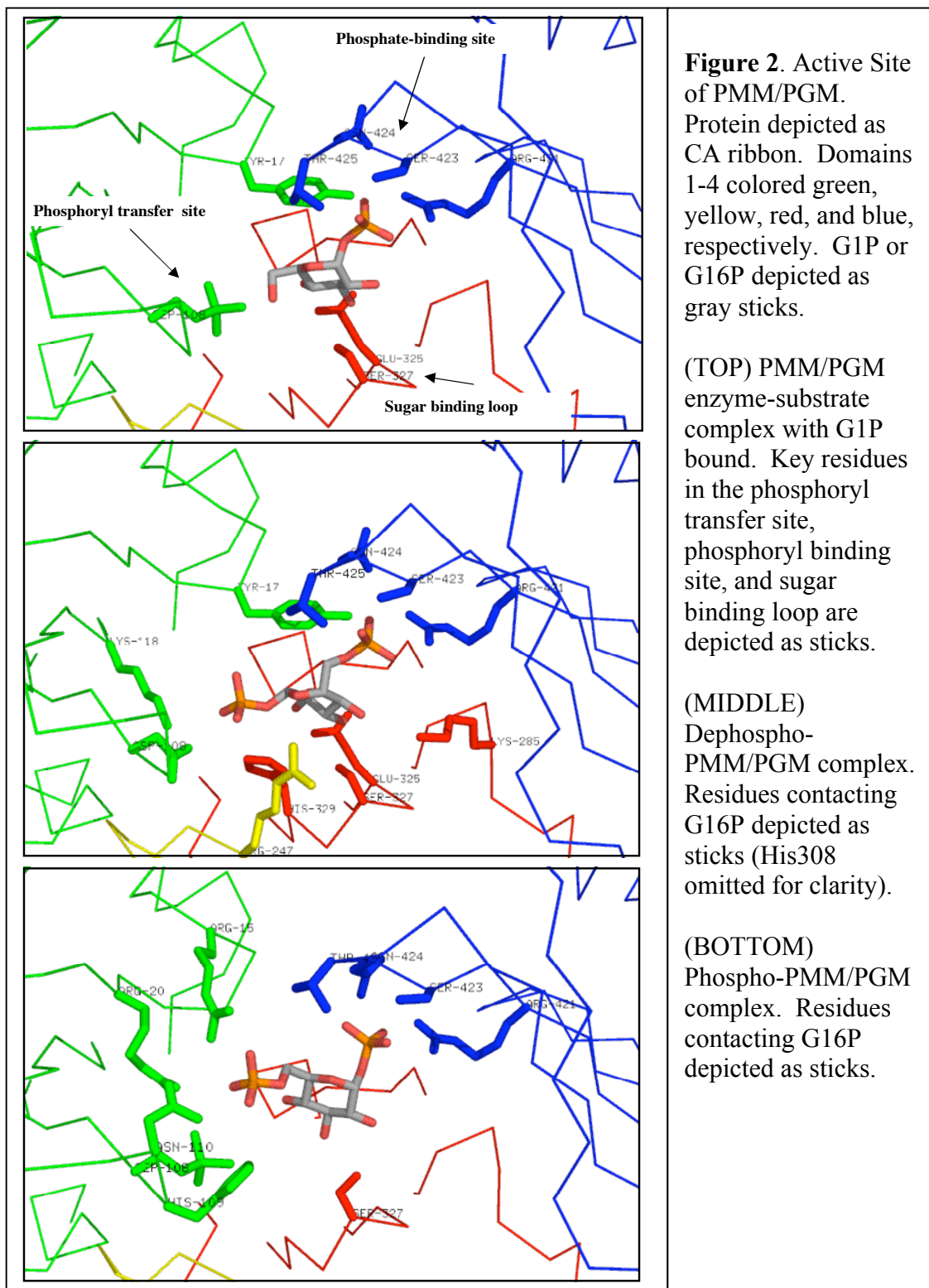


Figure 3. An F_o-F_c difference Fourier map (contoured at 2.7σ) showing electron density (gray) for G16P in the phospho-PMM/PGM complex. Phases for the map are from the beginning of the refinement process, immediately after the first round of rigid body and positional refinement and prior to extensive manual rebuilding. Substrate and solvent were not included in the model.

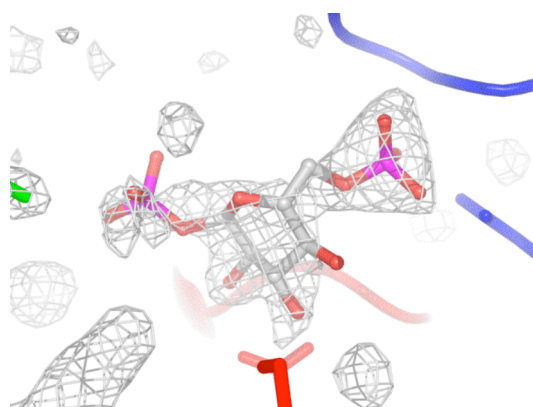
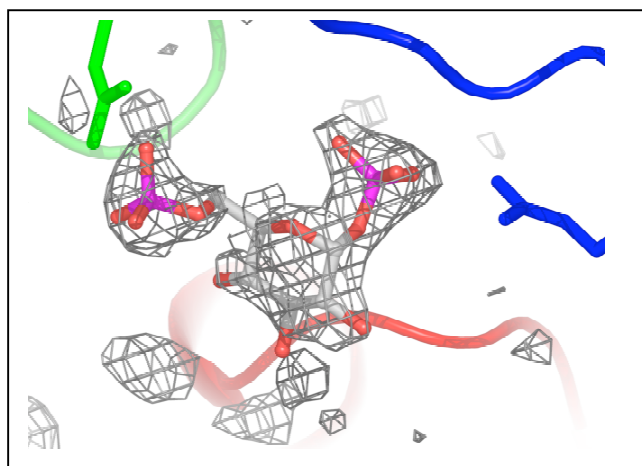


Figure 4. An F_o-F_c difference Fourier map (contoured at 3.0σ) showing electron density (gray) for G16P in the phospho-PMM/PGM complex. Phases for the map are from the beginning of the refinement process, immediately after the first round of rigid body and positional refinement and prior to extensive manual rebuilding. Substrate and solvent were not included in the model.



References

1. Regni, C., P.A. Tipton, and L.J. Beamer, *Crystal structure of PMM/PGM: an enzyme in the biosynthetic pathway of P. aeruginosa virulence factors*. Structure, 2002. **10**(2): p. 269-79.
2. Regni, C.A., P.A. Tipton, and L.J. Beamer, *Crystallization and initial crystallographic analysis of phosphomannomutase/phosphoglucomutase from Pseudomonas aeruginosa*. Acta Crystallogr. D, 2000. **56**(Pt 6): p. 761-2.
3. Regni, C., L.E. Naught, P.A. Tipton, and L.J. Beamer, *Structural basis of diverse substrate recognition by the enzyme PMM/PGM from P. aeruginosa*. Structure, 2004. **12**: p. 55-63.
4. Otwinowski, Z. and W. Minor, *Processing of X-ray diffraction data collected in oscillation mode*. Methods Enzymol., 1997. **276**: p. 307-326.
5. Pflugrath, J.W., *The finer things in X-ray diffraction data collection*. Acta Crystallogr D Biol Crystallogr, 1999. **55** (Pt 10): p. 1718-25.
6. Brünger, A.T., et al., *Crystallography & NMR system: A new software suite for macromolecular structure determination*. Acta Crystallogr. D, 1998. **54**(Pt 5): p. 905-21.
7. Murshudov, G.N., A.A. Vagin, A. Lebedev, K.S. Wilson, and E.J. Dodson, *Efficient anisotropic refinement of macromolecular structures using FFT*. Acta Crystallogr. D, 1999. **55**(Pt 1): p. 247-255.
8. Emsley, P. and K. Cowtan, *Coot: model-building tools for molecular graphics*. Acta Crystallogr D Biol Crystallogr, 2004. **60**(Pt 12 Pt 1): p. 2126-32.

9. No. 4, C.C.P., *The CCP4 suite: Programs for Protein Crystallography*. Acta Crystallogr. D, 1994. **50**: p. 760.
10. Vaguine, A.A., J. Richelle, and S.J. Wodak, *SFCHECK: a unified set of procedures for evaluating the quality of macromolecular structure-factor data and their agreement with the atomic model*. Acta Crystallogr. D, 1999. **55**(Pt 1): p. 191-205.
11. Laskowski, R.A., M.W. McArthur, D.S. Moss, and J.M. Thornton, *PROCHECK: A program to check the stereochemical quality of protein structures*. J. Appl. Crystallogr., 1993. **26**: p. 283-291.
12. Liang, J., H. Edelsbrunner, and C. Woodward, *Anatomy of protein pockets and cavities: measurement of binding site geometry and implications for ligand design*. Protein Sci., 1998. **7**(9): p. 1884-1897.
13. Jones, S. and J.M. Thornton, *Principles of protein-protein interactions*. Proc. Natl. Acad. Sci. USA, 1996. **93**(1): p. 13-20.
14. Hayward, S. and H.J. Berendsen, *Systematic analysis of domain motions in proteins from conformational change: new results on citrate synthase and T4 lysozyme*. Proteins, 1998. **30**(2): p. 144-54.
15. Shatsky, M., R. Nussinov, and H.J. Wolfson, *A method for simultaneous alignment of multiple protein structures*. Proteins, 2004. **56**(1): p. 143-56.
16. Maiti, R., G.H. Van Domselaar, H. Zhang, and D.S. Wishart, *SuperPose: a simple server for sophisticated structural superposition*. Nucleic Acids Res, 2004. **32**(Web Server issue): p. W590-4.

17. Esnouf, R.M., *An extensively modified version of MolScript that includes greatly enhanced coloring capabilities*. J. Mol. Graph. Model., 1997. **15**(2): p. 132-4.
18. DeLano, W.L., *The PyMOL Molecular Graphics System*. 2002, DeLano Scientific: San Carlos, CA.
19. Naught, L.E. and P.A. Tipton, *Kinetic Mechanism and pH Dependence of the Kinetic Parameters of Pseudomonas aeruginosa Phosphomannomutase/Phosphoglucomutase*. Arch Biochem Biophys, 2001. **396**(1): p. 111-8.
20. Shackelford, G.S., C.A. Regni, and L.J. Beamer, *Evolutionary trace analysis of the alpha-D-phosphohexomutase superfamily*. Protein Sci, 2004. **13**(8): p. 2130-8.
21. Naught, L.E. and P.A. Tipton, *Formation and reorientation of glucose 1,6-bisphosphate in the PMM/PGM reaction: transient-state kinetic studies*. Biochemistry, 2005. **44**(18): p. 6831-6.
22. Breyer, W.A. and B.W. Matthews, *A structural basis for processivity*. Protein Sci, 2001. **10**(9): p. 1699-711.

CHAPTER 7 CONCLUSION

Several themes emerge from the structural studies of PMM/PGM presented herein: Shape, charge, domain organization, and conformational change are critical for the enzyme's function. The scaffold for the chemistry of the reaction, housing the phosphoryl donor and the metal binding loop, is domains 1-2. Domain 3 serves as a platform for the substrate, shifting slightly relative to domains 1 and 2, and provides residues that bind the sugar ring. Domain 4 is the flexible "gate" which undergoes a conformational change and closes around the substrate. Overall, the surface of the protein is negatively charged, but the active site cleft is positively charged and has sufficient surface area to "trap" anionic substrates. In the active site, several side chains change conformations to bind the substrate and the intermediate. The subtle shifts that accompany ligand binding are exquisite, and reveal amazing complexity for an enzyme that catalyzes a seemingly simple reaction.

Many questions remain regarding this system and the α -phosphohexomutase superfamily, such as the structural basis for specificity and energetics of ligand binding. To address specificity, structural studies and computational methods will be useful. Structural characterization of the eukaryotic phosphoglucomutase (PGM) bound to its substrates and comparison with the PMM/PGM enzyme-substrate complexes may reveal a structural determinant for specificity that could be tested biochemically. In addition, a new algorithm to identify specificity-determining residues in related enzymes, surface patch ranking (SPR), may provide a starting-point for biochemical studies [1]. PMM/PGM and PGM are excellent candidates for this analysis; given their overall sequence identity is low. Furthermore, PMM/PGM is a good candidate for isothermal

titration calorimetry (ITC), to probe the energetics of ligand binding; the enzyme is highly soluble, and all the substrates are commercially available. Thermodynamic characterization of ligand binding in PMM/PGM, combined with the structural and kinetic studies already completed would facilitate inhibitor design.

In conclusion, the structures presented herein provide a visual framework for understanding the catalytic reaction of PMM/PGM, a ubiquitous enzyme. Future investigations could address several uncharacterized facets of the catalytic reaction and explore other members of the superfamily. In addition, PMM/PGM can serve as a model system for understanding the structural relationships between enzyme and substrate that have significant implications for catalysis in more complicated systems.

References

1. Yu, G.X., et al., *In silico discovery of enzyme-substrate specificity-determining residue clusters*. J Mol Biol, 2005. **352**(5): p. 1105-17.

VITA

Catherine A. Regni was born September 26, 1973, in Anchorage, Alaska, and grew up in Bellevue, Nebraska. After attending public schools in Nebraska, she attended the University of Missouri-Columbia and received a B.A. in History (1995). In 1997 she returned to her education and switched disciplines, completing prerequisites to enter the Biochemistry doctoral program (2000), and earned the Ph.D. degree in 2005. She is married to Dr. Agoston Jerga and has a daughter, Margit A. Jerga.